

The bosonic effective chiral Lagrangian with a light Higgs particle

Memoria de Tesis Doctoral realizada por
Juan Alberto Yepes
presentada ante el Departamento de Física Teórica
de la Universidad Autónoma de Madrid



Trabajo dirigido por la
Dra. María Belén Gavela Legazpi
Catedrática del Departamento de Física Teórica
y miembro del Instituto de Física Teórica, IFT-UAM/CSIC

Madrid, Septiembre de 2014

Agradecimientos

A mi familia, especialmente mi madre y abuelo a quienes quiero y debo mucho. A Belén Gavela, a quien agradezco todo su tiempo, paciencia y conocimientos aprendidos, y sin cuya ayuda, soporte y dirección este trabajo no hubiera sido posible. A Luis Ibáñez, quien permitió la financiacion de mis dos primeros años de doctorado mediante la red europea Marie Curie Initial Training Network-UNILHC era. A mis colegas y compañeros de trabajo Rodrigo Alonso, Luca Merlo, Stefano Rigolin y Juan Fraile, con quienes tuve discusiones realmente gratificantes y enriquecedoras a lo largo de estos cuatro años, discusiones fundamentales para el desarrollo de los resultados aquí presentados.

Y a Pablo Fernández, Cristian Setevich, Eric Endress, Andy de Ganseman, Manuel Sánchez, Ana María Matamoros, María Parejo, Magdalena Kazimieruk, Martina Brajković, Eva Rodríguez y Asunción, sin cuya compañía y momentos especiales este trabajo hubiera sido una quimera más.

Contents

Introduction	viii
Introducción	xii
1 Standard Model interactions	1
1.1 EWSB in the SM	3
1.2 SM flavour structure	4
1.3 Going beyond the Standard Model	8
2 Bosonic Chiral Lagrangian for a Light Dynamical “Higgs Particle”	13
2.1 The SM vs. σ -model parametrization	14
2.2 Chiral effective expansion and light Dynamical Higgs h	17
2.2.1 Pure gauge and gauge- h operator basis	19
2.2.2 CP-conserving $\Delta\mathcal{L}_{\text{CP}}$	20
2.2.3 CP-violating $\Delta\mathcal{L}_{\text{CP}}$	23
2.3 $\Delta\mathcal{L}_{\text{CP}}$ -phenomenology	25
2.3.1 CP-odd two-point functions	25
2.3.2 Triple gauge boson couplings	27
2.3.3 CP violation in Higgs couplings to gauge-boson pairs	36
3 Fermion-h sector and flavour effects	41
3.1 Fermion-gauge- h couplings	41
3.2 Operators suppressed by Λ_s	45
3.3 Phenomenological analysis	47
3.3.1 $\Delta F = 1$ and $\Delta F = 2$ observables	47
3.3.2 $\bar{B} \rightarrow X_s \gamma$ branching ratio	51
4 Conclusions	58
5 Conclusiones	62

APPENDIXES	66
A Useful Formulas for non-linear $d_\chi = 4$ basis	67
A.1 CP transformation properties	68
A.2 Relation with the linear representation	69
A.3 Formulae for the Phenomenological Analysis	69
A.3.1 $\Delta F = 2$ Wilson Coefficients	69
A.3.2 Approximate Analytical Expressions	73
B MFV in a Strong Higgs Dynamics scenario	75
B.1 Non Unitarity and CP Violation	75
B.2 $\Delta F = 1$ Observables	76
B.3 $\Delta F = 2$ Observables	78
B.4 Phenomenological analysis	81
C Linear siblings of the CP-odd chiral operators $\mathcal{S}_i(h)$	85
D Linear siblings of the operators \mathcal{X}_i	88
E Feynman rules	91
Bibliografía	101

List of Figures

1.1	CKM unitary triangle	8
2.1	Hierarchy representation of the involved scales	14
2.2	A CP-odd TGV coupling inducing a fermionic EDM interaction	29
2.3	Distribution of events with respect to p_T^Z for the 7 (14) TeV run assuming $\mathcal{L} = 4.64$ (300) fb^{-1} of integrated luminosity	34
2.4	Distribution of $pp \rightarrow \ell'^\pm \ell^+ \ell^- E_T^{\text{miss}}$ contributions with respect to $\cos \theta_\Xi$, for 300 fb^{-1} of integrated luminosity at 14 TeV	37
3.1	Tree-level Z -mediated FCNC from \mathcal{O}_{1-3}	48
3.2	W -mediated box diagrams for $\Delta F = 2$ transitions from \mathcal{O}_{2-4}	49
3.3	ε_K vs. $R_{BR/\Delta M}$ and $a_W - a_{CP}$ parameter space for ε_K and $R_{BR/\Delta M}$ inside their 3σ error ranges and $a_Z^d \in [-0.044, 0.009]$	50
3.4	$a_W - a_{CP}$ parameter space for ε_K and $BR(B^+ \rightarrow \sigma^+ \nu)/\Delta M_{B_d}$ inside their 3σ error ranges and $a_Z^d \in [-0.044, 0.009]$	54
3.5	$BR(\bar{B} \rightarrow X_s \gamma)$ vs. b_{eff}^d and $b_F^d - b_G^d$ parameter space	56
A.1	W -mediated box diagrams for the neutral kaon and B_q meson systems	71
B.1	Tree-level Z -mediated currents contributing to the FCNC operators \mathcal{Q}_n	77
B.2	ε_K , $\Delta M_{B_{d,s}}$ and $R_{BR/\Delta M}$ in the reduced $ V_{ub} - \gamma$ parameter space.	82
B.3	ε_K vs. $R_{BR/\Delta M}$ for different values of a_W , a_{CP} and a_Z^d , and $a_W - a_{CP}$ parameter space for ε_K and $R_{BR/\Delta M}$ inside their 3σ error ranges	83
B.4	A_{sl}^b vs. $S_{\psi\phi}$, for ε_K and $R_{BR/\Delta M}$ inside their 3σ error ranges	84

List of Tables

1.1	SM fermion field content and quantum numbers	2
1.2	SM interactions, gauge field content and quantum numbers	2
1.3	Bounds either on Λ or c_{ij} for some $\Delta F = 2$ operators of dimension 6	10
1.4	Bounds either on Λ or c_{ij} implementing MFV ansatz	12
2.1	Values of the cross section predictions for the process $pp \rightarrow \ell'^\pm \ell^+ \ell^- E_T^{\text{miss}}$.	33
2.2	Expected sensitivity on g_4^Z , $\tilde{\kappa}_Z$ and $\tilde{\lambda}_Z$ at the LHC, and the corresponding precision reachable on the non-linear operator coefficients	35
3.1	The magic numbers for $\Delta C_{7\gamma}(\mu_b)$ defined in Eq. (3.28)	53
B.1	FCNC bounds [191] on the combination of the operator coefficients a_Z^d . . .	77

Introduction

The recent LHC discovery of a new scalar resonance [1, 2] and its experimental confirmation as a particle resembling the Higgs boson [3–5] have finally established the Standard Model (SM) as a successful and consistent framework of electroweak symmetry breaking (EWSB). Even so, the hierarchy problem, related with the stabilization of the Higgs mass against larger physics scales which may communicate with the Higgs properties via radiative loop corrections, is still pending to be solved. Indeed, no new particles -which could indicate beyond the Standard Model (BSM) physics curing the problem- have been detected so far. Many models attempting to palliate the electroweak hierarchy problem have appeared in the last decades, such as the Minimal Supersymmetric extension of the SM (MSSM) [6–8] and several other BSM scenarios, playing a role at the TeV-scale.

The way in which the Higgs particle participates in the EWSB mechanism determines different BSM scenarios. In one class of models, the Higgs is introduced as an elementary scalar doublet transforming linearly under the SM gauge group $SU(2)_L \times U(1)_Y$. An alternative is to postulate its nature as emerging from a given strong dynamics sector at the TeV or slightly higher scale, in which the Higgs participates either as an EW doublet or as a member of other representations: a singlet in all generality. Both cases call for new physics (NP) around the TeV scale, but concrete BSM models of the former type (EWSB linear realisations) tend to propose the existence of lighter exotic resonances which have failed to show up in data so far.

The alternative case mentioned assumes a non-perturbative Higgs dynamics associated to a strong interacting sector at Λ_s -scale, with a explicitly non-linear implementation of the symmetry in the scalar sector. These strong dynamics frameworks all share a reminiscence of the long ago proposed “Technicolor” formalism [9–11], in which no Higgs particle was proposed in the low-energy physical spectrum and only three would-be-Goldstone bosons were present with an associated scale f identified with the electroweak scale $f = v \equiv 246$ GeV (respecting $f \geq \Lambda_s/4\pi$ [12]), and responsible a posteriori for the weak gauge boson masses. The experimental discovery of a light Higgs boson, not accompanied of extra resonances, has led to a revival of a variant of that idea: that the Higgs

particle h may be light because being itself a Goldstone boson resulting from the spontaneous breaking of a strong dynamics with symmetry group G at the scale Λ_s [13–18]. A subsequent source of explicit breaking of G would allow the Higgs boson to pick a small mass, much as the pion gets a mass in QCD, and develops a potential with a non-trivial minimum $\langle h \rangle$. Only via this explicit breaking would the EW gauge symmetry be broken and the electroweak scale v -defined from the W mass- be generated, distinct from f . Three scales enter thus in the game now: f , v and $\langle h \rangle$, although a model-dependent constraint will link them. The strength of non-linearity is quantified by a new parameter

$$\xi \equiv \frac{v^2}{f^2}, \quad (1)$$

such that, $f \sim v$ ($\xi \sim 1$) characterizes non-linear constructions, whilst $f \gg v$ ($\xi \ll 1$) labels regimes approaching the linear one. As a result, for non-negligible ξ there may be corrections to the size of the SM couplings observable at low energies due to new physics (NP) contributions.

A systematic and model-independent procedure to account for those corrections is their encoding via an Effective Field Theory (EFT) approach. The idea is to employ a non-linear σ model to account for the strong dynamics giving rise to the Goldstone bosons, that is the W^\pm and Z longitudinal components, and a posteriori to couple this effective Lagrangian to a scalar singlet h in a general way. In a given model, relations between the coefficients of the most general set of operators will hold, remnant of the initial EW doublet or other nature of the Higgs particle. But in the absence of an established model, it is worth to explore the most general Lagrangian, which may even account for scenarios other than those discussed above, for instance that in which the Higgs may be an “impostor” not related to EW symmetry breaking, such as a dark sector scalar, and other scenarios as for instance the presence of a dilaton. We will thus try to construct here the most general electroweak effective non-linear Lagrangian (often referred to also as “chiral” Lagrangian) in the presence of a light scalar h , restricted to the bosonic sector.

A very general characteristic differentiating linear from non-linear effective expansions goes as follows. In the SM and in BSM realizations of EWSB the EW scale v and the h particle enter in the Lagrangian in the form of polynomial dependences on $(h + v)$, with h denoting here the physical Higgs particle. In chiral realisations instead, that simple functional form changes and will be encoded by generic functionals $\mathcal{F}(h)$. To parametrize them, it may be useful a representation of the form [19]

$$\mathcal{F}(h) = g_0(h, v) + \xi g_1(h, v) + \xi^2 g_2(h, v) + \dots \quad (2)$$

where $g(h, v)$ are model-dependent functions of h and of v , once $\langle h \rangle$ is expressed in terms of ξ and v . Furthermore, for a generic h singlet, the number of independent operators

constituting a complete basis will be larger than that for linear realizations of EWSB, and also larger than that for the EW non-linear Lagrangian constructed long ago in the absence of a light scalar particle (the so-called Applequist-Longhitano-Feruglio effective Lagrangian [21–25]), entailing as a consequence a richer phenomenology.

The EFT developed here should provide the most general model-independent description of bosonic interactions in the presence of a light Higgs particle h : pure gauge, gauge- h and pure h couplings, up to four derivatives in the chiral expansion [19, 20]. We identified first [19] the tower of independent operators invariant under the simultaneous action of charge conjugation (C) and parity (P) transformations (named as CP-conserving or CP-even); next, the bosonic tower of CP-odd operators has also been determined [20].

While some of the operators in our CP-even and CP-odd bases had been individually identified in recent years in Refs. [26–29], the present analysis is the first determination of the complete set of independent bosonic operators and their impact. Some of the bosonic operators discussed in Chapter 2 had not been explored in previous literature on non-linear effective Lagrangians, but traded instead by fermionic ones via the equations of motion [30]. It is very interesting to identify and analyse the complete set of independent bosonic operators, though, both from the theoretical and from the phenomenological point of view. Theoretically, because they may shed a direct light on the nature of EWSB, which takes place precisely in the bosonic sector. Phenomenologically, because given the present and future LHC data, increasingly rich and precise constraints on gauge and gauge-Higgs couplings are becoming available, up to the point of becoming increasingly competitive with fermionic bounds in constraining BSM theories. This fact may be further strengthened with the post-LHC facilities presently under discussion.

One of the phenomenological explorations of CP-violation contained in this work deals with the differential features expected in the leading anomalous couplings and signals of non-linear realisations of EWSB versus linear ones. Phenomenological constraints resulting from limits on electric dipole moments (EDMs) and from present LHC data will be derived, and future prospects briefly discussed. We will go beyond interesting past and new proposals to search for Higgs boson CP-odd anomalous couplings to fermions and gauge bosons [31–67], which rank from purely phenomenological analysis to the identification of expected effective signals assuming either a linear or a non-linear realisation of EWSB.

Another aspect explored in this work is that of BSM flavour physics in the context of the EW chiral Lagrangian with a light Higgs particle h . While we will not attempt to derive in this case a complete fermionic and bosonic EFT basis, some salient features will be explored. This will be implemented in the framework of a very predictive and promising flavour tool: the so called Minimal Flavour Violation hypothesis (MFV) [69–71], based

on promoting the Yukawa couplings to *spurions* transforming under the global flavour symmetry that the SM exhibits in the limit of massless fermions (we restrict to the quark sector here): $G_f = SU(3)_{Q_L} \times SU(3)_{U_R} \times SU(3)_{D_R}$. In this setup, each operator is weighted by a coefficient made out of Yukawa couplings so as to make each term in the EFT Lagrangian G_f -invariant; those weights will for instance govern and maintain under safe control all the Flavour Changing Neutral Currents processes (FCNC). As a result, the low-energy predictions turn out to be suppressed by Yukawa couplings, i.e. by the observed quark masses and small mixing angles. Indeed, what data are telling us is that whatever is the BSM theory of flavour it should align at low-energies with SM predictions, in other words, with all flavour-changing effects resulting from the SM sources. The only source of flavour in the SM are Yukawa couplings and the MFV construction ensures precisely that Yukawa coupling are the only low-energy messengers of BSM flavour physics.

The content of this manuscript is organized as follows: Chapter 1 contains a brief SM description, followed by an also brief non-linear sigma model presentation and of the MFV ansatz. Chapter 2 develops the EFT approach for the EW chiral Lagrangian in the presence of a light scalar h . The corresponding complete basis of CP-even and CP-odd effective operators in the non-linear regime for the pure gauge, gauge- h and pure h sectors are listed in there¹. Phenomenological bounds on CP-odd couplings resulting from EDMs limits and from present LHC data are derived as well in Chapter 2. Chapter 3 is dedicated to flavour effects, and therefore, to the inclusion of the fermion-gauge and fermion-gauge- h sectors, within the assumed chiral EFT framework and the MFV ansatz. Finally, Chapter 4 summarizes the main results. Complementary tools and results are given in the appendices.

¹The $\mathcal{F}_i(h)$ functions will be restricted to CP-even ones, though.

Introducción

El reciente descubrimiento de una nueva resonancia de tipo escalar en el LHC [1, 2] y su confirmación experimental e identificación con el bosón de Higgs [3–5], han establecido finalmente al Modelo Estándar (ME) como marco consistente de rotura de la simetría electrodébil (RSE). Aun así, el problema de la jeraquía, relacionado con la estabilización de la masa del Higgs frente a mayores escalas de física que pueden comunicarse con las propiedades del Higgs vía correcciones radiativas, sigue sin ser resuelto. De hecho, nuevo contenido de partículas -el cual podría indicar física más allá del Modelo Estándar (MME) que cure el problema- no ha sido detectado hasta ahora. Muchos modelos que intentan resolver tal problema han aparecido en las últimas décadas, tales como la extensión Mínima Supersimétrica del Modelo Estándar (MSME) [6–8] y diversos modelos de MME a la escala del TeV.

La manera en que el bosón de Higgs participa del RSE determina dos escenarios diferentes. En un tipo de modelos, el Higgs es introducido como doblete escalar elemental que transforma linealmente bajo el grupo gauge $SU(2)_L \times U(1)_Y$ del ME. Una alternativa es postular su naturaleza como emergente de un sector dinámico fuerte a la escala del TeV o ligeramente mayor, en el cual el Higgs participa ya sea como un doblete electrodébil o como parte de otras representaciones: un singlete en toda generalidad. Ambos casos requieren de nueva física (NF) cerca de la escala del TeV, pero modelos concretos de MME del primer tipo (realizaciones lineales de RSE) tienden a proponer la existencia de resonancias exóticas livianas las cuales no han aparecido en los datos experimentales hasta ahora.

El caso alternativo asume una dinámica no-perturbativa del Higgs asociada al sector fuertemente interactuante a una escala Λ_s , con una implementación explícita de la simetría no-lineal en el sector escalar. Estos escenarios de dinámica fuerte comparten todos una reminiscencia del antiguo formalismo de “Technicolor” [9–11], sin partícula de Higgs en el espectro físico de bajas energías y solo tres bosones de Goldstone estando presentes con una escala asociada f identificada con la escala electrodébil (EE), $f = v \equiv 246$ GeV (con $f \geq \Lambda_s/4\pi$ [12]) y responsable a posteriori de la masas de los bosones de gauge. El

descubrimiento experimental de bosón de Higgs liviano, no acompañado de resonancias extra, ha llevado a un resurgimiento de una variante de esa idea: que la partícula de Higgs h puede ser liviana siendo así misma un bosón de Goldstone resultante del rompimiento espontáneo de una dinámica fuerte con grupo de simetría G a la escala Λ_s [13–18]. Una fuente subsecuente de rompimiento explícito de G permitiría al bosón de Higgs obtener su masa pequeña, así como el pión obtiene su masa en QCD, y desarrollar un potencial con un mínimo no trivial $\langle h \rangle$. Sólo mediante este rompimiento espontáneo la simetría de gauge electrodébil sería rota y la EE v -definida por la masa del bosón de gauge W - sería generada y distinta de la escala f . Tres escalas entran en el juego ahora: f , v y $\langle h \rangle$, y estarán vinculadas entre ellas mediante alguna relación dependiente del modelo. La no-linealidad del modelo está cuantificada por el nuevo parámetro

$$\xi \equiv \frac{v^2}{f^2}, \quad (3)$$

tal que $f \sim v$ ($\xi \sim 1$) caracteriza escenarios no-lineales, mientras que $f \gg v$ ($\xi \ll 1$) distingue a escenarios de régimen lineal. Como resultado, para valores no despreciables de ξ pueden haber correcciones al tamaño de los acoplos del ME debido a nuevas contribuciones de NF.

Un procedimiento sistemático para explicar esas correcciones consiste en codificarlas vía una Teoría Efectiva de Campos (TEC). La idea es emplear un modelo σ no-lineal para dar cuenta de la dinámica fuerte que da lugar a los bosones de Goldstone, que son las componentes longitudinales de los bosones de gauge W^\pm y Z , y acoplar a posteriori este Lagrangiano efectivo a un singlete escalar h del modo más general posible. En un modelo dado, se tendrán relaciones entre los coeficientes del conjunto más general de operadores, remanentes de un doblete electrodébil inicial o de otra naturaleza de la partícula de Higgs. Pero en ausencia de un modelo establecido como tal, vale la pena explorar el Lagrangiano más general, el cual puede dar cuenta de escenarios distintos a los descritos anteriormente, por ejemplo en los cuales el Higgs pueda ser un “impostor” no relacionado con la RSE, tal como un sector escalar oscuro, y otros escenarios que incluyan la presencia de un dilatón. Intentaremos construir aquí el Lagrangiano efectivo no-lineal más general (a menudo llamado Lagrangiano “quiral”) en presencia de un escalar liviano h , restringido al sector bosónico.

Una característica muy general que distingue expansiones efectivas lineales de no-lineales va como sigue. En el ME y en realizaciones MME de RSE, la EE v y la partícula h entran en el Lagrangiano en la forma de dependencias polinomiales en $(h + v)$, con h denotando la partícula de Higgs física. En realizaciones quirales, esa simple forma funcional cambia y será codificada mediante funcionales genéricas $\mathcal{F}(h)$. Para parametrizarlas,

puede ser útil una representación de la forma [19]

$$\mathcal{F}(h) = g_0(h, v) + \xi g_1(h, v) + \xi^2 g_2(h, v) + \dots \quad (4)$$

con $g(h, v)$ funciones de h y v , dependientes del modelo, una vez que $\langle h \rangle$ es expresada en términos de ξ and v . Además, para un singlete h genérico, el número de operadores independientes que constituye una base completa será mayor que para las realizaciones lineales de RSE, y también mayor que para los Lagrangianos electrodébiles no-lineales construidos años atrás en ausencia de una partícula escalar liviana (el llamado Lagrangiano efectivo de Applequist-Longhitano-Feruglio [21–25]), conllevando como consecuencia una fenomenología más rica.

La TEC aquí desarrollada debería proporcionar la descripción más general independiente del modelo de las interacciones bosónicas en presencia de una partícula de Higgs liviana h : puramente gauge, gauge- h y acoplos puramente h , hasta cuatro derivadas en la expansión quiral [19, 20]. Hemos identificado primeramente [19] la torre de operadores independientes invariantes bajo la acción simultánea de transformaciones de carga (C) y paridad (P) (denominados operadores que conservan CP); la torre bosónica de operadores que violan la simetría CP también ha sido determinada [20].

Mientras algunos de los operadores que conservan y violan CP han sido individualmente identificados en años recientes en las Refs. [26–29], el análisis presente es la primera determinación del conjunto completo de operadores independientes bosónicos y de su impacto. Algunos de los operadores bosónicos discutidos en el Capítulo 2 no habían sido explorados en literatura previa de Lagrangianos efectivos no-lineales, pero sí reemplazados por operadores fermiónicos vía ecuaciones de movimiento [30]. Es muy interesante identificar y analizar el conjunto completo de operadores bosónicos, desde el punto de vista teórico y fenomenológico. Teóricamente, porque pueden arrojar alguna luz en la naturaleza de la RSE, la cual tiene lugar justamente en el sector bosónico. Fenomenológicamente, porque dado el potencial de los datos presentes y futuros del LHC, cotas más precisas en acoplos gauge y gauge-Higgs son disponibles, llegando a ser competitivas con límites fermiónicos que acotan teorías MME. Característica ésta que puede ser fortalecida con las facilidades del LHC a futuro.

Una de las exploraciones fenomenológicas de violación de CP contenidas en éste trabajo trata con las características diferenciales esperadas en acoplos anómalos y señales de realizaciones no-lineales de la RSE versus realizaciones lineales. Cotas fenomenológicas de límites de momentos dipolares eléctricos (MDEs) y de datos presentes del LHC son derivadas a posteriori, y futuras perspectivas son brevemente discutidas. En este trabajo iremos más allá de las interesantes propuestas pasadas y actuales para buscar acoplos anómalos que violan CP a los fermiones y bosones de gauge [31–67], los cuales van desde

análisis puramente fenomenológicos a identificación de señales efectivas asumiendo ya bien sean realizaciones lineales o no-lineales de la RSE.

Otro aspecto explorado en este trabajo es de física de sabor MME en el contexto de Lagrangianos quirales electrodébiles con un Higgs liviano h . Si bien no vamos a intentar derivar en este caso una completa base de TEC fermiónica y bosónica, algunas características serán exploradas. Esto será implementado es un escenario de una herramienta de sabor muy predictivo y prometedor: la llamada hipótesis de Violación Mínima de Sabor (VMS) [69–71], basada en acoplos de Yukawa propuestos como *espuriones* transformando bajo la simetría global que el ME exhibe en el límite de fermiones no masivos (restringimos aquí al sector de quarks): $G_f = SU(3)_{Q_L} \times SU(3)_{U_R} \times SU(3)_{D_R}$. En este escenario, cada operador es sopesado por un coeficiente construido a base de acoplos de Yukawa con el fin de hacer cada término en el Lagrangiano de TEC invariante bajo G_f ; dichos coeficientes gobernarán y mantendrán bajo control, por ejemplo, todos los procesos de corrientes neutras que cambian el sabor (CNCS). Como resultado, las predicciones de bajas energías resultan estar suprimidas por la dependencia en acoplos de Yukawa, es decir masas de quarks y ángulos de mezcla. Ciertamente, lo que los datos experimentales nos dicen es que cualquiera sea la teoría MME de sabor, ella debe alinearse a bajas energías con las predicciones del ME, en otras palabras, con todos los efectos que cambian sabor y que resultan de las fuentes de ME. La única fuente de sabor en el ME son los acoplos de Yukawa, y la hipótesis de VMS asegura precisamente que los acoplos de Yukawa sean los únicos mensajeros a bajas energías de física de sabor MME.

El contenido de éste manuscrito está organizado como sigue: Capítulo 1 contiene una breve descripción de las principales características del ME, seguida por una breve presentación del modelo σ no-lineal y de la hipótesis de VMS. El Capítulo 2 desarrolla el escenario de TEC para el Lagrangiano quiral electrodébil en presencia de un escalar liviano h . La base completa de operadores no-lineales efectivos que conservan y violan la simetría CP en el sector gauge y gauge- h es igualmente listada en dicho capítulo ². Cotas fenomenológicas en acoplos que violan CP y provenientes de límites de MDEs y de datos del LHC son presentados en el Capítulo 2. El Capítulo 3 es dedicado a efectos de sabor, y por consiguiente, a la inclusión de los sectores fermion-gauge y fermion-gauge- h , dentro del marco quiral de TEC y la hipótesis de VMS asumidos. Finalmente, el Capítulo 5, resume los principales resultados de este trabajo. Resultados y herramientas complementarias son dados en los apéndices.

²Las funciones $\mathcal{F}_i(h)$ serán restringidas funciones que conservan CP.

Chapter 1

Standard Model interactions

The known physical interactions playing a role in nature are described by the following forces: electromagnetic, weak, strong and gravitational. The first three form part of the so called *Standard Model* of particle physics (SM), a local invariant gauge theory built upon the group $SU(3)_c \times SU(2)_L \times U(1)_Y$, with $SU(3)_c$ the color group for the Chromodynamics theory [72–74], and $SU(2)_L \times U(1)_Y$ the electroweak group unifying in a single picture electromagnetic and weak interactions, the so called Electroweak theory (EW) [75–77]. Gravitation remains to be properly incorporated in the SM framework as no viable and convincing quantum picture for it has emerged so far. The SM lagrangian density is written as

$$\mathcal{L}_{\text{SM}} = \mathcal{L}_{\text{QCD}} + \mathcal{L}_{\text{EW}} + \mathcal{L}_{\text{Scalar}} + \mathcal{L}_{\text{Yukawa}} , \quad (1.1)$$

where the QCD and EW sectors are described by

$$\begin{aligned} \mathcal{L}_{\text{QCD}} + \mathcal{L}_{\text{EW}} = & -\frac{1}{4} G_{\mu\nu}^a G_a^{\mu\nu} - \frac{1}{4} W_{\mu\nu}^i W_i^{\mu\nu} - \frac{1}{4} B_{\mu\nu} B^{\mu\nu} + \\ & + i \bar{Q}_L \not{D} Q_L + i \bar{u}_R \not{D} u_R + i \bar{d}_R \not{D} d_R + i \bar{L} \not{D} L + i \bar{e}_R \not{D} e_R , \end{aligned} \quad (1.2)$$

the first line accounting for the strength of the gauge kinetic tensor

$$\begin{aligned} G_{\mu\nu}^a &= \partial_\mu G_\nu^a - \partial_\nu G_\mu^a - g_s f^{abc} G_\mu^b G_\nu^c , \\ W_{\mu\nu}^i &= \partial_\mu W_\nu^i - \partial_\nu W_\mu^i - i g \epsilon^{ijk} W_\mu^j W_\nu^k , \\ B_{\mu\nu} &= \partial_\mu B_\nu - \partial_\nu B_\mu , \end{aligned} \quad (1.3)$$

the second one for the lepton and quark kinetic terms with

$$D_\mu = \partial_\mu + i \frac{g_s}{2} G_\mu^a \lambda^a + i \frac{g}{2} W_\mu^i \tau_i + i g' Y B_\mu \quad (1.4)$$

covariant derivative with λ^a Gell-Mann and τ_i Pauli matrices acting on $SU(3)_c$ color and $SU(2)_L$ indices respectively, Y the corresponding $U(1)_Y$ hypercharge quantum number assigned from $Q_\psi = T_{3,\psi} + Y_\psi$, where ψ covers the left handed lepton and quark doublets $L^T = (\nu_L, e_L)$ and $Q^T = (u_L, d_L)$ respectively, as well as the right handed electron and quark fields e_R , u_R and d_R , respectively. The coupling constants g_s , g and g' correspond to each symmetry group respectively, and color and flavour indices are omitted. The SM interactions of the gauge and fermion fields are normalized in Tables 1.1 and 1.2.

Matter field	$SU(3)_c$	$T_3 [SU(2)_L]$	$Y [U(1)_Y]$
$\begin{pmatrix} u_L \\ d_L \end{pmatrix}$	3 3	$+\frac{1}{2}$ $-\frac{1}{2}$	$+\frac{1}{6}$ $+\frac{1}{6}$
u_R	3	0	$+\frac{2}{3}$
d_R	3	0	$-\frac{1}{3}$
<hr/>			
$\begin{pmatrix} \nu_L \\ e_L \end{pmatrix}$	1 1	$+\frac{1}{2}$ $-\frac{1}{2}$	$-\frac{1}{2}$ $-\frac{1}{2}$
e_R	1	0	-1

Table 1.1: SM fermion field content and their quantum numbers.

Interaction	Gauge group	Gauge field	$SU(3)_c$	$SU(2)_L$	$Y [U(1)_Y]$
Strong	$SU(3)_c$	G_μ^a	8	1	0
Weak	$SU(2)_L$	W_μ^a	1	3	0
Hypercharge	$U(1)_Y$	B_μ	1	1	0

Table 1.2: SM interactions and their gauge field content (before EWSB) and quantum numbers.

1.1 EWSB in the SM

The scalar sector in (1.1), represented by the $SU(3)_c$ color singlet $SU(2)_L$ doublet field Φ , defined as

$$\Phi(x) = \begin{pmatrix} \Phi^+ \\ \Phi^0 \end{pmatrix} = \frac{1}{\sqrt{2}} \begin{pmatrix} \phi_1(x) - i\phi_2(x) \\ h(x) + i\phi_3(x) \end{pmatrix}, \quad (1.5)$$

and its covariant derivative as

$$D_\mu \Phi = \left(\partial_\mu + i \frac{g}{2} W_\mu^i \tau_i + i \frac{g'}{2} B_\mu \right) \Phi, \quad (1.6)$$

has a corresponding lagrangian

$$\mathcal{L}_{Scalar} = (D_\mu \Phi)^\dagger (D^\mu \Phi) - V(\Phi), \quad (1.7)$$

$$V(\Phi) = \mu^2 \Phi^\dagger \Phi + \lambda (\Phi^\dagger \Phi)^2, \quad (1.8)$$

where \mathcal{L}_{Scalar} is invariant under $SU(3)_c \times SU(2)_L \times U(1)_Y$. Necessarily λ is positive to have a stable potential and, as soon as the potential gets minimized by the conditions $\mu^2 < 0$ and $\lambda > 0$ at the vacuum expectation value (VEV)

$$\langle \Phi^\dagger \Phi \rangle = v^2 = -\frac{\mu^2}{2\lambda} \quad (1.9)$$

the ground state will lose the SM invariance, keeping just the electromagnetic $U(1)_{em}$ invariance, and triggering thus EWSB. In polar coordinates, Φ can be written as

$$\Phi(x) = \frac{1}{\sqrt{2}} \exp \left[i \frac{\tau \cdot \pi(x)}{2v} \right] \begin{pmatrix} 0 \\ v + h(x) \end{pmatrix}, \quad (1.10)$$

and reabsorbing the triplet of Goldstone bosons, $\pi = (\pi^1, \pi^2, \pi^3)$, by $SU(2)_L$ -rotations (i.e. going to the unitary gauge)

$$\Phi(x) \implies \frac{1}{\sqrt{2}} \begin{pmatrix} 0 \\ v + h(x) \end{pmatrix} \quad (1.11)$$

the scalar kinetic term will reduce to

$$(D_\mu \Phi)^\dagger (D^\mu \Phi) = \frac{1}{2} (\partial_\mu h)^2 + M_W^2 W_\mu^+ W^{-\mu} \left(1 + \frac{h}{v} \right)^2 + \frac{1}{2} M_Z^2 Z_\mu^2 \left(1 + \frac{h}{v} \right)^2, \quad (1.12)$$

with W_μ^\pm and Z_μ fields defined as

$$W_\mu^\pm = \frac{1}{\sqrt{2}} (W_\mu^1 \mp i W_\mu^2), \quad \begin{pmatrix} Z_\mu \\ A_\mu \end{pmatrix} = \begin{pmatrix} c_W & -s_W \\ s_W & c_W \end{pmatrix} \begin{pmatrix} W_\mu^3 \\ B_\mu \end{pmatrix}, \quad (1.13)$$

and the parameters and masses

$$s_W = \sin \theta_W = \frac{g'}{\sqrt{g^2 + g'^2}}, \quad c_W = \cos \theta_W = \frac{g}{\sqrt{g^2 + g'^2}}, \quad (1.14)$$

$$M_W = \frac{1}{2} g v, \quad M_Z = \frac{g v}{2 \cos \theta_W}. \quad (1.15)$$

Also from the scalar potential one obtains

$$M_h^2 = 2 \lambda v^2 = -2 \mu^2. \quad (1.16)$$

The Lagrangian term in Eq. (1.12), exhibits SM interactions coupled to the light Higgs h , up to quadratic powers. Later on, when dealing with a non-linear EFT approach, this interaction will be considered in a more general manner by incorporating a generic h dependence, including higher powers of h . This will be implemented not only for the corresponding non-linear kinetic term, but also extended to any effective operator in the approach.

Finally, fermion masses can be accounted via EWSB through the Yukawa interactions, they are described in the next section as well as the SM flavour dynamics stemming from the Yukawa interactions.

1.2 SM flavour structure

Quarks and charged leptons become massive via gauge invariant Yukawa coupled to the SM Higgs doublet as

$$\mathcal{L}_{\text{Yukawa}} = \overline{Q}_L Y^u \tilde{\Phi} u_R + \overline{Q}_L Y^d \Phi d_R + \bar{L} Y^e \Phi e_R + \text{h.c.}, \quad \tilde{\Phi} = i \tau_2 \Phi^*, \quad (1.17)$$

with Y^u , Y^d and Y^e denoting Yukawa coupling matrices. Triggering EWSB via the Higgs field VEV value v , the Yukawa interactions in Eq. (1.17) result in quark and charged lepton mass matrices

$$M_u = Y^u \frac{v}{\sqrt{2}}, \quad M_d = Y^d \frac{v}{\sqrt{2}}, \quad M_e = Y^e \frac{v}{\sqrt{2}}, \quad (1.18)$$

with $v = \langle \Phi \rangle \simeq 246$ GeV. The mass matrices can be diagonalized by rewriting the quark flavour states (u', d') to the mass eigenstates (u, d) ,

$$\begin{aligned} u_L &= V_{u_L} u'_L, & u_R &= V_{u_R} u'_R, \\ d_L &= V_{d_L} d'_L, & d_R &= V_{d_R} d'_R, \end{aligned} \quad (1.19)$$

with V being unitary such that

$$V_{u_L}^T M_u V_{u_R} = \text{diag}(m_u, m_c, m_t), \quad V_{d_L}^T M_d V_{d_R} = \text{diag}(m_d, m_s, m_b). \quad (1.20)$$

Masses matrices $M_{u,d}$ are simultaneously diagonalized, remaining therefore no SM flavor changing neutral Higgs-mediated current at tree level. Electromagnetic and neutral EW-currents are also diagonal in the mass basis, e.g., $\bar{u}'_L \gamma_\mu u'_L Z^\mu \Rightarrow \bar{u}_L \gamma_\mu u_L Z^\mu$, and thus no flavor changing neutral Z^0 - γ currents (FCNC) in the SM.

The charged current sector (CC) behaves differently, as they involve, in the mass basis, two different unitary matrices: those from the up and down sectors respectively, and being misaligned in the flavour space in general

$$\mathcal{L}_{\text{CC}} = \frac{g}{\sqrt{2}} W_\mu^+ \bar{u}'_L \gamma^\mu d'_L \Rightarrow \frac{g}{\sqrt{2}} W_\mu^+ \bar{u}_L \gamma^\mu V d_L, \quad V = V_{u_L}^\dagger V_{d_L} = \begin{pmatrix} V_{ud} & V_{us} & V_{ub} \\ V_{cd} & V_{cs} & V_{cb} \\ V_{td} & V_{ts} & V_{tb} \end{pmatrix}, \quad (1.21)$$

with $V = V_{u_L}^\dagger V_{d_L}$ Cabibbo-Kobayashi-Maskawa (CKM) matrix [78, 79]. Flavour changing current processes thus appear in the SM charged current sector.

Neutrino masses lead to an analogous situation in the mass basis

$$\mathcal{L}_{\text{CC}} = \frac{g}{\sqrt{2}} W_\mu^+ \bar{\nu}'_L \gamma^\mu e'_L \Rightarrow \frac{g}{\sqrt{2}} W_\mu^+ \bar{\nu}_L \gamma^\mu U e_L, \quad U = V_\nu^\dagger V_{e_L} = \begin{pmatrix} U_{e1} & U_{e2} & U_{e3} \\ U_{\mu 1} & U_{\mu 2} & U_{\mu 3} \\ U_{\tau 1} & U_{\tau 2} & U_{\tau 3} \end{pmatrix}, \quad (1.22)$$

with $U = V_\nu^\dagger V_{e_L}$ being the Pontecorvo-Maki-Nakagawa-Sakata (PMNS) matrix describing flavour mixing for the lepton sector [80, 81]. Massless neutrinos as in the SM allow us to choose $V_\nu = V_{e_L}$ such that $U = \mathbb{I}_{3 \times 3}$. Nonetheless, BSM extensions with massive neutrinos require a non-trivial U . Note that for the Majorana neutrino case U contains a priori two

physical phases more than the CKM matrix for quarks, which are Dirac fermions. In fact for the Majorana neutrino case, U can be written in the standard parametrization as

$$U = \begin{pmatrix} c_{12}c_{13} & s_{12}c_{13} & s_{13}e^{-i\delta} \\ -s_{12}c_{23} - c_{12}s_{23}s_{13}e^{i\delta} & c_{12}c_{23} - s_{12}s_{23}s_{13}e^{i\delta} & s_{23}c_{13} \\ s_{12}s_{23} - c_{12}c_{23}s_{13}e^{i\delta} & -c_{12}s_{23} - s_{12}c_{23}s_{13}e^{i\delta} & c_{23}c_{13} \end{pmatrix} U_P \quad (1.23)$$

with $s_{ij} = \sin \theta_{ij}$, $c_{ij} = \cos \theta_{ij}$, and U_P the diagonal matrix $U_P = \text{diag}(e^{i\alpha_1/2}, e^{i\alpha_2/2}, m_t)$, where α_1 , α_2 and α_3 are the Majorana phases¹.

As a conclusion the diagonalization of the mass matrices leads to the quark mixing pattern and no Flavor Changing Neutral Currents (FCNC) at tree level in the SM. The same thing happens for the leptonic sector once neutrino masses are turned on.

Quark mixing matrix

Mixing between generations is explicitly manifested in the quark charged weak currents as seen in Eq. (1.21). Conventionally, the mixing may be described as assigned to the down quark sector as $d'_L = V d_L$, although what counts is the relative misalignment of the up and down quark sectors. The CKM matrix is unitary as it is the product of two unitary matrices. An $n \times n$ unitary matrix is described by n^2 real-valued parameters, $n(n-1)/2$ of them being real (angles) and $n(n+1)/2$ phases, all the latter with no physical meaning as $2n-1$ can be absorbed by quark rephasings. Indeed, for the n -family case, the $2n$ -rephasings $u_{L,\alpha} \rightarrow e^{i\theta_\alpha^u} u_{L,\alpha}$ and $d_{L,\alpha} \rightarrow e^{i\theta_\alpha^d} d_{L,\alpha}$, with $\alpha = 1, \dots, n$, lead the CKM-matrix element $V_{\alpha\beta}$ to $V_{\alpha\beta} \rightarrow V_{\alpha\beta} e^{i(\theta_\beta^d - \theta_\alpha^u)}$, and factorizing one phase as a global overall phase, it tends to $2n-1$ effective rephasings, and therefore $(n-1)(n-2)/2$. For the CKM matrix case, one has 3 mixing angles and 1 CP -violating phase, all that parametrized as [82]

$$V = \begin{pmatrix} c_{12}c_{13} & s_{12}c_{13} & s_{13}e^{-i\delta} \\ -s_{12}c_{23} - c_{12}s_{23}s_{13}e^{i\delta} & c_{12}c_{23} - s_{12}s_{23}s_{13}e^{i\delta} & s_{23}c_{13} \\ s_{12}s_{23} - c_{12}c_{23}s_{13}e^{i\delta} & -c_{12}s_{23} - s_{12}c_{23}s_{13}e^{i\delta} & c_{23}c_{13} \end{pmatrix}, \quad (1.24)$$

with $s_{ij} = \sin \theta_{ij}$, $c_{ij} = \cos \theta_{ij}$, and δ the phase, responsible for all the CP -violating phenomena in the SM flavour changing processes. Experimentally the mixing among quark families is small, with $s_{13} \ll s_{23} \ll s_{12} \ll 1$, and a convention may be introduced to account for this hierarchy, the so called Wolfenstein parametrization [83]

¹Only two relative phases, $\alpha_{21} \equiv \alpha_2 - \alpha_1$ and $\alpha_{31} \equiv \alpha_3 - \alpha_1$ are physical, the remaining one being absorbed by redefining the fields. For the Dirac neutrino case, such phases are also absorbable via field redefinitions of the right handed neutrinos.

$$s_{12} = \lambda = \frac{|V_{us}|}{\sqrt{|V_{us}|^2 + |V_{us}|^2}}, \quad s_{23} = A \lambda^2 = \lambda \left| \frac{V_{cb}}{V_{us}} \right|,$$

$$s_{13} e^{i\delta} = V_{ub}^* = A \lambda^3 (\rho + i \eta) = \frac{A \lambda^3 (\bar{\rho} + i \bar{\eta}) \sqrt{1 - A^2 \lambda^4}}{\sqrt{1 - \lambda^2} [1 - A^2 \lambda^4 (\bar{\rho} + i \bar{\eta})]}. \quad (1.25)$$

Written in terms of λ , A , $\bar{\rho}$ and $\bar{\eta}$, and expanded up to order $\mathcal{O}(\lambda^4)$ it reads:

$$V = \begin{pmatrix} 1 - \lambda^2/2 & \lambda & A \lambda^3 (\rho - i \eta) \\ -\lambda & 1 - \lambda^2/2 & A \lambda^2 \\ A \lambda^3 (1 - \rho - i \eta) & -A \lambda^2 & 1 \end{pmatrix} + \mathcal{O}(\lambda^4). \quad (1.26)$$

The unitarity of the CKM matrix imposes the relations

$$\sum_i V_{ij} V_{ik}^* = \delta_{jk}, \quad \sum_j V_{ij} V_{kj}^* = \delta_{ik}. \quad (1.27)$$

In consequence, six vanishing combinations are obtained, which can be represented as triangles in the complex plane, all of them with the same area. It is useful to define the Jarlskog invariant J , a phase convention-independent measure of CP -violation defined by

$$\text{Im} [V_{ij} V_{kl} V_{il}^* V_{kj}^*] = J \sum_{m,n} \epsilon_{ikm} \epsilon_{jln}. \quad (1.28)$$

A very useful unitary triangle results from the relation $V_{ud} V_{ub}^* + V_{cd} V_{cb}^* + V_{td} V_{tb}^* = 0$, normalized by the experimentally well determined product $V_{cd} V_{cb}^*$, and projected on the $\bar{\rho}$ - $\bar{\eta}$ plane. Such triangle is shown in Fig. 1.1, and the angles it gives rise to defined as

$$\begin{aligned} \alpha &= \arg \left(-\frac{V_{tb}^* V_{td}}{V_{ub}^* V_{ud}} \right), \\ \beta &= \arg \left(-\frac{V_{cb}^* V_{cd}}{V_{tb}^* V_{td}} \right), \\ \gamma &= \arg \left(-\frac{V_{ub}^* V_{ud}}{V_{cb}^* V_{cd}} \right). \end{aligned} \quad (1.29)$$

One of the aims of the ongoing research in flavour physics research intends to overconstrain the CKM elements, comparing many measurements.

In Chapter 3 slightly modifications are induced in the angles of the unitary triangle from the framework assumed there.

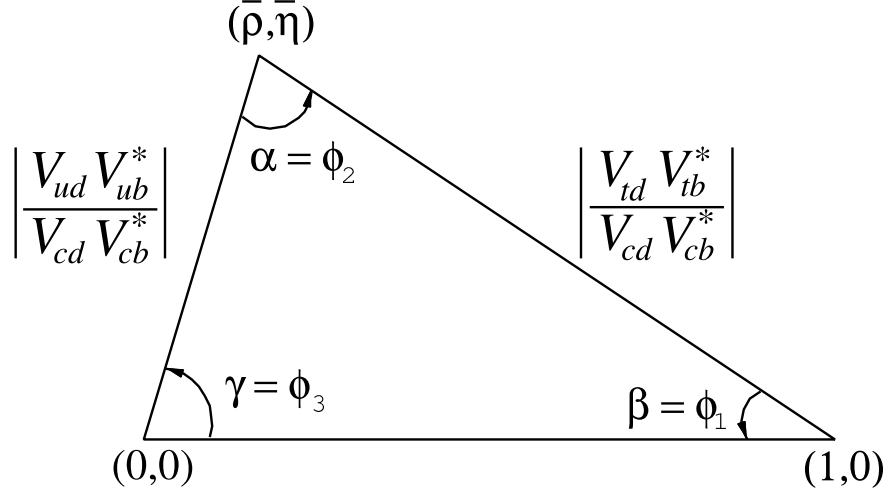


Figure 1.1: CKM unitary triangle.

1.3 Going beyond the Standard Model

For the sake of description, I will first discuss SM extensions in the linear EWSB context, i.e. with the explicit presence of a Higgs doublet properly transforming under the SM gauge group, and later on will focus on non-linear EWSB realizations.

The BSM signals can be tackled by assuming the existence of NP at some scale Λ above the electroweak one, i.e. $v \ll \Lambda$, and encoding NP interactions in a set of effective operators \mathcal{O}_i such that their Lagrangian will be

$$\delta\mathcal{L} = \sum_i \frac{c_i}{\Lambda^2} \mathcal{O}_i + \text{h.c.} + \dots, \quad (1.30)$$

where \mathcal{O}_i are generic gauge invariant effective operators of dimension six, emerging after integrating out new degrees of freedom at the scale Λ , scale that can be bounded by experimental constraints. Dots in Eq. (1.30) account for operators of dimension higher than six, in principle less relevant as they are suppressed by higher powers of the NP scale. Among these operators, we can have

- Pure gauge interactions

$$\mathcal{O}_W = \varepsilon^{ijk} W_\mu^{i\nu} W_\nu^{j\rho} W_\rho^{k\mu}, \quad \mathcal{O}_{\widetilde{W}} = \varepsilon^{ijk} \widetilde{W}_\mu^{i\nu} W_\nu^{j\rho} W_\rho^{k\mu}. \quad (1.31)$$

- Pure scalar interactions as

$$\mathcal{O}_\Phi = (\Phi^\dagger \Phi)^3, \quad \mathcal{O}_{\Phi \square} = (\Phi^\dagger \Phi) \square (\Phi^\dagger \Phi). \quad (1.32)$$

- Yukawa-like interactions coupled to Φ

$$\mathcal{O}_{\Phi u} = (\Phi^\dagger \Phi) (\bar{Q}_L \tilde{\Phi} u_R), \quad \mathcal{O}_{\Phi d} = (\Phi^\dagger \Phi) (\bar{Q}_L \Phi d_R). \quad (1.33)$$

- Gauge- Φ interactions

$$\mathcal{O}_{\Phi W} = \Phi^\dagger \Phi W_{\mu\nu}^i W^{i\mu\nu}, \quad \mathcal{O}_{\Phi B} = \Phi^\dagger \Phi B_{\mu\nu} B^{\mu\nu}, \quad \mathcal{O}_{\Phi WB} = \Phi^\dagger \tau^i \Phi W_{\mu\nu}^i B^{\mu\nu}, \quad (1.34)$$

$$\mathcal{O}_{\Phi \tilde{W}} = \Phi^\dagger \Phi \tilde{W}_{\mu\nu}^i W^{i\mu\nu}, \quad \mathcal{O}_{\Phi \tilde{B}} = \Phi^\dagger \Phi \tilde{B}_{\mu\nu} B^{\mu\nu}, \quad \mathcal{O}_{\Phi \tilde{W}B} = \Phi^\dagger \tau^i \Phi \tilde{W}_{\mu\nu}^i B^{\mu\nu}. \quad (1.35)$$

- Magnetic penguin-like operators

$$\mathcal{O}_{uW} = (\bar{Q}_L \sigma^{\mu\nu} u_R) \tau^i \tilde{\Phi} W_{\mu\nu}^i, \quad \mathcal{O}_{uB} = (\bar{Q}_L \sigma^{\mu\nu} u_R) \tilde{\Phi} B_{\mu\nu}, \quad (1.36)$$

$$\mathcal{O}_{dW} = (\bar{Q}_L \sigma^{\mu\nu} d_R) \tau^i \Phi W_{\mu\nu}^i, \quad \mathcal{O}_{dB} = (\bar{Q}_L \sigma^{\mu\nu} d_R) \Phi B_{\mu\nu}. \quad (1.37)$$

- Fermion vector currents coupled to scalar gauge currents

$$\mathcal{O}_{\Phi q}^{(1)} = (\Phi^\dagger i \overleftrightarrow{D}_\mu \Phi) (\bar{Q}_L \gamma^\mu Q_L), \quad \mathcal{O}_{\Phi u} = (\Phi^\dagger i \overleftrightarrow{D}_\mu \Phi) (\bar{u}_R \gamma^\mu u_R), \quad (1.38)$$

$$\mathcal{O}_{\Phi q}^{(3)} = (\Phi^\dagger i \overleftrightarrow{D}_\mu^j \Phi) (\bar{Q}_L \tau^j \gamma^\mu Q_L), \quad \mathcal{O}_{\Phi d} = (\Phi^\dagger i \overleftrightarrow{D}_\mu \Phi) (\bar{d}_R \gamma^\mu d_R). \quad (1.39)$$

Colour and generation indices are implicit. Operators containing gluon- Φ , gluon self-interactions, gluon magnetic penguin-like operators, as well as operators properly having lepton fields instead of quark fields (either left or right handed fields), are all them fully listed in Refs. [84, 85]. Four fermion operators are also included in those references, and summing up a total of 59 independent dimension-six operators, so long as B -conservation is imposed and finally reported in Refs. [85]. Many studies of the effective Lagrangian in Eq. (1.30) for the linear expansion have been carried out over the years, analysing its effects on Higgs production and decay [87, 88], with a revival of activity [89, 90] after the Higgs discovery [91, 92] (see also Refs. [64, 93–119] for studies of Higgs couplings in alternative and related frameworks).

Operator	Bounds on Λ in TeV		Bounds on c_{ij}		Observables
	Re	Im	Re	Im	
$(\bar{s}_L \gamma^\mu d_L)^2$	9.8×10^2	1.6×10^4	9.0×10^{-7}	3.4×10^{-9}	$\Delta m_K; \epsilon_K$
$(\bar{s}_R d_L)(\bar{s}_L d_R)$	1.8×10^4	3.2×10^5	6.9×10^{-9}	2.6×10^{-11}	$\Delta m_K; \epsilon_K$
$(\bar{c}_L \gamma^\mu u_L)^2$	1.2×10^3	2.9×10^3	5.6×10^{-7}	1.0×10^{-7}	$\Delta m_D; q/p , \phi_D$
$(\bar{c}_R u_L)(\bar{c}_L u_R)$	6.2×10^3	1.5×10^4	5.7×10^{-8}	1.1×10^{-8}	$\Delta m_D; q/p , \phi_D$
$(\bar{b}_L \gamma^\mu d_L)^2$	5.1×10^2	9.3×10^2	3.3×10^{-6}	1.0×10^{-6}	$\Delta m_{B_d}; S_{\psi K_S}$
$(\bar{b}_R d_L)(\bar{b}_L d_R)$	1.9×10^3	3.6×10^3	5.6×10^{-7}	1.7×10^{-7}	$\Delta m_{B_d}; S_{\psi K_S}$
$(\bar{b}_L \gamma^\mu s_L)^2$	1.1×10^2		7.6×10^{-5}		Δm_{B_s}
$(\bar{b}_R s_L)(\bar{b}_L s_R)$	3.7×10^2		1.3×10^{-5}		Δm_{B_s}

Table 1.3: Bounds on Λ assuming $c_{ij} = 1$, or alternatively, bounds on c_{ij} assuming $\Lambda = 1$ TeV (here the coefficient c_i in Eq. (1.30) has been replaced by c_{ij} as the corresponding operator implies two family indexes). Some operators $\Delta F = 2$ of dimension 6 has been used, and experimental bounds from the corresponding observables have been implemented. Table from Ref. [86].

Assuming now the adimensional coefficients c_i to be of order one, which is a reasonable assumption for generic new physics, the lower bounds for Λ can even reach the level of thousands of TeV, which would preclude any related observation in foreseen experiments. This is shown in Table 1.3, extracted from Ref. [86]. Notice that the lower limits on the scale Λ are in many cases of the order $\mathcal{O}(10^3 - 10^4)$ TeV, reaching 10^5 TeV in the case of the contribution of the operator $(\bar{s}_R d_L)(\bar{s}_L d_R)$ to the CP-violating parameter in neutral kaon decays ϵ_K (defined in Appendix C). This implies that, if some NP appears at a scale $\Lambda < 10^4$ TeV, then the flavour and CP structure of the NP theory has to be highly non trivial. One way-out would be to assume some hypothesis allowing us to write the effective Lagrangian as

$$\delta \mathcal{L} = \sum_i \frac{c_i}{\Lambda^2} \alpha_i \mathcal{O}_i + \text{h.c.}, \quad (1.40)$$

where α_i are small parameters controlled by some hypothesis, preferably a symmetry justifying such suppression, such that Λ could be lower and near the TeV region, if the Lagrangian in Eq. (1.40) is in agreement with all current data and with coefficients c_i of the order $\mathcal{O}(1)$.

Minimal Flavour Violation

The smallness of α_i could be caused by some flavour hypothesis, a flavour symmetry. The most popular attempt in this direction is the so called Minimal Flavour Violation hypothesis (MFV) [69–71], based on the flavour symmetry which the SM kinetic terms exhibit [120–127]

$$G_f = SU(3)_{Q_L} \times SU(3)_{U_R} \times SU(3)_{D_R} \quad (1.41)$$

with $SU(2)_L$ doublet Q_L and singlets U_R and D_R transforming under it as

$$Q_L \sim (3, 1, 1), \quad U_R \sim (1, 3, 1), \quad D_R \sim (1, 1, 3). \quad (1.42)$$

To recover G_f in the presence of Yukawa interactions, the MFV ansatz promotes Yukawa couplings to be *spurions* transforming under G_f as

$$Y_U \sim (3, \bar{3}, 1), \quad Y_D \sim (3, 1, \bar{3}). \quad (1.43)$$

Quark masses and mixings are correctly reproduced once these spurion fields get background values as

$$Y_U = V^\dagger \mathbf{y}_U, \quad Y_D = \mathbf{y}_D, \quad (1.44)$$

with $\mathbf{y}_{U,D}$ diagonal matrices whose elements are the Yukawa eigenvalues, and V a unitary matrix that in good approximation coincides with the CKM matrix. The flavour group G_f is broken by these background values, providing therefore contributions to FCNC observables suppressed by specific combinations of quark mass hierarchies and mixing angles. Indeed, a G_f -invariant coupling

$$\lambda_F \equiv Y_U Y_U^\dagger + Y_D Y_D^\dagger, \quad (1.45)$$

transforming as $(8, 1, 1)$ under G_f , will govern FCNC processes for 4-fermion operators by inserting it into the effective operators from the assumed EFT framework. As a nice feature, low-energy effects are suppressed by the quark masses and mixing angles encoded in λ_F , not contradicting therefore the FCNC experimental bounds. In this way, one obtains parameters α_i equal to some power of the CKM matrix elements (depending on the specific operator \mathcal{O}_i), in such a way that a scale $\Lambda \sim 10$ TeV can be allowed by all experimental data. This is illustrated in Table 1.4 from Ref. [71], where the complete basis of gauge-invariant 6-dimensional FCNC operators has been constructed for the case of a linearly realized SM Higgs sector, in terms of the SM fields and the Y_U and Y_D spurions. Operators of dimension $d > 6$ are usually neglected due to the additional suppression

Minimally flavour violating dimension six operator	main observables	Λ [TeV]	
		−	+
$\mathcal{O}_0 = \frac{1}{2}(\bar{Q}_L \lambda_{\text{FC}} \gamma_\mu Q_L)^2$	$\epsilon_K, \Delta m_{B_d}$	6.4	5.0
$\mathcal{O}_{F1} = H^\dagger (\bar{D}_R \lambda_d \lambda_{\text{FC}} \sigma_{\mu\nu} Q_L) F_{\mu\nu}$	$B \rightarrow X_s \gamma$	9.3	12.4
$\mathcal{O}_{G1} = H^\dagger (\bar{D}_R \lambda_d \lambda_{\text{FC}} \sigma_{\mu\nu} T^a Q_L) G_{\mu\nu}^a$	$B \rightarrow X_s \gamma$	2.6	3.5
$\mathcal{O}_{\ell 1} = (\bar{Q}_L \lambda_{\text{FC}} \gamma_\mu Q_L) (\bar{L}_L \gamma_\mu L_L)$	$B \rightarrow (X) \ell \bar{\ell}, K \rightarrow \pi \nu \bar{\nu}, (\pi) \ell \bar{\ell}$	3.1	2.7
$\mathcal{O}_{\ell 2} = (\bar{Q}_L \lambda_{\text{FC}} \gamma_\mu \tau^a Q_L) (\bar{L}_L \gamma_\mu \tau^a L_L)$	$B \rightarrow (X) \ell \bar{\ell}, K \rightarrow \pi \nu \bar{\nu}, (\pi) \ell \bar{\ell}$	3.4	3.0
$\mathcal{O}_{H1} = (\bar{Q}_L \lambda_{\text{FC}} \gamma_\mu Q_L) (H^\dagger i D_\mu H)$	$B \rightarrow (X) \ell \bar{\ell}, K \rightarrow \pi \nu \bar{\nu}, (\pi) \ell \bar{\ell}$	1.6	1.6
$\mathcal{O}_{q5} = (\bar{Q}_L \lambda_{\text{FC}} \gamma_\mu Q_L) (\bar{D}_R \gamma_\mu D_R)$	$B \rightarrow K \pi, \epsilon'/\epsilon, \dots$	~ 1	

Table 1.4: Bounds either on Λ or c_{ij} (again c_{ij} instead of c_i , as the implied operators have two family indexes) implementing MFV ansatz. Notice the TeV scales for Λ compared with those in Table 1.3. Table from Ref. [71].

in terms of the cut-off scale. NP may be also as low as few TeV in several distinct contexts [128–131].

As the non-linear EWSB setup is considered in this thesis work, the MFV ansatz has to be realized in such a context as well, and will be developed in Chapter 3, by including additionally the light Higgs particle contribution in the framework.

Chapter 2

Bosonic Chiral Lagrangian for a Light Dynamical “Higgs Particle”

If the EWSB is non-linear, the low energy effective Lagrangian can be parametrized via a chiral formalism. This leads to deal with a non-linear σ -model construction, useful to parametrize Goldstone field contributions. Additionally, realistic approaches have to account for a light Higgs particle, explaining thus gauge- h interactions and pure Higgs h -interactions. When building up the non-linear realization of the Goldstone boson mechanism implemented with a light Higgs, in general four scales may be relevant, Λ_s , f , $\langle h \rangle$ and v :

- i) Λ_s denotes the strong dynamics scale and the characteristic size of the heavy resonances (in the context of QCD, it corresponds to $\Lambda_{\chi SB}$, the scale of the chiral symmetry breaking [12]).
- ii) The Goldstone boson scale f , satisfying $\Lambda_s \leq 4\pi f$ (in the context of QCD, it corresponds to the pion coupling constant f_π).
- iii) $\langle h \rangle$ refers to the order parameter of EW symmetry breaking, around which the physical scalar h oscillates.
- iv) EW scale v , defined through $M_W = gv/2$.

Diagrammatically, these scales can be arranged as in Fig. 2.1. In a general model $\langle h \rangle \neq v$ and this leads to an $\langle h \rangle$ -dependence in the low-energy Lagrangian through a generic functional form $\mathcal{F}(h + \langle h \rangle)$. In non-linear realizations such as Technicolor-like models, it may happen that $\langle h \rangle = v = f$. In the setup considered here with a light h , they do not need to coincide, and typically a relation links v , $\langle h \rangle$ and f . Thus, a total of three scales

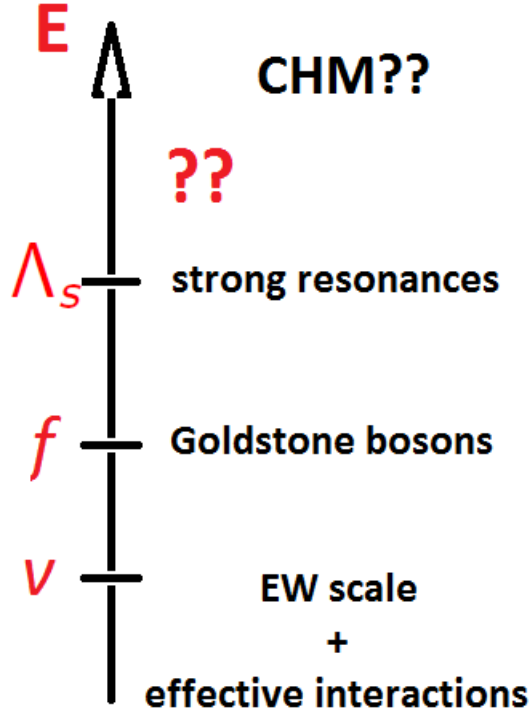


Figure 2.1: Hierarchy representation of the involved scales, where the arrow sense points towards higher energies and CHM stands for Composite Higgs Models.

will be useful in the analysis, for instance Λ_s , f and v . Indeed, the ratio of the two latter measures the strength of non-linearity and is quantified by a new parameter

$$\xi \equiv \frac{v^2}{f^2}, \quad (2.1)$$

such that ξ encodes the strength of the effects at the electroweak scale for theories which exhibit strong coupling at the new physics scale $\Lambda_s \leq 4\pi f$, and measuring thus the degree of non-linearity for the low-energy effective theory, with $f \gg v$ ($\xi \ll 1$) pointing towards linear regime, whereas $f \sim v$ ($\xi \sim 1$) to the non-linear ones.

2.1 The SM vs. σ -model parametrization

A hidden global symmetry is underlying the Lagrangians in Eq. (1.7) and (1.8). Instead of introducing the scalar fields as a complex doublet as in Eq. (1.5), an adimensional 2×2 matrix field can be used in order to highlight that symmetry

$$\mathbf{U}(x) = \frac{1}{v} [\sigma(x) + i \tau \cdot \pi(x)], \quad (2.2)$$

with $\sigma(x)$ being a scalar field and $\pi(x) = (\pi_1(x), \pi_2(x), \pi_3(x))$ the triplet of would-be Goldstone boson fields. $\mathbf{U}(x)$ can be linked to the doublet representation if the corresponding isospin 1/2 and hypercharge -1 field $\tilde{\Phi}$ is introduced, and the following correspondence is assumed, see Eq. (1.5)

$$(\pi_1(x), \pi_2(x), \pi_3(x)) = (-\phi_2(x), \phi_1(x), -\phi_3(x)) , \quad (2.3)$$

obtaining thus

$$\mathbf{U}(x) \equiv \frac{\sqrt{2}}{v} \begin{pmatrix} \tilde{\Phi}(x) & \Phi(x) \end{pmatrix} = \frac{\sqrt{2}}{v} \begin{pmatrix} \Phi^{0*}(x) & \Phi^+(x) \\ -\Phi^-(x) & \Phi^0(x) \end{pmatrix} . \quad (2.4)$$

Writing the scalar potential in Eq. (1.8) in terms of $\mathbf{U}(x)$

$$V(\mathbf{U}) = \frac{1}{4} \lambda \left[\frac{v^2}{2} \text{Tr}(\mathbf{U}^\dagger \mathbf{U}) + \frac{\mu^2}{\lambda} \right]^2 \quad (2.5)$$

emerges the aforementioned hidden global symmetry, $SU(2)_L \times SU(2)_R$ with $\mathbf{U}(x)$ transforming under it as

$$\mathbf{U} \rightarrow L \mathbf{U} R^\dagger , \quad L \equiv e^{i \epsilon_L \cdot \tau/2} , \quad R \equiv e^{i \epsilon_R \cdot \tau/2} \quad (2.6)$$

with the L and R global transformations $L \in SU(2)_L$ and $R \in SU(2)_R$, and $\epsilon_{L,R}$ global parameters. Imposing now local $SU(2)_L \times U(1)$ gauge invariance, $\Phi(x)$ transforms as

$$\Phi(x) \rightarrow \Phi'(x) = e^{i[-\epsilon_0(x) + \epsilon(x) \cdot \tau]/2} \Phi(x) \quad (2.7)$$

and therefore $\mathbf{U}(x)$ will do it as

$$\mathbf{U}(x) \rightarrow L(x) \mathbf{U}(x) R^\dagger(x) , \quad L(x) = e^{i \epsilon \cdot \tau/2} , \quad R(x) = e^{i \epsilon_0(x) \tau_3/2} \quad (2.8)$$

being possible to introduce its associated covariant derivative as

$$\mathcal{D}_\mu \mathbf{U} \equiv \partial_\mu \mathbf{U} + \frac{i g}{2} \tau_i W_\mu^i \mathbf{U} - \frac{i g'}{2} B_\mu \mathbf{U} \tau_3 , \quad (2.9)$$

and therefore the Lagrangians in Eq. (1.7) and (1.8), which are $SU(2)_L \times U(1)$ gauge invariant, can be rewritten as

$$\mathcal{L}_{Scalar} = \frac{v^2}{4} \text{Tr} \left((\mathcal{D}^\mu \mathbf{U})^\dagger \mathcal{D}_\mu \mathbf{U} \right) - V(\mathbf{U}) . \quad (2.10)$$

Triggering now EWSB with $\mu^2 < 0$ and $\lambda > 0$, the unitary relation holds $\langle \mathbf{U}^\dagger \mathbf{U} \rangle = \mathbb{I}_{2 \times 2}$ and the global symmetry breaks down to the custodial one, i.e. $SU(2)_L \times SU(2)_R \Rightarrow SU(2)_V$.

Decoupling Higgs: non-linear σ -model

The latter unitary relation implies $\sigma^2 + \pi^2 = v^2$, and by replacing $\sigma = \sqrt{v^2 - \pi^2}$ in $\mathbf{U}(x)$

$$\mathbf{U}(x) = \sqrt{1 - \frac{\pi^2(x)}{v^2}} + \frac{i \tau \cdot \pi(x)}{v}, \quad (2.11)$$

the σ -particle is removed from the physical spectrum¹, obtaining therefore a $SU(2)_L \times U(1)$ Yang-Mills theory coupled to a non-linear σ -model²

$$\mathcal{L} = \frac{v^2}{4} \text{Tr} \left((\mathcal{D}^\mu \mathbf{U})^\dagger \mathcal{D}_\mu \mathbf{U} \right) - V(\mathbf{U}) - \frac{1}{4} W_{\mu\nu}^i W_i^{\mu\nu} - \frac{1}{4} B_{\mu\nu} B^{\mu\nu}, \quad (2.14)$$

where the $SU(2)_L \times U(1)$ strength gauge kinetic sector has been introduced and the space-time dependence of \mathbf{U} is implicit there and below. To construct the effective Lagrangian are introduced two chiral objects, a vector \mathbf{V}_μ and a scalar \mathbf{T} , transforming covariantly under the SM gauge group

$$\begin{aligned} \mathbf{T} &= \mathbf{U} \tau_3 \mathbf{U}^\dagger, & \mathbf{T} &\rightarrow L \mathbf{T} L^\dagger, \\ \mathbf{V}_\mu &= (\mathcal{D}_\mu \mathbf{U}) \mathbf{U}^\dagger, & \mathbf{V}_\mu &\rightarrow L \mathbf{V}_\mu L^\dagger, \end{aligned} \quad (2.15)$$

and with these the Eq. (2.14) can be rewritten as

$$\mathcal{L} = \mathcal{L}_{VV} - V(\mathbf{U}) - \frac{1}{4} W_{\mu\nu}^i W_i^{\mu\nu} - \frac{1}{4} B_{\mu\nu} B^{\mu\nu}, \quad (2.16)$$

where now \mathcal{L}_{VV} is the Lagrangian containing two derivative operators (remind that mass dimension comes from gauge fields and derivatives applied on \mathbf{U} only) and expressed as

$$\mathcal{L}_{VV} = -\frac{v^2}{4} \text{Tr} (\mathbf{V}^\mu \mathbf{V}_\mu) + c_T \frac{v^2}{4} \text{Tr} (\mathbf{T} \mathbf{V}_\mu) \text{Tr} (\mathbf{T} \mathbf{V}^\mu). \quad (2.17)$$

\mathbf{V}_μ -antihermiticity has been used for the first term, and the second operator is the two derivative custodial symmetry breaking operator inducing a shift in the mass M_Z with respect to the mass M_W . This coupling tends to be unacceptably large in naive models

¹Goldstone bosons degrees of freedom can also be encoded in a local invariant exponential representation as

$$\mathbf{U}(x) = e^{i\tau \cdot \pi(x)/v}, \quad \mathbf{U}(x) \rightarrow L(x) \mathbf{U}(x) R^\dagger(x), \quad (2.12)$$

with $i = 1, 2, 3$, such that $\mathbf{U}(x)$ can be expanded as

$$\mathbf{U}(x) = \cos \left(\frac{\tilde{\pi}}{v} \right) + \sin \left(\frac{\tilde{\pi}}{v} \right) \frac{i \tau \cdot \pi(x)}{\tilde{\pi}}, \quad \tilde{\pi}(x) = \sqrt{\pi_i(x) \pi^i(x)} \quad (2.13)$$

²Gauge fixing and Faddeev-Popov Lagrangians are not discussed here as quantizations issues will not be relevant for the analysis below.

of a strong interacting Higgs sector, from the original technicolor formulation [9, 10] to its modern variants, if not opportunely protected by some additional custodial symmetry. Quantitatively, realistic models need to limit the intensity of this induced coupling to $c_T < 0.001$, as it is well-known.

The above construction has been repeatedly used in the past to represent a hypothetical dynamical sector of EWSB, with a heavy (decoupled) Higgs particle, by identifying the Higgs particle with σ . Nowadays we know that the Higgs is light, so it is compelling and necessary to generalize the effective Lagrangian to still account for a strong dynamics with a light Higgs.

2.2 Chiral effective expansion and light Dynamical Higgs h

The transformation properties of the three longitudinal degrees of freedom of the weak gauge bosons will still be encoded³ in the dimensionless unitary matrix $\mathbf{U}(x)$ in Eq. (2.2). The adimensionality of $\mathbf{U}(x)$ is the key to understand that the dimension of the leading low-energy operators, describing the dynamics of the scalar sector and the tower of operators differs for a non-linear Higgs sector [21–25] ($\xi \sim 1$) and a purely linear regime ($\xi \ll 1$), as insertions of $\mathbf{U}(x)$ do not exhibit a scale suppression.

Linear regime

For $\xi \ll 1$ the hierarchy between $d \geq 4$ effective operators mimics the linear expansion, where the operators are written in terms of the Higgs doublets Φ : couplings with higher number of (physical) Higgs legs are suppressed compared to the SM renormalizable ones, due to higher powers of $1/f$ or, in other words, of ξ . The power of ξ keeps then track of the h -dependence of the higher dimension operators.

In the extreme linear limit $\langle h \rangle = v$, the Higgs sector enters in the tower of operators through powers of the SM Higgs doublet Φ and its derivatives. It is illustrative to write Φ and its covariant derivative in terms of the Goldstone bosons matrix \mathbf{U} and the physical

³Notice that in this low-energy expression for $\mathbf{U}(x)$, the scale associated to the eaten GBs is v and not f . Technically, the scale v appears through a redefinition of the GB fields so as to have canonically normalized kinetic terms.

scalar h :

$$\begin{aligned}\Phi &= \frac{(v+h)}{\sqrt{2}} \mathbf{U} \begin{pmatrix} 0 \\ 1 \end{pmatrix}, \\ D_\mu \Phi &= \frac{(v+h)}{\sqrt{2}} \mathcal{D}_\mu \mathbf{U} \begin{pmatrix} 0 \\ 1 \end{pmatrix} + \frac{\partial_\mu h}{\sqrt{2}} \mathbf{U} \begin{pmatrix} 0 \\ 1 \end{pmatrix},\end{aligned}\tag{2.18}$$

with $\mathcal{D}_\mu \mathbf{U}$ being the covariant derivative previously defined in Eq. (2.9). The Higgs kinetic energy term in the linear expansion reads then

$$(D^\mu \Phi)^\dagger (D_\mu \Phi) = \frac{1}{2} (\partial_\mu h)^2 - \frac{v^2}{4} \left(1 + \frac{h}{v}\right)^2 \text{Tr}(\mathbf{V}_\mu \mathbf{V}^\mu).\tag{2.19}$$

Notice that the right-hand side of this equation contains, besides of the h -kinetic term, part of the Lagrangian $\mathcal{L}_{d_\chi=2}$ in Eq. (2.14) for $f \rightarrow \infty$, i.e. $\xi = 0$, and $a = b = c = 1$ (disregarding higher order terms in h/f), which corresponds to the SM case. Also notice a $(1 + \frac{h}{v})$ -structure coupled to the non-derivative term, feature that the tower of $d \geq 4$ operators would inherit generically encoded as a h -dependence in powers of $(v+h)/f = \xi^{1/2}(1 + h/v)$, and of $\partial_\mu h/f^2$ [26–28]. This motivates and reinforces a realistic chiral expansion accounting for a light Higgs h contribution and their interactions with the SM particle content. That feature is achieved in the effective chiral approach by introducing a generic polynomial expansion on h [19]

$$\mathcal{F}(h) = g_0(h, v) + \xi g_1(h, v) + \xi^2 g_2(h, v) + \dots\tag{2.20}$$

with $g(h, v)$ model-dependent functions of h and of v , once $\langle h \rangle$ is expressed in terms of ξ and v . As large ξ is, more terms in the expansion are considered and higher h -powers retained.

A priori, the $\mathcal{F}(h)$ functions would also inherit the aforementioned universal behavior in powers of $(1 + h/v)$ such that any operator weighted by ξ^n would have a corresponding expected dependence $\mathcal{F}(h) = (1 + h/v)^{2n}$. Nevertheless, the use of the equations of motion and integration by parts to construct the basis below will translate into combinations of operator coefficients, which lead to a generic h dependence that, for instance at order ξ (i.e. for $d = 6$ operators), reads [19]

$$\mathcal{F}_i(h) = 1 + 2 a_i \frac{h}{v} + b_i \frac{h^2}{v^2},\tag{2.21}$$

where a_i and b_i are expected to be $\mathcal{O}(1)$. An obvious extrapolation applies to couplings weighted by higher powers of ξ (i.e. for $d > 6$ operators).

Non-linear regime

For $\xi \approx 1$, the ξ dependence does not entail a suppression of operators compared to the renormalisable SM operators and the chiral expansion should instead be adopted, although it should be clarified at which level the effective expansion on h/f should stop. In fact, for any BSM theory in the non-linear regime the dependence on h will be a general function. For instance, in the $SO(5)/SO(4)$ strong-interacting model with a composite light Higgs [132], the tower of higher-dimension operators is weighted by powers of $\sin((\langle h \rangle + h)/f)$, and in this case $\xi = \sin^2(\langle h \rangle/f)$. Below, the $\mathcal{F}(h)$ functions encode the non-linear interactions of the light h and will be considered completely general polynomials of $\langle h \rangle$ and h (not including derivatives of h). Notice that, when using the equations of motion and integration by parts to relate operators, $\mathcal{F}(h)$ would be assumed to be redefined when convenient, much as one customarily redefines the constant operator coefficients.

2.2.1 Pure gauge and gauge- h operator basis

As for the gauge- h sector is concerned, all gauge invariant CP-conserving and CP-violating operators are listed in this work up to four derivatives. The connection to the linear regime will be made manifest exploiting the operator dependence on ξ . The effective chiral Lagrangian can thus be decomposed as

$$\mathcal{L}_{\text{chiral}} = \mathcal{L}_{SM} + \Delta\mathcal{L}_{CP} + \Delta\mathcal{L}_{CP}, \quad (2.22)$$

where the first term is the usual SM chiral term

$$\begin{aligned} \mathcal{L}_{SM} = & \frac{1}{2}(\partial_\mu h)(\partial^\mu h) - \frac{1}{4}B_{\mu\nu}B^{\mu\nu} - \frac{1}{4}W_{\mu\nu}^iW_i^{\mu\nu} - \frac{1}{4}G_{\mu\nu}^aG_a^{\mu\nu} - V(h) \\ & - \frac{(v+h)^2}{4}\text{Tr}(\mathbf{V}_\mu\mathbf{V}^\mu) + i\bar{Q}\not{D}Q + i\bar{L}\not{D}L \\ & - \frac{v+h}{\sqrt{2}}(\bar{Q}_L\mathbf{U}\mathbf{Y}_QQ_R + \text{h.c.}) - \frac{v+h}{\sqrt{2}}(\bar{L}_L\mathbf{U}\mathbf{Y}_LL_R + \text{h.c.}) \\ & - \frac{g_s^2}{16\pi^2}\theta_s G_{\mu\nu}^a\tilde{G}_{\rho\sigma}^a. \end{aligned} \quad (2.23)$$

As it can be seen the first line of \mathcal{L}_{SM} accounts for the Higgs and strength gauge kinetic sectors and also the scalar potential $V(h)$, the second line provides W and Z -masses plus gauge- h interactions VVh and $VVhh$ ($V = W, Z$), as well as the fermion kinetic terms,

whilst third line provides Yukawa terms for both of the quark and lepton sector, with Yukawa matrices

$$\mathbf{Y}_Q \equiv \mathbf{diag}(Y_U, Y_D), \quad \mathbf{Y}_L \equiv \mathbf{diag}(Y_\nu, Y_l), \quad (2.24)$$

and L_R and Q_R doublets grouping the corresponding leptons and quarks right handed fields. Finally, the last term in Eq. (2.23) corresponds to the well-known total derivative CP-odd gluonic coupling, for which the notation used is that in which the dual field-tensor of any field strength $X_{\mu\nu}$ is defined as $\tilde{X}^{\mu\nu} \equiv \frac{1}{2}\epsilon^{\mu\nu\rho\sigma}X_{\rho\sigma}$.

Finally, the departures with respect to the SM Lagrangian \mathcal{L}_{SM} are encoded in the remaining part $\Delta\mathcal{L}_{CP} + \Delta\mathcal{L}_{CP}$ of \mathcal{L}_{chiral} in Eq. (2.22). In the follow the CP-even contributions $\Delta\mathcal{L}_{CP}$ are analysed.

2.2.2 CP-conserving $\Delta\mathcal{L}_{CP}$

CP-even contributions are encoded in $\Delta\mathcal{L}_{CP}$ as [19]

$$\begin{aligned} \Delta\mathcal{L}_{CP} = & \xi [c_B \mathcal{P}_B(h) + c_W \mathcal{P}_W(h) + c_G \mathcal{P}_G(h) + c_C \mathcal{P}_C(h) + c_T \mathcal{P}_T(h) + c_\Phi \mathcal{P}_\Phi + c_{\square\Phi} \mathcal{P}_{\square\Phi}] + \\ & + \xi \sum_{i=1}^{10} c_i \mathcal{P}_i(h) + \xi^2 \sum_{i=11}^{25} c_i \mathcal{P}_i(h) + \xi^4 c_{26} \mathcal{P}_{26}(h). \end{aligned} \quad (2.25)$$

First line in $\Delta\mathcal{L}_{CP}$ accounts for the kinetic gauge terms, custodial breaking $\mathcal{P}_T(h)$ and custodial conserving operators $\mathcal{P}_C(h)$, all of them coupled to $\mathcal{F}(h)$

$$\begin{aligned} \mathcal{P}_B(h) &= -\frac{1}{4} B_{\mu\nu} B^{\mu\nu} \mathcal{F}_B(h) \\ \mathcal{P}_W(h) &= -\frac{1}{4} W_{\mu\nu}^a W_a^{\mu\nu} \mathcal{F}_W(h) \\ \mathcal{P}_G(h) &= -\frac{1}{4} G_{\mu\nu}^a G_a^{\mu\nu} \mathcal{F}_G(h) \\ \mathcal{P}_C(h) &= -\frac{v^2}{4} \text{Tr}(\mathbf{V}^\mu \mathbf{V}_\mu) \mathcal{F}_C(h) \\ \mathcal{P}_T(h) &= \frac{v^2}{4} \text{Tr}(\mathbf{T} \mathbf{V}^\mu) \text{Tr}(\mathbf{T} \mathbf{V}_\mu) \mathcal{F}_T(h), \end{aligned} \quad (2.26)$$

and the second line containing the effective CP-even operator basis $\mathcal{P}_i(h)$, weighted by the corresponding ξ -powers, and with c_i the operator coefficient corresponding to each one of the operators $\mathcal{P}_i(h)$. Such weighting is done for keeping track the corresponding linear siblings to each one of the operators $\mathcal{P}_i(h)$, where linear sibling means basically a

determined operator made out of gauge fields and with the explicit presence of the SM Higgs doublet Φ . The corresponding siblings are listed in Appendix C.

The guideline to establish the complete set of pure gauge and pure gauge- h operators consists in

- Straightforwardly to couple strength gauge kinetic sector to $\mathcal{F}(h)$.
- Directly to couple the already existing CP-even operators in the literature.
- Consider operators containing $\mathcal{D}_\mu \mathbf{V}^\mu$ and no derivatives of $\mathcal{F}(h)$.
- Consider also operators with one or two derivatives of $\mathcal{F}(h)$.
- Those operators that were disregarded via integration by parts has to be reconsidered as they will give rise to extra operators depending on derivatives of $\mathcal{F}(h)$.

After this procedure is done, we are able to provide the complete tower of effective chiral operators accounting for pure gauge and gauge- h interactions (initially listed in Ref. [19]) and extended a posteriori with pure Higgs interactions (in Ref. [133]) as

$$\begin{aligned}
\mathcal{P}_1(h) &= g g' B_{\mu\nu} \text{Tr}(\mathbf{T} W^{\mu\nu}) \mathcal{F}_1(h), & \mathcal{P}_{14}(h) &= 2 g \text{Tr}(\mathbf{T} \mathbf{V}_\mu) \text{Tr}\left(\mathbf{V}_\nu \widetilde{W}_{\rho\lambda}\right) \mathcal{F}_{14}(h), \\
\mathcal{P}_2(h) &= i g' B_{\mu\nu} \text{Tr}(\mathbf{T} [\mathbf{V}^\mu, \mathbf{V}^\nu]) \mathcal{F}_2(h), & \mathcal{P}_{15}(h) &= \text{Tr}(\mathbf{T} \mathcal{D}_\mu \mathbf{V}^\mu) \text{Tr}(\mathbf{T} \mathcal{D}_\nu \mathbf{V}^\nu) \mathcal{F}_{15}(h), \\
\mathcal{P}_3(h) &= i g \text{Tr}(W_{\mu\nu} [\mathbf{V}^\mu, \mathbf{V}^\nu]) \mathcal{F}_3(h), & \mathcal{P}_{16}(h) &= \text{Tr}([\mathbf{T}, \mathbf{V}_\nu] \mathcal{D}_\mu \mathbf{V}^\mu) \text{Tr}(\mathbf{T} \mathbf{V}^\nu) \mathcal{F}_{16}(h), \\
\mathcal{P}_4(h) &= i g' B_{\mu\nu} \text{Tr}(\mathbf{T} \mathbf{V}^\mu) \partial^\nu \mathcal{F}_4(h), & \mathcal{P}_{17}(h) &= i g \text{Tr}(\mathbf{T} W_{\mu\nu}) \text{Tr}(\mathbf{T} \mathbf{V}^\mu) \partial^\nu \mathcal{F}_{17}(h), \\
\mathcal{P}_5(h) &= i g \text{Tr}(W_{\mu\nu} \mathbf{V}^\mu) \partial^\nu \mathcal{F}_5(h), & \mathcal{P}_{18}(h) &= \text{Tr}(\mathbf{T} [\mathbf{V}_\mu, \mathbf{V}_\nu]) \text{Tr}(\mathbf{T} \mathbf{V}^\mu) \partial^\nu \mathcal{F}_{18}(h), \\
\mathcal{P}_6(h) &= (\text{Tr}(\mathbf{V}_\mu \mathbf{V}^\mu))^2 \mathcal{F}_6(h), & \mathcal{P}_{19}(h) &= \text{Tr}(\mathbf{T} \mathcal{D}_\mu \mathbf{V}^\mu) \text{Tr}(\mathbf{T} \mathbf{V}_\nu) \partial^\nu \mathcal{F}_{19}(h), \\
\mathcal{P}_7(h) &= \text{Tr}(\mathbf{V}_\mu \mathbf{V}^\mu) \partial_\nu \partial^\nu \mathcal{F}_7(h), & \mathcal{P}_{20}(h) &= \text{Tr}(\mathbf{V}_\mu \mathbf{V}^\mu) \partial_\nu \mathcal{F}_{20}(h) \partial^\nu \mathcal{F}'_{20}(h), \\
\mathcal{P}_8(h) &= \text{Tr}(\mathbf{V}_\mu \mathbf{V}_\nu) \partial^\mu \mathcal{F}_{20}(h) \partial^\nu \tilde{\mathcal{F}}_8(h), & \mathcal{P}_{21}(h) &= (\text{Tr}(\mathbf{T} \mathbf{V}_\mu))^2 \partial_\nu \mathcal{F}_{21}(h) \partial^\nu \mathcal{F}'_{21}(h), \\
\mathcal{P}_9(h) &= \text{Tr}((\mathcal{D}_\mu \mathbf{V}^\mu)^2) \mathcal{F}_9(h), & \mathcal{P}_{22}(h) &= (\text{Tr}(\mathbf{T} \mathbf{V}_\mu) \partial^\mu \mathcal{F}_{22}(h))^2, \\
\mathcal{P}_{10}(h) &= \text{Tr}(\mathbf{V}_\nu \mathcal{D}_\mu \mathbf{V}^\mu) \partial^\nu \mathcal{F}_{10}(h), & \mathcal{P}_{23}(h) &= \text{Tr}(\mathbf{V}_\mu \mathbf{V}^\mu) (\text{Tr}(\mathbf{T} \mathbf{V}_\nu))^2 \mathcal{F}_{23}(h), \\
\mathcal{P}_{11}(h) &= (\text{Tr}(\mathbf{V}_\mu \mathbf{V}_\nu))^2 \mathcal{F}_{11}(h), & \mathcal{P}_{24}(h) &= \text{Tr}(\mathbf{V}_\mu \mathbf{V}_\nu) \text{Tr}(\mathbf{T} \mathbf{V}^\mu) \text{Tr}(\mathbf{T} \mathbf{V}^\nu) \mathcal{F}_{24}(h), \\
\mathcal{P}_{12}(h) &= g^2 (\text{Tr}(\mathbf{T} W^{\mu\nu}))^2 \mathcal{F}_{12}(h), & \mathcal{P}_{25}(h) &= (\text{Tr}(\mathbf{T} \mathbf{V}_\mu))^2 \partial_\nu \partial^\nu \mathcal{F}_{25}(h), \\
\mathcal{P}_{13}(h) &= i g \text{Tr}(\mathbf{T} W_{\mu\nu}) \text{Tr}(\mathbf{T} [\mathbf{V}^\mu, \mathbf{V}^\nu]) \mathcal{F}_{13}(h), & \mathcal{P}_{26}(h) &= (\text{Tr}(\mathbf{T} \mathbf{V}_\mu) \text{Tr}(\mathbf{T} \mathbf{V}_\nu))^2 \mathcal{F}_{26}(h),
\end{aligned} \tag{2.27}$$

Finally, concerning pure Higgs operators, the two derivative operator \mathcal{P}_Φ and the four derivative one $\mathcal{P}_{\square\Phi}$ in $\Delta\mathcal{L}_{\text{CP}}$, weighted both of them by ξ , are

$$\mathcal{P}_\Phi(h) = \frac{1}{2} (\partial_\mu h)^2 \mathcal{F}_\Phi(h), \quad \mathcal{P}_{\square\Phi} = \frac{1}{v^2} (\square h)^2 \mathcal{F}_{\square\Phi}(h). \quad (2.28)$$

Additionally, more pure Higgs operators with linear siblings of dimension higher than 6 (i.e. weighted by $\xi^{\geq 2}$) are possible, like $\mathcal{P}_{D\Phi}(h)$ [134, 135] and $\mathcal{P}_{\Delta\Phi}$

$$\mathcal{P}_{D\Phi}(h) = \frac{1}{v^4} ((\partial_\mu h)(\partial^\mu h))^2 \mathcal{F}_{D\Phi}(h), \quad \mathcal{P}_{\Delta\Phi} = \frac{1}{v^3} (\partial_\mu h)^2 \square h. \quad (2.29)$$

These operators correspond to three major categories: a) pure gauge and gauge- h operators $\mathcal{P}_{1-3}(h)$, $\mathcal{P}_6(h)$, $\mathcal{P}_{11-14}(h)$, $\mathcal{P}_{23-24}(h)$ and $\mathcal{P}_{26}(h)$ which result from a direct extension of the original Appelquist-Longhitano chiral Higgsless basis already considered in Refs. [21–25] with additional $\mathcal{F}(h)$ insertions. They appear in the Lagrangian with different powers of ξ . b) Operators containing the contraction $\mathcal{D}_\mu \mathbf{V}^\mu$ and no derivatives of $\mathcal{F}(h)$. c) Operators with one or two derivatives of $\mathcal{F}(h)$.

In all the effective operators listed so far, the light Higgs dependence is encoded through the generic $\mathcal{F}_i(h)$ -functions of the scalar singlet h defined as [19]

$$\mathcal{F}_i(h) \equiv 1 + 2 a_i \frac{h}{v} + b_i \frac{h^2}{v^2} + \dots, \quad (2.30)$$

with dots standing for terms with higher powers in h/v which will not be considered below. It is worth to comment that the standard structure $\text{Tr}(\mathbf{V}_\mu \mathbf{V}^\mu)$ together with the custodial breaking term $\text{Tr}(\mathbf{T} \mathbf{V}_\mu) \text{Tr}(\mathbf{T} \mathbf{V}^\mu)$, as well as the Yukawa terms of the SM Lagrangian in Eq. (2.23), can be extended in a more general manner by coupling them to the corresponding light Higgs dependence functions. In fact

$$-\frac{v^2}{4} \text{Tr}(\mathbf{V}^\mu \mathbf{V}_\mu) \mathcal{F}_C(h), \quad c_T \xi \frac{v^2}{4} \text{Tr}(\mathbf{T} \mathbf{V}^\mu) \text{Tr}(\mathbf{T} \mathbf{V}_\mu) \mathcal{F}_T(h), \quad (2.31)$$

$$-\frac{v}{\sqrt{2}} (\bar{Q}_L \mathbf{U} \mathbf{Y}_Q \mathcal{F}_Q(h) Q_R + \text{h.c.}) - \frac{v}{\sqrt{2}} (\bar{L}_L \mathbf{U} \mathbf{Y}_L \mathcal{F}_L(h) L_R + \text{h.c.}), \quad (2.32)$$

where $\mathcal{F}_H(h)$, $\mathcal{F}_C(h)$, $\mathcal{F}_T(h)$, $\mathcal{F}_Q(h)$ and $\mathcal{F}_L(h)$ defined similarly as in Ec. (2.19), and with $\mathcal{F}_Q(h)$ and $\mathcal{F}_L(h)$ diagonal 2×2 matrices defined as

$$\mathcal{F}_Q(h) \equiv \mathbf{diag}(\mathcal{F}_U(h), \mathcal{F}_D(h)), \quad \mathcal{F}_L(h) \equiv \mathbf{diag}(\mathcal{F}_\nu(h), \mathcal{F}_l(h)), \quad (2.33)$$

where the entries $\mathcal{F}_{U,D}(h)$ and $\mathcal{F}_{\nu,l}(h)$ are as in Eq. (2.19). For the particular cases of $\mathcal{F}_C(h)$ and $\mathcal{F}_Y(h)$, specific forms (alike in Eq. (2.20)) were already provided in the literature [26, 27] as

$$\mathcal{F}_C(h) = \left(1 + 2a \frac{h}{v} + b \frac{h^2}{v^2} + \dots \right),$$

$$\mathcal{F}_{U,D}(h) = \left(1 + c_{U,D} \frac{h}{v} + \dots \right).$$

The constants a , b and $c_{U,D}$ are model-dependent parameters, and specifically, a and c_T parameters are constrained from electroweak precision tests as $0.7 \lesssim a \lesssim 1.2$ [106] and $-1.7 \times 10^{-3} < c_T \xi < 1.9 \times 10^{-3}$ [28] at 95% CL.

The Lagrangian $\mathcal{L}_{gauge-h}$ is useful in describing an extended class of “Higgs” models:

- Mimicking the SM scenario with a linear Higgs sector after neglecting higher h -powers, and if $\langle h \rangle = v$, $a = b = c_{U,D} = c_l = 1$ as well as $\mathcal{F}_\nu(h) = 0$ as the neutrinos are massless in the SM.
- Technicolor-like ansatz (for $f \sim v$ and omitting all terms in h) and intermediate situations with a light scalar h from composite/holographic Higgs models [11, 13–18, 132, 136, 137] (in general for $f \neq v$)
- Dilaton-like scalar frameworks [134, 138–143] (for $f \sim v$), where the dilaton participates to the electroweak symmetry breaking.

In concrete models, electroweak corrections imply $\xi \lesssim 0.2 - 0.4$ [144], even though the ξ parameter will be free and general here, only accounting for the constraints on custodial symmetry through limits on the $d = 2$ and higher-dimensional chiral operator coefficients.

So far, all the aforementioned operators are invariant under CP transformations and the CP-even gauge- h effective operator basis was established in Eqs. (2.25)–(2.27). Taking into consideration the corresponding CP-violating counterpart, such basis is enlarged and completed through $\Delta\mathcal{L}_{CP}$. The latter contribution is considered in the follow.

2.2.3 CP-violating $\Delta\mathcal{L}_{CP}$

The effective CP-odd lagrangian expansion $\Delta\mathcal{L}_{CP}$ will be parametrised as [20]

$$\begin{aligned}
\Delta \mathcal{L}_{\mathcal{CP}} = & \xi \left[c_{2D} \mathcal{S}_{2D}(h) + c_{\tilde{B}} \mathcal{S}_{\tilde{B}}(h) + c_{\tilde{W}} \mathcal{S}_{\tilde{W}}(h) + c_{\tilde{G}} \mathcal{S}_{\tilde{G}}(h) \right] + \\
& + \xi \sum_{i=1}^3 c_i \mathcal{S}_i(h) + \xi^2 \sum_{i=4}^{14} c_i \mathcal{S}_i(h) + \xi^3 \sum_{i=15}^{16} c_i \mathcal{S}_i(h),
\end{aligned} \tag{2.34}$$

where c_i are model-dependent constant coefficients and

$$\begin{aligned}
\mathcal{S}_{\tilde{B}}(h) &\equiv -\frac{1}{2} g'^2 B^{\mu\nu} \tilde{B}_{\mu\nu} \mathcal{F}_{\tilde{B}}(h), & \mathcal{S}_7(h) &\equiv g \text{Tr}(\mathbf{T} [W^{\mu\nu}, \mathbf{V}_\mu]) \partial_\nu \mathcal{F}_7(h), \\
\mathcal{S}_{\tilde{W}}(h) &\equiv -\frac{1}{2} g^2 \text{Tr} \left(W^{\mu\nu} \tilde{W}_{\mu\nu} \right) \mathcal{F}_{\tilde{W}}(h), & \mathcal{S}_8(h) &\equiv 2 g^2 \text{Tr} \left(\mathbf{T} \tilde{W}^{\mu\nu} \right) \text{Tr}(\mathbf{T} W_{\mu\nu}) \mathcal{F}_8(h), \\
\mathcal{S}_{\tilde{G}}(h) &\equiv -\frac{1}{2} g_s^2 G^{a\mu\nu} \tilde{G}_{\mu\nu}^a \mathcal{F}_{\tilde{G}}(h), & \mathcal{S}_9(h) &\equiv 2i g \text{Tr} \left(\tilde{W}^{\mu\nu} \mathbf{T} \right) \text{Tr}(\mathbf{T} \mathbf{V}_\mu) \partial_\nu \mathcal{F}_9(h), \\
\mathcal{S}_{2D}(h) &\equiv i \frac{v^2}{4} \text{Tr}(\mathbf{T} \mathcal{D}^\mu \mathbf{V}_\mu) \mathcal{F}_{2D}(h), & \mathcal{S}_{10}(h) &\equiv i \text{Tr}(\mathbf{V}^\mu \mathcal{D}^\nu \mathbf{V}_\nu) \text{Tr}(\mathbf{T} \mathbf{V}_\mu) \mathcal{F}_{10}(h), \\
\mathcal{S}_1(h) &\equiv 2g g' \tilde{B}^{\mu\nu} \text{Tr}(\mathbf{T} W_{\mu\nu}) \mathcal{F}_1(h), & \mathcal{S}_{11}(h) &\equiv i \text{Tr}(\mathbf{T} \mathcal{D}^\mu \mathbf{V}_\mu) \text{Tr}(\mathbf{V}^\nu \mathbf{V}_\nu) \mathcal{F}_{11}(h), \\
\mathcal{S}_2(h) &\equiv 2i g' \tilde{B}^{\mu\nu} \text{Tr}(\mathbf{T} \mathbf{V}_\mu) \partial_\nu \mathcal{F}_2(h), & \mathcal{S}_{12}(h) &\equiv i \text{Tr}([\mathbf{V}^\mu, \mathbf{T}] \mathcal{D}^\nu \mathbf{V}_\nu) \partial_\mu \mathcal{F}_{12}(h), \\
\mathcal{S}_3(h) &\equiv 2i g \text{Tr} \left(\tilde{W}^{\mu\nu} \mathbf{V}_\mu \right) \partial_\nu \mathcal{F}_3(h), & \mathcal{S}_{13}(h) &\equiv i \text{Tr}(\mathbf{T} \mathcal{D}^\mu \mathbf{V}_\mu) \partial^\nu \partial_\nu \mathcal{F}_{13}(h), \\
\mathcal{S}_4(h) &\equiv g \text{Tr}(W^{\mu\nu} \mathbf{V}_\mu) \text{Tr}(\mathbf{T} \mathbf{V}_\nu) \mathcal{F}_4(h), & \mathcal{S}_{14}(h) &\equiv i \text{Tr}(\mathbf{T} \mathcal{D}^\mu \mathbf{V}_\mu) \partial^\nu \mathcal{F}_{14}(h) \partial_\nu \mathcal{F}'_{14}(h), \\
\mathcal{S}_5(h) &\equiv i \text{Tr}(\mathbf{V}^\mu \mathbf{V}^\nu) \text{Tr}(\mathbf{T} \mathbf{V}_\mu) \partial_\nu \mathcal{F}_5(h), & \mathcal{S}_{15}(h) &\equiv i \text{Tr}(\mathbf{T} \mathbf{V}^\mu) \text{Tr}(\mathbf{T} \mathbf{V}^\nu)^2 \partial_\mu \mathcal{F}_{15}(h), \\
\mathcal{S}_6(h) &\equiv i \text{Tr}(\mathbf{V}^\mu \mathbf{V}_\mu) \text{Tr}(\mathbf{T} \mathbf{V}^\nu) \partial_\nu \mathcal{F}_6(h), & \mathcal{S}_{16}(h) &\equiv i \text{Tr}(\mathbf{T} \mathcal{D}^\mu \mathbf{V}_\mu) \text{Tr}(\mathbf{T} \mathbf{V}^\nu)^2 \mathcal{F}_{16}(h),
\end{aligned} \tag{2.35}$$

with the $\mathcal{F}_i(h)$ -functions for all operators⁴ but $\mathcal{S}_{\tilde{G}}(h)$, being defined as in Eq. (2.30). $\mathcal{F}_{\tilde{G}}(h)$ will be understood to be also of this form but for the first term in Eq. (2.30), as the Higgs-independent part of $\mathcal{S}_{\tilde{G}}(h)$ has already been included in the SM Lagrangian, Eq. (2.23).

Note that the number of independent operators in the non-linear expansion turned out to be larger than for the analogous basis in the linear expansion [133, 145], a generic feature when comparing both type of effective Lagrangians; see Appendix C. The basis is also larger than that for chiral expansions developed in the past for the case of a very heavy Higgs particle (i.e. absent at low energies) [21–23, 25], as: i) terms which in the absence of the $\mathcal{F}_i(h)$ functions were shown to be equivalent via total derivatives, are now independent; ii) new terms including derivatives of h appear.

⁴The Higgs-independent term in this functional is physically irrelevant for operators $\mathcal{S}_{\tilde{B}}(h)$, $\mathcal{S}_{\tilde{W}}(h)$, $\mathcal{S}_{2D}(h)$.

The Lagrangian in Eqs. (2.25) and (2.34) describes both of the CP-conserving and CP-violating low-energy effects of a high-energy strong dynamics responsible for the electroweak GBs, coupled to a generic scalar singlet h . For the former case, the gauge- h CP-even sector, the phenomenology that $\Delta\mathcal{L}_{\text{CP}}$ in Eqs. (2.25) entails, is analysed in Ref. [133], where the complete sets of gauge and gauge-Higgs operators are considered, the Feynman rules for the non-linear expansion are derived, and additionally, are considered possible discriminating signals including decorrelation in the non-linear case of signals correlated in the linear one, for instance, some pure gauge versus gauge-Higgs couplings and also between couplings with the same number of Higgs legs. Furthermore, in Ref. [133], are analysed some anomalous signals expected at first order in the non-linear realization that may appear only at higher orders of the linear one, and vice versa. The impact of both type of discriminating signals on LHC physics is also studied there.

For this Thesis work the phenomenology impact implied by the CP-violating contribution encoded in $\Delta\mathcal{L}_{\text{CP}}$ is analysed following the Ref. [20], and presented in detail in the next subsection.

2.3 $\Delta\mathcal{L}_{\text{CP}}$ -phenomenology

The physical impact of the operators in the CP-odd bosonic basis determined previously is analysed below. Some phenomenological bounds and future prospects are discussed as well.

2.3.1 CP-odd two-point functions

Only the operators $\mathcal{S}_{2D}(h)$ and $\mathcal{S}_{13}(h)$ among those defined in Eq. (2.35) may a priori induce renormalisation effects on the fields and couplings of the SM Lagrangian. $\mathcal{S}_{2D}(h)$ is a two-derivative coupling and thus part of the leading order of the chiral expansion; in contrast, note that it has no analogue in the leading order of the linear expansion –in other words in the SM Lagrangian– as its lower-dimensional linear sibling would be a dimension six ($d = 6$) operator, see Appendix B.

$\mathcal{S}_{2D}(h)$ and $\mathcal{S}_{13}(h)$ contain two-point functions which explicitly break the CP symmetry and as a consequence the Lagrangian eigenstates may not be CP-eigenstates. Those two couplings result in a mixing of h with the Goldstone bosons which in the SM give masses to the W and Z bosons, see below. Their physical impact reduces simply to anomalous CP-odd Higgs-fermion and Higgs- Z couplings, as it is shown detailed in the next.

Consider the linear combination of the two operators $\mathcal{S}_{2D}(h)$ and $\mathcal{S}_{13}(h)$, together with the h -kinetic term and the gauge-boson mass term in the Lagrangian of Eq. (2.22), and

let us focus first on their contribution to two-point functions:

$$\begin{aligned}
\mathcal{L}_{\text{chiral}} &\supset \frac{1}{2} \partial^\mu h \partial_\mu h - \frac{(v+h)^2}{4} \text{Tr}(\mathbf{V}^\mu \mathbf{V}_\mu) + \xi c_{2D} \mathcal{S}_{2D}(h) + \xi^2 c_{13} \mathcal{S}_{13}(h) \\
&\supset \frac{1}{2} \partial^\mu h \partial_\mu h + \frac{v^2}{4} \text{Tr}(\partial^\mu \mathbf{U}^\dagger \partial_\mu \mathbf{U}) + \frac{i}{2} v \text{Tr}[\mathbf{T}(\partial_\mu \partial^\mu \mathbf{U}) \mathbf{U}^\dagger] (\hat{a}_{2D} h + \frac{4}{v^2} \hat{a}_{13} \square h) + \\
&\quad + \frac{i}{2} g' B^\mu \left\{ \frac{v^2}{4} \text{Tr}[(\partial_\mu \mathbf{U}) \tau_3 \mathbf{U}^\dagger - \mathbf{U} \tau_3 (\partial_\mu \mathbf{U}^\dagger)] + i \xi v \left[\hat{a}_{2D} \partial_\mu h + \frac{4}{v^2} \hat{a}_{13} \xi \partial_\mu (\square h) \right] \right\} \\
&\quad + \frac{i}{2} g W_\mu^i \left\{ \frac{v^2}{4} \text{Tr}[(\partial^\mu \mathbf{U}^\dagger) \tau^i \mathbf{U} - \mathbf{U}^\dagger \tau^i (\partial^\mu \mathbf{U})] - \frac{iv}{2} \xi \left[\hat{a}_{2D} \partial_\mu h + \frac{4}{v^2} \hat{a}_{13} \xi \partial_\mu (\square h) \right] \text{Tr}(\mathbf{T} \tau^i) \right\},
\end{aligned} \tag{2.36}$$

where for simplicity the definitions

$$\hat{a}_i \equiv c_i a_i \tag{2.37}$$

have been implemented, with c_i being the operator coefficients in Eq. (2.34) and a_i the coefficients of the terms linear in the Higgs field in Eq. (2.30).

In what concerns the Lagrangian two-point functions, the dependence on \hat{a}_{2D} and \hat{a}_{13} in Eq. (2.36) can be reabsorbed via a phase redefinition of the Goldstone boson \mathbf{U} matrix defined either in Eq. (2.4), (2.11), or (2.12), of the form

$$\mathbf{U} = \tilde{\mathbf{U}} \exp \left[-\frac{i}{v} \xi \left(\hat{a}_{2D} h + 4 \hat{a}_{13} \xi \frac{\square h}{v^2} \right) \tau_3 \right], \tag{2.38}$$

at first order in the \hat{a}_i coefficients. This redefinition is a non-linear version of the simple Higgs-field redefinition proposed in Ref. [146] when analysing the effective linear axion Lagrangian. $\tilde{\mathbf{U}}$ is then the resulting physical matrix of the Goldstone bosons eaten by the W and Z bosons, to be identified with the identity in the unitary gauge. The gauge-fixing terms can now be written in the standard form,

$$\begin{aligned}
\mathcal{L}_B^{\text{GF}} &= -\frac{1}{4\eta} \text{Tr} \left\{ \left[\partial_\mu B^\mu - \frac{i}{4} \eta g' v^2 (\tilde{\mathbf{U}} \tau_3 - \tau_3 \tilde{\mathbf{U}}^\dagger) \right]^2 \right\} \\
\mathcal{L}_W^{\text{GF}} &= -\frac{1}{\eta} \text{Tr} \left\{ \left[\partial_\mu W^\mu + \frac{i}{8} \eta g v^2 (\tilde{\mathbf{U}} - \tilde{\mathbf{U}}^\dagger) \right]^2 \right\},
\end{aligned} \tag{2.39}$$

removing all mixed gauge boson-Goldstone bosons and gauge boson- h two-point couplings.

After the redefinition in Eq. (2.38), restraining to vertices involving at most two Higgs particles⁵ and at first order on the operator coefficients, the SM Lagrangian Eq. (2.23)

⁵ Vertices cubic in h and originated by S_{2D} and S_{13} result: i) from the impact of Eq. (2.38) on the standard term $\propto \text{Tr}(\mathbf{V}^\mu \mathbf{V}_\mu)$ combined with the h^2 dependence of its $(v+h)^2$ prefactor; ii) from the third order in the h expansion of the $F_i(h)$ functions. If considered, they would induce for instance additional contributions to the vertex in Eq. (FR.26).

gets physical corrections given by

$$\Delta\mathcal{L}_{\text{Yukawa}} + \Delta\mathcal{L}_{\text{Bosonic}}, \quad (2.40)$$

with

$$\Delta\mathcal{L}_{\text{Yuk}} = \frac{i}{v} \xi \left(\hat{a}_{2D} h + 4 \hat{a}_{13} \xi \frac{\square h}{v^2} \right) \frac{(v+h)}{\sqrt{2}} \left(\bar{Q}_L \tilde{\mathbf{U}} \mathbf{Y}_Q \tau_3 Q_R - \text{h.c.} \right) + [Q_{L,R} \implies L_{L,R}], \quad (2.41)$$

and

$$\begin{aligned} \Delta\mathcal{L}_{\text{Bos}} = & -i \xi \left(1 + \frac{h}{v} \right) \partial_\mu h \text{Tr} \left(\mathbf{T} \left(\partial^\mu \tilde{\mathbf{U}} \right) \tilde{\mathbf{U}}^\dagger \right) \left(\hat{a}_{2D} h + 4 \hat{a}_{13} \xi \frac{\square h}{v^2} \right) \\ & - i \xi \text{Tr} \left(\mathbf{T} \left(\partial_\mu \partial^\mu \tilde{\mathbf{U}} \right) \tilde{\mathbf{U}}^\dagger \right) \left[\left(\hat{a}_{2D} - \frac{\hat{b}_{2D}}{4} \right) h^2 + 4 \left(\hat{a}_{13} - \frac{\hat{b}_{13}}{2} \right) \xi \frac{h \square h}{v^2} \right. \\ & \quad \left. - 2 \hat{b}_{13} \xi \frac{\partial_\nu h \partial^\nu h}{v^2} + \frac{h^2}{2v} \left(\hat{a}_{2D} h + 4 \hat{a}_{13} \xi \frac{\square h}{v^2} \right) \right] \\ & - \xi \left[g \text{Tr} (\mathbf{T} W^\mu) - g' B^\mu \right] \left[\left(\hat{a}_{2D} - \frac{\hat{b}_{2D}}{2} \right) h \partial_\mu h + 4 \left(\hat{a}_{13} - \frac{\hat{b}_{13}}{2} \right) \xi \frac{h \partial^\mu \square h}{v^2} \right. \\ & \quad \left. - 2 \hat{b}_{13} \xi \left(\frac{\square h \partial_\mu h}{v^2} + 2 \frac{\partial_\nu h \partial_\mu \partial^\nu h}{v^2} \right) \right. \\ & \quad \left. + \frac{h^2}{2v} \left(\hat{a}_{2D} \partial_\mu h + 4 \hat{a}_{13} \xi \frac{\partial_\mu \square h}{v^2} \right) \right] \end{aligned} \quad (2.42)$$

where $\hat{b}_i \equiv c_i b_i$. The “tilde” over $\tilde{\mathbf{U}}$ will be dropped from now on.

Anomalous qqh , $\ell\ell h$ and Zhh vertices follow; the corresponding Feynman rules can be found in Appendix D. It is worth to remark that if a generic $\mathcal{F}_i(h)$ function is considered also for the Yukawa terms instead of the SM-like dependence in Eq. (2.23), further quartic $qqhh$ and $\ell\ell hh$ anomalous vertices will be revealed in addition to those shown in Eq. (2.41). The consideration of these two-Higgs exotic interactions it is postponed to a future analysis [20]. Furthermore, it is easy to derive the form of couplings involving three Higgs particles from the formulae above.

In addition to the tree-level impact discussed, $\mathcal{S}_{2D}(h)$ and $\mathcal{S}_{13}(h)$ induce one-loop corrections to the Higgs gauge-boson couplings, see Sec. 2.3.3, which in turn can be bounded from the strong experimental limits on fermionic EDMs, see Eq. (2.75).

2.3.2 Triple gauge boson couplings

The operators in Eq. (2.35) induce tree-level modifications of the self-couplings of the electroweak gauge bosons as well as of the Higgs-gauge boson vertices involving three or more particles: their impact on the Feynman rules of the theory are given in Appendix D.

The focus is first now on the CP-violating triple gauge boson couplings $W^+W^-\gamma$ and W^+W^-Z , originated from the operators in Eq. (2.35). Following Ref. [147], the CP-odd sector of the Lagrangian that describes triple gauge boson vertices (TGVs) can be parametrised as:

$$\mathcal{L}_{\text{eff, CP}}^{WWV} = g_{WWV} \left(g_4^V W_\mu^\dagger W_\nu (\partial^\mu V^\nu + \partial^\nu V^\mu) - i\tilde{\kappa}_V W_\mu^\dagger W_\nu \tilde{V}^{\mu\nu} - i\frac{\tilde{\lambda}_V}{M_W^2} W_\sigma^\dagger W_\nu^\mu \tilde{V}^{\nu\sigma} + \right. \\ \left. + \tilde{g}_6^V (W_\nu^\dagger \partial_\mu W^\mu + W_\nu \partial_\mu W^{\dagger\mu}) V^\nu + \tilde{g}_7^V W_\mu^\dagger W^\mu \partial^\nu V_\nu \right), \quad (2.43)$$

where $V \equiv \{\gamma, Z\}$ and $g_{WW\gamma} \equiv e = g \sin \theta_W$, $g_{WWZ} = g \cos \theta_W$. In this equation $W_{\mu\nu}^\pm$ and $V_{\mu\nu}$ stand exclusively for the kinetic part of the corresponding gauge field strengths, and the dual tensor $\tilde{V}_{\mu\nu}$ has been defined in Sect. 2.2.1. In writing Eq. (2.43) have been introduced the coefficients \tilde{g}_6^V and \tilde{g}_7^V associated to operators that contain the contraction $\mathcal{D}_\mu \mathbf{V}^\mu$; its $\partial_\mu \mathbf{V}^\mu$ part vanishes only for on-shell gauge bosons; in all generality $\mathcal{D}_\mu \mathbf{V}^\mu$ insertions could only be disregarded in the present context when fermion masses are neglected. In the SM all couplings in Eq. (2.43) vanish.

Electromagnetic gauge invariance requires $g_4^\gamma = 0$, while the CP-odd bosonic operators in Eq. (2.35) give the following contributions to the phenomenological coefficients in Eq. (2.43):

$$\begin{aligned} \tilde{\kappa}_\gamma &= -\frac{4e^2}{s_\theta^2} \xi (c_1 + 2c_8 \xi), & \tilde{\kappa}_Z &= \frac{4e^2}{c_\theta^2} \xi \left(c_1 - 2\frac{c_\theta^2}{s_\theta^2} c_8 \xi \right), \\ g_4^Z &= \frac{e^2}{2c_\theta^2 s_\theta^2} c_4 \xi^2, & \tilde{g}_6^Z &= \frac{e^2}{2c_\theta^2 s_\theta^2} (c_4 + c_{10}) \xi^2, \\ \tilde{g}_7^Z &= -\frac{e^2}{2c_\theta^2 s_\theta^2} (c_4 - 2c_{11}) \xi^2, & \tilde{g}_6^\gamma &= \tilde{g}_7^\gamma = \tilde{\lambda}_\gamma = \tilde{\lambda}_Z = 0. \end{aligned} \quad (2.44)$$

For completeness, note that there is an additional contribution to the ZZZ vertex of the form:

$$\mathcal{L}_{\text{eff, CP}}^{3Z} = \tilde{g}_{3Z} Z_\mu Z^\mu \partial_\nu Z^\nu, \quad (2.45)$$

with

$$\tilde{g}_{3Z} = \frac{e^3}{2c_\theta^3 s_\theta^3} \xi^2 (c_{10} + c_{11} + 2c_{16} \xi), \quad (2.46)$$

which, alike to the phenomenological couplings \tilde{g}_6^V and \tilde{g}_7^V in Eq. (2.43), vanishes for on-shell Z bosons and in general can be disregarded in the present context when the masses of fermions coupling to the Z are neglected.

The strongest constraints on CP violation in the $W^+W^-\gamma$ vertex arise from its contributions to fermionic EDMs that they can induce at one-loop, while constraints on CP-

violating W^+W^-Z couplings can be obtained from the study of gauge-boson production at colliders. Later on further analysis is done in these two types of signals.

CP violation in $WW\gamma$: fermionic EDMs

Electric dipole moments for quarks and leptons are generically the best windows on BSM sources of CP-violation, due to the combination of the very stringent experimental bounds with the fact that they tend to be almost free from SM background contributions: fermionic EDMs are suppressed in the SM beyond two electroweak boson exchange, while in most BSM theories they are induced at one-loop level.

Although none of the operators in the chiral basis above – Eq. (2.35) – induces tree-level contributions to EDMs, two of them, $\mathcal{S}_1(h)$ and $\mathcal{S}_8(h)$, contain gauge boson couplings involving the photon, of the form

$$+ \frac{i}{2} \epsilon_{\mu\nu\rho\sigma} W_\mu^+ W_\nu^- A^{\rho\sigma}, \quad (2.47)$$

where $A^{\rho\sigma}$ denotes the photon field strength, see Eqs.(2.43) and (2.44) and Appendix D. This coupling induces in turn a one-loop contribution to fermion EDMs, see Fig. 2.2.

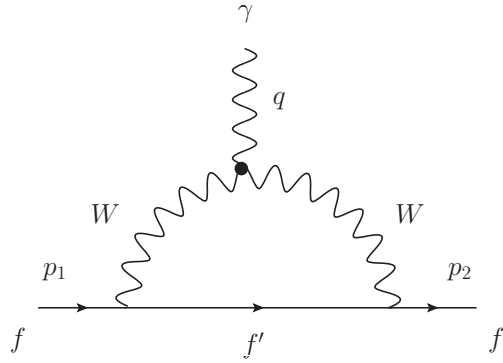


Figure 2.2: A CP-odd TGV coupling inducing a fermionic EDM interaction.

The amplitude corresponding to this Feynman diagram can be parametrised as

$$\mathcal{A}_f \equiv -i d_f \bar{u}(p_2) \sigma_{\mu\nu} q^\nu \gamma^5 u(p_1), \quad (2.48)$$

where d_f denotes the fermionic EDM strength. The corresponding integral diverges logarithmically; assuming a physical cut-off Λ_s for the high energy BSM theory and following

the generic computation in Ref. [148], it is obtained the contribution from $\mathcal{S}_1(h)$ and $\mathcal{S}_8(h)$:

$$d_f = \xi (c_1 + 2 \xi c_8) \frac{e^3 G_F T_{3L} \csc^2 \theta_W}{\sqrt{2} \pi^2} m_f \left[\log \left(\frac{\Lambda_s^2}{M_W^2} \right) + \mathcal{O}(1) \right], \quad (2.49)$$

where T_{3L} stands for the fermion weak isospin, θ_W denotes the Weinberg angle and G_F the Fermi coupling constant. The present experimental bound on the electron EDM [149],

$$\left| \frac{d_e}{e} \right| < 8.7 \times 10^{-29} \text{ cm}, \quad \text{at 90\% CL}, \quad (2.50)$$

implies then a limit

$$\left| \xi (c_1 + 2 c_8 \xi) \left[\log \left(\frac{\Lambda_s^2}{M_W^2} \right) + \mathcal{O}(1) \right] \right| < 5.2 \times 10^{-5}. \quad (2.51)$$

Using as values for the constituent quark masses $m_u = m_d = m_N/3$, the experimental limit on the neutron EDM [150],

$$\left| \frac{d_n}{e} \right| < 2.9 \times 10^{-26} \text{ cm}, \quad \text{at 90\% CL}, \quad (2.52)$$

allows to set an even stronger limit on the combination of $\mathcal{S}_1(h)$ and $\mathcal{S}_8(h)$ operator coefficients:

$$\left| \xi (c_1 + 2 c_8 \xi) \left[\log \left(\frac{\Lambda_s^2}{M_W^2} \right) + \mathcal{O}(1) \right] \right| < 2.8 \times 10^{-5}. \quad (2.53)$$

Weaker but more direct bounds on these operators can be imposed from the study of $W\gamma$ production at colliders. For example the recent study in Ref. [151] concluded that the future 14 TeV LHC data with 10 fb^{-1} can place a 95% CL bound

$$|\tilde{\kappa}_\gamma| \leq 0.05 \implies |\xi (c_1 + 2 c_8 \xi)| \leq 0.03. \quad (2.54)$$

CP violation in WWZ : Collider bounds and signatures

At present the strongest direct constraints on CP-violating effects in the WWZ vertex are imposed by the combination of results using the LEP collaboration studies on the observation of the angular distribution of W 's and their decay products in WW production at LEPII [152–154]. The combination yields the following 1σ (68% CL) constraints [82]

$$-0.47 \leq g_4^Z \leq -0.13, \quad -0.14 \leq \tilde{\kappa}_Z \leq -0.06, \quad -0.16 \leq \tilde{\lambda}_Z \leq -0.02, \quad (2.55)$$

which in terms of the coefficients of operators in Eq. (2.35) and the TGV couplings in Eq. (2.44) implies

$$-1.8 \leq c_4 \xi^2 \leq -0.50, \quad -0.29 \leq \xi \left(c_1 - 2 \frac{c_\theta^2}{s_\theta^2} c_8 \xi \right) \leq -0.13. \quad (2.56)$$

Note that the bounds in Eq. (2.55) are obtained assuming one effective coupling in Eq. (2.43) being different from zero at a time, which is consistent with the predictions from the dynamical Higgs Lagrangian, Eq. (2.44), since different operators lead to independent modifications of the effective couplings g_4^Z and $\tilde{\kappa}_Z$.

In what concerns Tevatron and LHC data, anomalous CP-odd TGV interactions have not been studied in detail yet. To fill this gap, it is presented in this work our analysis of the LHC potential to measure deviations or set exclusion bounds on CP-odd WWZ anomalous TGVs, extending our preliminary study [155]. At LEP the experimental analyses which lead to the bounds in Eq. (2.55) were based on the study of the angular distributions of the final state particles in the event. In contrast, at the LHC, the higher collision energy – well above the WW and WZ thresholds – makes the use of kinematic variables related to the energy of the event more suitable for the measurement of TGV.

The study in Ref. [155] concluded that the $pp \rightarrow W^\pm Z$ process has higher potential to observe g_4^Z than the $pp \rightarrow W^+W^-$ channel, while both channels have a similar power to study $\tilde{\kappa}_Z$ and $\tilde{\lambda}_Z$. Furthermore, it was also discussed the use of several kinematic distributions to characterize the presence of a non-vanishing CP-violating coupling and the use of some asymmetries to characterize its CP nature. So far the LHC has already collected almost 25 times more data than the luminosity considered in that preliminary study which it is updated in here. In addition, this update takes advantage of a more realistic background evaluation, by using the results of the experimental LHC analysis on other anomalous TGV interactions [156]⁶.

In this section it is studied the process

$$pp \rightarrow \ell'^\pm \ell^+ \ell^- E_T^{\text{miss}}, \quad (2.57)$$

where $\ell^{(\prime)} = e$ or μ . The main background for the detection of anomalous TGV interactions is the irreducible SM production of $W^\pm Z$ pairs. In addition there are further reducible backgrounds like W or Z production with jets, ZZ production followed by the leptonic decay of the Z 's with one charged lepton escaping detection, and $t\bar{t}$ pair production.

We simulate the signal and the SM irreducible background using an implementation of the anomalous vertices g_4^Z , $\tilde{\kappa}_Z$, and $\tilde{\lambda}_Z$ in FeynRules [157] interfaced with MadGraph 5 [158] for event generation. We account for the different detection efficiencies by rescaling our simulation of the SM production of $W^\pm Z$ pairs to the values quoted by ATLAS [156] for the study of $\Delta\kappa_Z$, g_1^Z and λ_Z . However, we have also cross-checked the results using a setup where the signal simulation is based on the same FeynRules [157] and MadGraph5 [158] implementation, interfaced then with PYTHIA [159] for parton shower and

⁶This strategy was also the starting point for the study of the CP conserving, but C and P violating coupling g_5^Z presented in Ref. [133].

hadronization, and with PGS 4 [160] for detector simulation. Finally, the reducible backgrounds for the 7 TeV data analysis are obtained from the simulations presented in the ATLAS search [156], and they are properly rescaled for the 8 and 14 TeV runs.

In order to make our simulations more realistic, we closely follow the TGV analysis performed by ATLAS [156]. The kinematic study of the $W^\pm Z$ production starts with the usual detection and isolation cuts on the final state leptons. Muons and electrons are considered if their transverse momentum with respect to the collision axis z , $p_T \equiv \sqrt{p_x^2 + p_y^2}$, and their pseudorapidity $\eta \equiv \frac{1}{2} \ln \frac{|\vec{p}| + p_z}{|\vec{p}| - p_z}$, satisfy

$$\begin{aligned} p_T^\ell &> 15 \text{ GeV}, & |\eta^\mu| &< 2.5, \\ |\eta^e| &< 1.37 & \text{or} & 1.52 < |\eta^e| < 2.47. \end{aligned} \quad (2.58)$$

To guarantee the isolation of muons (electrons), we require that the scalar sum of the p_T of the particles within $\Delta R \equiv \sqrt{\Delta\eta^2 + \Delta\phi^2} = 0.3$ of the muon (electron), excluding the muon (electron) track, is smaller than 15% (13%) of the charged lepton p_T . In the cases when the final state contains both muons and electrons, a further isolation requirement has been imposed:

$$\Delta R_{e\mu} > 0.1. \quad (2.59)$$

It is also required that at least two leptons with the same flavour and opposite charge are present in the event and that their invariant mass is compatible with the Z mass, i.e.

$$M_{\ell^+\ell^-} \in [M_Z - 10, M_Z + 10] \text{ GeV}. \quad (2.60)$$

In what follows we refer to p^Z as the momentum of this $\ell^+\ell^-$ pair, $p^Z \equiv p^{\ell^+} + p^{\ell^-}$. We further impose that a third lepton is present which passes the above detection requirements and whose transverse momentum satisfies in addition

$$p_T^{\ell'} > 20 \text{ GeV}. \quad (2.61)$$

Moreover, with the purpose of suppressing most of the $Z + \text{jets}$ and other diboson production backgrounds, we require

$$E_T^{\text{miss}} > 25 \text{ GeV} \quad \text{and} \quad M_T^W > 20 \text{ GeV}, \quad (2.62)$$

where E_T^{miss} is the missing transverse energy and the transverse mass is $M_T^W = \sqrt{2p_T^{\ell'} E_T^{\text{miss}} (1 - \cos(\Delta\phi))}$, with $p_T^{\ell'}$ being the transverse momentum of the third lepton, and $\Delta\phi$ the azimuthal angle between the missing transverse momentum and the third lepton. Finally, it is required that at least one electron or one muon has a transverse momentum complying with

$$p_T^{e(\mu)} > 25 \text{ (20) GeV}. \quad (2.63)$$

Our Monte Carlo simulations have been tuned to the ATLAS ones [156], so as to incorporate more realistic detection efficiencies. Initially, a global k -factor is introduced to account for the higher order corrections to the process in Eq. (2.57) by comparing our leading order predictions to the NLO ones used in the ATLAS search [156], leading to $k \sim 1.7$. Next, we compare our results after cuts with the ones quoted by ATLAS in Table 1 of Ref. [156]. We tune our simulation by applying a correction factor per flavour channel (eee , $ee\mu$, $e\mu\mu$ and $\mu\mu\mu$) that is almost equivalent to introducing a detection efficiency of $\epsilon^e = 0.8$ (0.95) for electrons (muons). These efficiencies have been employed in our simulations for signal and backgrounds.

After the selection procedure, in the presence of anomalous TGVs the cross section for the process $pp \rightarrow \ell'^\pm \ell^+ \ell^- E_T^{\text{miss}}$ can be qualitatively described by:

$$\sigma = \sigma_{\text{bck}} + \sigma_{SM} + \sum_{i,j \geq i} \sigma_{\text{ano}}^{ij} g_{\text{ano}}^i g_{\text{ano}}^j. \quad (2.64)$$

Here σ_{SM} corresponds to the irreducible SM $W^\pm Z$ background, while σ_{bck} stands for all background sources except for the SM EW $W^\pm Z$ production. Additionally σ_{ano}^{ij} are the pure anomalous contributions. Notice that because of the CP-violating nature of the anomalous couplings there is no interference between those and the SM contributing to the total cross section. Furthermore in the present study we assume only one coupling departing from its SM value at a time (i.e. always $i = j$) which, as mentioned above, is consistent with the expectations from the dynamical Higgs effective operators, Eq. (2.44), since they lead to independent modifications of the two relevant effective couplings g_4^Z and $\tilde{\kappa}_Z$. We present in Table 2.1 the values of σ_{SM} , σ_{bck} and σ_{ano} for center-of-mass energies of 7, 8 and 14 TeV⁷.

COM Energy	σ_{SM} (fb)	σ_{bck} (fb)	$\sigma_{\text{ano}}^{g_4^Z}$ (fb)	$\sigma_{\text{ano}}^{\tilde{\kappa}_z}$	$\sigma_{\text{ano}}^{\tilde{\lambda}_z}$
7 TeV	47.7	14.3	846	56.0	1914
8 TeV	55.3	16.8	1117	67.7	2556
14 TeV	97.0	29.0	3034	134	7471

Table 2.1: Values of the cross section predictions for the process $pp \rightarrow \ell'^\pm \ell^+ \ell^- E_T^{\text{miss}}$ after applying all the cuts described in the text. σ_{SM} is the SM contribution coming from EW $W^\pm Z$ production, σ_{ano}^i are the pure anomalous contributions and σ_{bck} corresponds to all the background sources except for the electroweak SM $W^\pm Z$ production.

⁷For completeness we make our study for the most general CP-violating WWZ vertex in Eq. (2.43) and evaluate the sensitivity to $\tilde{\lambda}^Z$ as well, even though this coupling is generated at higher order in the chiral expansion as shown in Eq. (2.44).

In order to quantify the reachable sensitivity on the determination of the different anomalous TGVs, advantage has been taken in this analysis of the fact that anomalous TGVs enhance the cross sections at high energies. Ref. [155] shows that the variables M_{WZ}^{rec} (the reconstructed WZ invariant mass), $p_T^{\ell \text{ max}}$ and p_T^Z are able to trace well this energy dependence, leading to similar sensitivities to the anomalous TGVs. Here, we chose p_T^Z because this variable is strongly correlated with the subprocess center-of-mass energy (\hat{s}), and, furthermore, it can be directly reconstructed with good precision from the measured lepton momenta. In the left (right) panel of Fig. 2.3 we show the number of expected events with respect to the transverse momentum of the Z candidate for the 7 (14) TeV run, assuming an integrated luminosity of $\mathcal{L} = 4.64$ (300) fb^{-1} . The figure captures the enhancement of events at the higher values of p_T^Z that the presence of anomalous TGV interactions causes. We can also observe how the effect of $\tilde{\kappa}_Z$ is weaker than the effect of introducing g_4^Z or $\tilde{\lambda}_Z$.

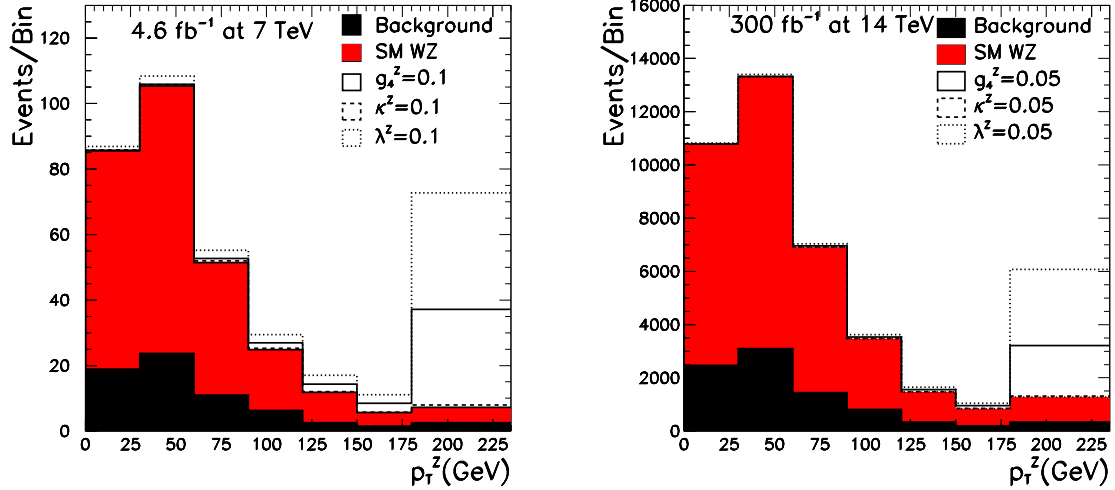


Figure 2.3: Distribution of events with respect to p_T^Z for the 7 (14) TeV run assuming $\mathcal{L} = 4.64$ (300) fb^{-1} of integrated luminosity in the left (right) panel. The black histogram contains all background sources, except for the SM $W^\pm Z$ production, the red histogram represents the sum of all the backgrounds and finally the solid (dashed) [dotted] distribution corresponds to the addition of the contribution of an anomalous TGV with a value $g_4^Z = 0.1$ ($\tilde{\kappa}_Z = 0.1$) [$\tilde{\lambda}_Z = 0.1$] for the 7 TeV run and $g_4^Z = 0.05$ ($\tilde{\kappa}_Z = 0.05$) [$\tilde{\lambda}_Z = 0.05$] for the 14 TeV run. The last bin contains all the events with $p_T^Z > 180$ GeV.

We have followed two procedures to estimate the LHC potential to probe anomalous CP-violating couplings. In a more conservative approach, we have performed a simple

event counting analysis assuming that the number of observed events corresponds to the SM prediction, and we look for the values of the corresponding anomalous couplings which are inside the 68% and 95% CL allowed regions. In this case an additional cut $p_T^Z > 90$ GeV was applied in the analysis to enhance the sensitivity [155]. On a second analysis, a simple χ^2 has been built based on the contents of the different bins of the p_T^Z distribution, with the binning shown in Fig. 2.3. Once again, it is assumed that the observed p_T^Z spectrum corresponds to the SM expectations and we seek the values of the corresponding anomalous couplings that are inside the 68% and 95% allowed regions. In general the binned analysis yields 10% – 30% better sensitivity. The results of the binned analysis are presented in Table 2.2.

	68% C.L. range		95% C.L. range	
	7+8 TeV	7+8+14 TeV	7+8 TeV	7+8+14 TeV
g_4^Z	(-0.019, 0.019)	(-0.007, 0.007)	(-0.027, 0.027)	(-0.010, 0.010)
$\tilde{\kappa}_Z$	(-0.12, 0.12)	(-0.047, 0.047)	(-0.17, 0.17)	(-0.067, 0.067)
$\tilde{\lambda}_Z$	(-0.012, 0.012)	(-0.004, 0.004)	(-0.018, 0.018)	(-0.006, 0.006)
c_4	(-0.074, 0.074)	(-0.027, 0.027)	(-0.10, 0.10)	(-0.039, 0.039)
$c_1 - 2\frac{c_\theta^2}{s_\theta^2}c_8$	(-0.25, 0.25)	(-0.099, 0.099)	(-0.36, 0.36)	(-0.14, 0.14)

Table 2.2: Expected sensitivity on g_4^Z , $\tilde{\kappa}_Z$ and $\tilde{\lambda}_Z$ at the LHC, and the corresponding precision reachable on the non-linear operator coefficients. We assume $\mathcal{L} = 4.64 \text{ fb}^{-1}$ for the 7 TeV run, $\mathcal{L} = 19.6 \text{ fb}^{-1}$ for the 8 TeV one and $\mathcal{L} = 300 \text{ fb}^{-1}$ for the future 14 TeV expectations.

From Table 2.2 we read that the 7 and 8 TeV data sets could clearly increase the existing limits on g_4^Z , and consequently on c_4 , and the future 14 TeV run would rapidly approach the few per cent level. Conversely, as it was expected, the reachable sensitivity on $\tilde{\kappa}_Z$ is weaker. Nevertheless, the future 14 TeV run has the potential to improve the direct bounds that LEP was able to derive, and settle consequently the strongest direct available limits on the corresponding combination of c_1 and c_8 couplings. Notice that this combination is different from the c_1 and c_8 combination contributing to $\tilde{\kappa}_\gamma$, which is bounded from EDM measurements, see Eqs. (2.44) and (2.54). Thus, both measurements are complementary.

Up to this point the analysis that we have performed has not benefitted from the CP-odd nature of the TGV interactions. Different studies [155, 161–163] have addressed the CP-odd nature of the anomalous TGVs by constructing some CP-odd or \hat{T} -odd observable. In particular, in Ref. [162] it was shown that ideally in $pp \rightarrow W^\pm Z$ an asymmetric

observable based on the sign of the cross-product $p_q \cdot (p_Z \times p_{\ell'})$ could be a direct probe of CP-violation, where here p_q is the four-momentum of the incoming quark. At the LHC, however, p_q cannot be fully determined and for this reason we build instead as a reconstructable correlated sign variable

$$\Xi_{\pm} \equiv \text{sign}(p^{\ell'})_z \text{sign}(p^{\ell'} \times p^Z)_z, \quad (2.65)$$

where z is the collision axis. We define the sign-weighted cross section as

$$\Delta\sigma \equiv \int d\sigma \Xi_{\pm} \equiv \sum_i g_{\text{ano}}^i \Delta\sigma_{\text{ano}}^i. \quad (2.66)$$

A CP-odd TGV gives a measurable contribution to this sign-weighted cross section which is linearly dependent on the coupling. On the contrary the SM background is symmetric with respect to Ξ_{\pm} and it gives a null contribution to the sign-weighted cross section in Eq. (2.66). This behaviour is illustrated in Fig. 2.4 where we show the distribution of events at 14 TeV, assuming 300 fb^{-1} of integrated luminosity, with respect to the related variable

$$\cos\theta_{\Xi} \equiv \cos\theta^{\ell'} \cos\theta^{Z \times \ell'}, \quad (2.67)$$

where the angles are defined with respect to the z axis. In this form $\text{sign}(\cos\theta_{\Xi}) = \Xi_{\pm}$.

The corresponding sign-weighted cross sections at 14 TeV are

$$\Delta\sigma_{\text{ano}}^{g_4^Z} = -59 \text{ fb}, \quad \Delta\sigma_{\text{ano}}^{\tilde{\kappa}_Z} = -9.7 \text{ fb}, \quad \Delta\sigma_{\text{ano}}^{\tilde{\lambda}_Z} = -137 \text{ fb}. \quad (2.68)$$

With a luminosity of 300 fb^{-1} this CP-violation induced asymmetry could be observed with 95% CL above the statistical fluctuations of the SM background for

$$|g_4^Z| \geq 0.02, \quad |\tilde{\kappa}_Z| \geq 0.13, \quad |\tilde{\lambda}_Z| \geq 0.01, \quad (2.69)$$

or what is equivalent for

$$|c_4 \xi^2| \geq 0.08, \quad \left| \xi \left(c_1 - 2 \frac{c_\theta^2}{s_\theta^2} c_8 \xi \right) \right| \geq 0.27. \quad (2.70)$$

2.3.3 CP violation in Higgs couplings to gauge-boson pairs

The effective operators described in Eq. (2.35) also give rise to CP-odd interactions involving the Higgs particle and two gauge bosons, to which we refer as HVV couplings. The CP-odd interactions can be phenomenologically parametrized as

$$\begin{aligned} \mathcal{L}_{\text{eff},CP}^{\text{HVV}} = & \tilde{g}_{Hgg} h G_{\mu\nu}^a \tilde{G}^{a\mu\nu} + \tilde{g}_{H\gamma\gamma} h A_{\mu\nu} \tilde{A}^{\mu\nu} + \tilde{g}_{HZ\gamma} h A_{\mu\nu} \tilde{Z}^{\mu\nu} \\ & + \tilde{g}_{HZZ}^{(2)} h Z_{\mu\nu} \tilde{Z}^{\mu\nu} + \tilde{g}_{HWW}^{(2)} h W_{\mu\nu}^+ \tilde{W}^{-\mu\nu} \\ & + \left[\tilde{g}_{HWW}^{(1)} (W_{\mu\nu}^+ W^{-\mu} \partial^\nu h) + \text{h.c.} \right] + \left[\tilde{g}_{HWW}^{(5)} (\partial_\mu W^{+\mu} W_\nu^- \partial^\nu h) + \text{h.c.} \right], \end{aligned} \quad (2.71)$$

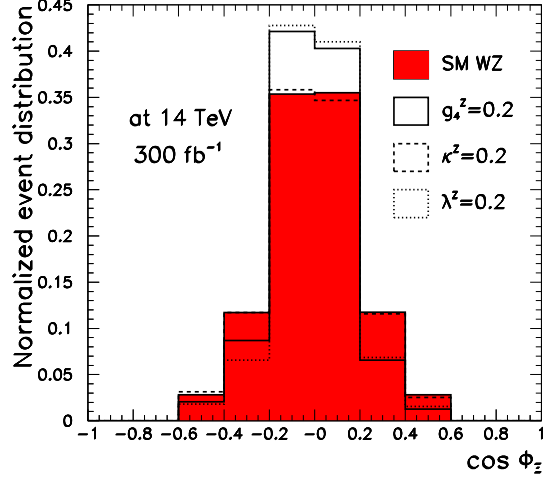


Figure 2.4: Distribution of $pp \rightarrow \ell'^\pm \ell^\pm \ell^- E_T^{\text{miss}}$ contributions with respect to $\cos \theta_\Xi$, for 300 fb^{-1} of integrated luminosity collected at 14 TeV, after the cuts described from Eqs. (2.58)–(2.62). The sign-symmetric electroweak SM $W^\pm Z$ distribution is shown as the red histogram and the distribution for the SM plus the contribution of $g_4^Z = 0.2$ ($\tilde{\lambda}_Z = 0.2$) [$\tilde{\lambda}_Z = 0.2$] is shown as the solid (dashed) [dotted] line. All the distributions are normalized to one for an easier comparison.

with tree level contributions

$$\begin{aligned}
\tilde{g}_{Hgg} &= -\frac{g_S^2}{v} \hat{a}_{\tilde{G}} \xi, & \tilde{g}_{H\gamma\gamma} &= \frac{4e^2}{v} \xi \left(-\frac{1}{4} \hat{a}_{\tilde{B}} + \hat{a}_8 \xi + \hat{a}_1 - \frac{1}{8} \hat{a}_{\tilde{W}} \right), \\
\tilde{g}_{HZ\gamma} &= -\frac{8e^2 s_\theta}{v c_\theta} \xi \left[-\frac{1}{4} \hat{a}_{\tilde{B}} - \frac{c_\theta^2}{2s_\theta^2} \left(-\frac{1}{4} \hat{a}_{\tilde{W}} + 2\hat{a}_8 \xi \right) + \frac{1}{8s_\theta^2} (2\hat{a}_2 + \hat{a}_3 + 2\hat{a}_9 \xi) - \frac{c_{2\theta}}{2s_\theta^2} \hat{a}_1 \right], \\
\tilde{g}_{HZZ}^{(2)} &= \frac{4e^2 s_\theta^2}{v c_\theta^2} \xi \left(-\frac{1}{4} \hat{a}_{\tilde{B}} + \frac{c_\theta^4}{s_\theta^4} \hat{a}_8 \xi - \frac{c_\theta^2}{s_\theta^2} \hat{a}_1 + \frac{1}{2s_\theta^2} \hat{a}_2 - \frac{c_\theta^4}{8s_\theta^4} \hat{a}_{\tilde{W}} - \frac{c_\theta^2}{2s_\theta^4} \hat{a}_9 \xi - \frac{c_\theta^2}{4s_\theta^4} \hat{a}_3 \right), \\
\tilde{g}_{HWW}^{(2)} &= -\frac{2e^2}{v s_\theta^2} \xi \left(\frac{1}{2} \hat{a}_{\tilde{W}} + \hat{a}_3 \right), & \tilde{g}_{HWW}^{(1)} &= \frac{2e^2}{v s_\theta^2} i \hat{a}_7 \xi^2, & \tilde{g}_{HWW}^{(5)} &= -\frac{2e^2}{v s_\theta^2} i \hat{a}_{12} \xi^2,
\end{aligned} \tag{2.72}$$

and where the \hat{a}_i coefficients have been defined in Eq. (2.37). Additionally, the effective CP-odd Higgs-fermion couplings induced by the mixing effects described in Sec. 2.3.1 generate one-loop induced HVV couplings such as

$$\tilde{g}_{Hgg} = \frac{\alpha_S}{8\pi v} \xi \left(\hat{a}_{2D} - \frac{4p_h^2}{v^2} \hat{a}_{13} \xi \right) F_{\text{odd}}^{\text{CP}}(x_f) = \frac{3}{8} \frac{\alpha_S}{\alpha_{\text{em}}} \tilde{g}_{H\gamma\gamma}, \tag{2.73}$$

where $F_{\text{odd}}^{\text{CP}}(x_f)$ is the form factor from the fermionic one-loop processes [164], that in the limit of high fermion masses ($x_f \equiv 4M_f^2/M_h^2 \gg 1$) is approximately $F_{\text{odd}}^{\text{CP}} = 1$, almost

equal to the form factor for the CP-even Yukawa-fermion contribution to $hG_{\mu\nu}^a G^{a\mu\nu}$ and $hA_{\mu\nu} A^{\mu\nu}$ in the same limit, $F_{\text{even}}^{\text{CP}}(x_f)$. In addition to effects on the Higgs signals, these operators, together with those giving direct contributions to $\tilde{g}_{H\gamma\gamma}$ in Eq. (2.72) give also a contribution to the fermion EDMs [165] of the form⁸

$$d_f = \frac{e^3 m_f}{\pi^2 v^2} \xi \left[-\frac{1}{4} \hat{a}_{\tilde{B}} + \hat{a}_8 \xi + \hat{a}_1 - \frac{1}{8} \hat{a}_{\tilde{W}} + \frac{1}{48\pi^2} \hat{a}_{2D} \left(F_{\text{odd}}^{\text{CP}}(x_{\text{top}}) + \frac{2}{3} F_{\text{even}}^{\text{CP}}(x_{\text{top}}) \right) \right] \times \times \left[\log \frac{\Lambda_s^2}{m_H^2} + \mathcal{O}(1) \right], \quad (2.74)$$

whose size can be constrained, for example, from the present bound on the electron EDM in Eq.(2.52):

$$\left| \xi \left[-\frac{1}{4} \hat{a}_{\tilde{B}} + \hat{a}_8 \xi + \hat{a}_1 - \frac{1}{8} \hat{a}_{\tilde{W}} + \frac{1}{48\pi^2} \hat{a}_{2D} \left(F_{\text{odd}}^{\text{CP}}(x_{\text{top}}) + \frac{2}{3} F_{\text{even}}^{\text{CP}}(x_{\text{top}}) \right) \right] \times \times \left[\log \left(\frac{\Lambda_s^2}{m_H^2} \right) + \mathcal{O}(1) \right] \right| < 5.6 \times 10^{-5}. \quad (2.75)$$

Measuring the CP properties of the Higgs couplings is a subject with an extensive literature before and after the Higgs discovery. For the sake of concreteness we focus here on the experimental results on the most studied channel, $h \rightarrow ZZ \rightarrow \ell^+ \ell^- \ell'^+ \ell'^-$, for which combined results of the full 7+8 TeV LHC runs have been presented both by CMS [166,167] and ATLAS [168,169] collaborations.

Historically the key observables for measuring the CP properties of the Higgs in this channel were established in the seminal works in Refs [31–33], that were followed by an abundant literature on their applications to the LHC [34–40]. Most of these early phenomenological studies were based on the study of single variable observables. Most recently, an almost together with the first LHC collisions, two different new multivariable methods [41,42] were proposed to use all the kinematic information of the event as input into the likelihood, to compare and exclude between different Higgs spin and parity hypothesis. These phenomenological studies set the roots of the first LHC experimental analyses of spin and CP properties of the Higgs in this channel [166–169].

In particular the results of the experimental constraints from the CMS analysis [166, 167] can be translated into the language of the effective operators of a light dynamical Higgs in Eq. (2.35). With this purpose we notice that in Ref. [167] the $h \rightarrow ZZ$ vertex is

⁸In writing Eq. (2.74) we have only considered the relevant loop of top quarks in the loop-induced part of the $h\gamma\gamma$ vertex (both CP-odd and CP-even) generated by $\mathcal{S}_{2D}(h)$ and we have neglected the corresponding $\mathcal{O}(m_f^2/m_H^2)$ contribution from $\mathcal{S}_{13}(h)$.

described using the notation in [41]:

$$A(h \rightarrow ZZ) = v^{-1} \left(d_1 m_Z^2 \epsilon_1^* \epsilon_2^* + d_2 f_{\mu\nu}^{*(1)} f^{\mu\nu*(2)} + d_3 f_{\mu\nu}^{*(1)} \tilde{f}^{\mu\nu*(2)} \right), \quad (2.76)$$

where $f_{\mu\nu}^{(i)} = \epsilon_\mu^i q_\nu^i - \epsilon_\nu^i q_\mu^i$, $\tilde{f}_{\mu\nu}^{(i)} = \frac{1}{2} \epsilon_{\mu\nu\alpha\beta} f^{\alpha\beta(i)} = \epsilon_{\mu\nu\alpha\beta} \epsilon_i^\alpha q_i^\beta$, with $\epsilon^{1,2}$ being the polarization vectors of the Z bosons and $q_{1,2}$ the corresponding four-momenta. In the SM $d_1 = 2i$, while d_2 only receives marginally contributions from high order diagrams, that can be safely neglected leading to $d_2 = d_3 = 0$. The d_3 term is CP-odd and its interference with the CP-conserving terms d_1 or d_2 leads to the CP-violating signals that are analyzed.

The effective operators in Eq. (2.35) give a non-vanishing contribution to d_3 which, from Eqs. (2.71) and (2.72), reads

$$d_3 = -2i v \tilde{g}_{HZZ}^{(2)}, \quad (2.77)$$

while as long as no CP-conserving operators are considered $d_2 = 0$ and $d_1 = d_{1,SM}$.

In Ref. [167] a measure of CP-violation in the $h \rightarrow ZZ^* \rightarrow 4l$ observables was defined as

$$f_{d_3} = \frac{|d_3|^2 \sigma_3}{|d_1|^2 \sigma_1 + |d_3|^2 \sigma_3}, \quad (2.78)$$

where σ_1 (σ_3) corresponds to the cross section for the process $h \rightarrow ZZ$ when $d_1 = 1$ ($d_3 = 1$) and $d_3 = 0$ ($d_1 = 1$). For $M_h = 125.6$ GeV, $\frac{\sigma_1}{\sigma_3} = 6.36$. In Ref. [167] f_{d_3} was fitted as one of the parameters of the multivariable analysis, obtaining the measured value

$$f_{d_3} = 0.00^{+0.17}_{-0.00} \quad \Rightarrow \quad \frac{|d_3|}{|d_1|} = 0.00^{+1.14}_{-0.00}, \quad (2.79)$$

pointing to the CP-even nature of the state. Furthermore, 95% CL exclusion bounds on f_{d_3} were derived,

$$f_{d_3} < 0.51 \quad \Rightarrow \quad \frac{|d_3|}{|d_1|} < 2.57. \quad (2.80)$$

We can directly translate the bounds in Eq. (2.80) to 68(95)% CL constraints on the coefficients of the relevant CP-violating operators,

$$\left| \xi \left(-\frac{1}{4} \hat{a}_{\tilde{B}} + \frac{c_\theta^4}{s_\theta^4} \hat{a}_8 \xi - \frac{c_\theta^2}{s_\theta^2} \hat{a}_1 + \frac{1}{2s_\theta^2} \hat{a}_2 - \frac{c_\theta^4}{8s_\theta^4} \hat{a}_{\tilde{W}} - \frac{c_\theta^2}{2s_\theta^4} \hat{a}_9 \xi - \frac{c_\theta^2}{4s_\theta^4} \hat{a}_3 \right) \right| \leq 10.3 \text{ (23.3)}. \quad (2.81)$$

In Ref. [170] the same analysis was applied to derive the future expectations when $300(3000)$ fb^{-1} are collected at 14 TeV. The corresponding expected sensitivities at 95% CL are

$$f_{d_3} \leq 0.13 \text{ (0.04)} \quad \text{for} \quad 300 \text{ (3000)} \text{ fb}^{-1}. \quad (2.82)$$

They can be translated into the following sensitivity at 95% CL to the relevant combination of operators:

$$\left| \xi \left(-\frac{1}{4} \hat{a}_{\tilde{B}} + \frac{c_\theta^4}{s_\theta^4} \hat{a}_8 \xi - \frac{c_\theta^2}{s_\theta^2} \hat{a}_1 + \frac{1}{2s_\theta^2} \hat{a}_2 - \frac{c_\theta^4}{8s_\theta^4} \hat{a}_{\tilde{W}} - \frac{c_\theta^2}{2s_\theta^4} \hat{a}_9 \xi - \frac{c_\theta^2}{4s_\theta^4} \hat{a}_3 \right) \right| \leq 8.8 \quad (4.6), \quad (2.83)$$

for 300 (3000) fb^{-1} .

Observables to study the CP properties of the Higgs couplings have also been proposed in the production channel $pp \rightarrow hjj$ followed by the Higgs decay into $\tau^+\tau^-$, W^+W^- , or $\gamma\gamma$ [43–53]. Depending on the kinematic cuts imposed, the study is most sensitive to CP-violating effects in the hWW (from $\mathcal{S}_{\tilde{W}}(h)$, $\mathcal{S}_3(h)$ and/or $\mathcal{S}_7(h)$) and hZZ (from $\mathcal{S}_{\tilde{B}}(h)$, $\mathcal{S}_{\tilde{W}}(h)$, $\mathcal{S}_1(h)$, $\mathcal{S}_2(h)$, $\mathcal{S}_3(h)$, $\mathcal{S}_8(h)$ and/or $\mathcal{S}_9(h)$) vertices contributing to Higgs production through vector boson fusion, or in the hgg vertex (from $\mathcal{S}_{\tilde{G}}(h)$, and from loop induced $\mathcal{S}_{2D}(h)$ and $\mathcal{S}_{13}(h)$) contributing to production by gluon fusion. The sensitivity to CP violating observables in associated production processes $pp \rightarrow hZ \rightarrow b\bar{b}\ell^+\ell^-$ and $pp \rightarrow hW \rightarrow \ell^+ jj E_T^{\text{miss}}$ has also been studied in Refs. [51, 54–58], and in pure gluon fusion production followed by Higgs decay into $\gamma\gamma$ or to $Z\gamma$ [59–62].

Finally, it is also possible to quantify the potential to observe or bound CP-odd interactions from global analyses of the Higgs signal strengths [63–65]. However in this case the analysis does not contain any genuinely CP-violating observable and consequently it is always sensitive to combinations of CP-even and CP-odd interactions.

So far only the pure gauge and gauge- h sector have been analysed for the effective chiral approach. As soon as the fermion sector is coupled to the gauge fields, Flavor physics has to be analysed also, as it will be sensitive to the assumed flavor prescription for the fermion-gauge couplings. In Chapter 3 the Minimal Flavor Violation (MFV) hypothesis is assumed and implemented within the the effective chiral approach previously described.

Chapter 3

Fermion- h sector and flavour effects

In the previous chapters, the gauge and gauge- h sectors were tackled via an effective chiral Lagrangian formalism and the tower of effective CP-conserving and CP-violating operators was also established. Now, if we extend this formalism in order to cover the fermion sector, flavour physics has to be accounted for some flavour prescription. We are considering non-linear EWSB scenarios, and when facing flavour we will do it via the MFV ansatz, where NP operator coefficients will have a flavour structure dictated by such hypothesis, within a strong dynamics at the scale Λ_s and in the presence of a light Higgs particle. For the case of a Higgs degree of freedom integrated out from the physical spectrum, the MFV hypothesis was already analysed in the presence of a strong interacting dynamics and introduced in Ref. [171], where the relevant flavour-changing chiral operators at the leading order of the expansion were listed. A realistic approach leads to couple them to a light scalar Higgs, and to consider as well their main loop-induced effects as in Ref. [68]. A more complete and extended list of this type of operators can be found in the Ref. [30]. In here we only focus on those ones relevant for flavour-changing processes and couple to a light Higgs contribution [68].

3.1 Fermion-gauge- h couplings

Fermion-gauge operators involving two right-handed (RH) or two left-handed (LH) fields can be constructed by implementing the chiral building blocks \mathbf{T} and \mathbf{V}_μ defined in Eq. (2.15), and FCNC processes could appear from them if a MFV ansatz, encoded in the spurion coupling λ_F of Eq. (1.34), is incorporated in the approach.

A total of four independent chiral operators containing LH fermion fields¹ can be

¹Only operators built with two LH fermions can induce flavour-changing effects at leading order in the spurion expansion, and therefore terms with two RH fermions will not be considered here.

constructed [171–174], namely:

$$\begin{aligned}\mathcal{O}_1 &= \frac{i}{2} \bar{Q}_L \lambda_F \gamma^\mu \{ \mathbf{T}, \mathbf{V}_\mu \} Q_L, & \mathcal{O}_2 &= i \bar{Q}_L \lambda_F \gamma^\mu \mathbf{V}_\mu Q_L, \\ \mathcal{O}_3 &= i \bar{Q}_L \lambda_F \gamma^\mu \mathbf{T} \mathbf{V}_\mu \mathbf{T} Q_L, & \mathcal{O}_4 &= \frac{1}{2} \bar{Q}_L \lambda_F \gamma^\mu [\mathbf{T}, \mathbf{V}_\mu] Q_L.\end{aligned}\tag{3.1}$$

Under CP-transformations, the set $\mathcal{O}_1 - \mathcal{O}_3$ turn out to be CP-even, while \mathcal{O}_4 transforms as CP-odd [171]. The remarkable presence of the CP-odd operator \mathcal{O}_4 , violating CP at leading order in this framework with no complex coefficients introduced (as in Refs. [175, 176]), is a slight modification of the MFV ansatz² with respect to the standard MFV hypothesis with EWSB linearly realized in Ref. [71], the which exhibits at its leading order ($d = 6$) four operators involving the Higgs field and two fermions, named \mathcal{O}_{H_1} , \mathcal{O}_{H_2} , \mathcal{O}_{G_1} and \mathcal{O}_{F_1} . Only two of them, \mathcal{O}_{H_1} and \mathcal{O}_{H_2} , produce the same low-energy effects (for energy $E \ll v$) than our operators \mathcal{O}_1 and \mathcal{O}_2 , connected by the correspondences

$$\mathcal{O}_1 \iff \mathcal{O}_{H_1} = -i (\bar{Q}_L \lambda_{FC} \gamma^\mu Q_L) (\Phi^\dagger \overleftrightarrow{D}_\mu \Phi)$$

$$\mathcal{O}_2 \iff \mathcal{O}_{H_2} = -i (\bar{Q}_L \lambda_{FC} \gamma^\mu \tau^i Q_L) (\Phi^\dagger \tau_i \overleftrightarrow{D}_\mu \Phi)$$

whereas the linear *siblings* of our leading operators \mathcal{O}_3 and \mathcal{O}_4 in Eq. (A.12) have not been considered in Ref. [71], as they would have dimension $d = 8$ in the linear realization,

$$\mathcal{O}_3 \iff \mathcal{O}_{H_3} = -i (\bar{Q}_L \lambda_{FC} \gamma^\mu \tau^i Q_L) (H^\dagger \tau_i H) (H^\dagger \overleftrightarrow{D}_\mu H)$$

$$\mathcal{O}_4 \iff \mathcal{O}_{H_4} = -i \epsilon^{ijk} (\bar{Q}_L \lambda_{FC} \gamma^\mu \tau_i Q_L) (H^\dagger \tau_j H) (H^\dagger \tau_k \overleftrightarrow{D}_\mu H).$$

Conversely, the siblings of the other two operators in the linear expansion, \mathcal{O}_{G_1} and \mathcal{O}_{F_1} , do not appear at dimension $d_\chi = 4$ in the non-linear expansion, as they are only at

²Our only requirement is the invariance under the flavour group \mathcal{G}_f for all operators built out of the SM model fields (and \mathbf{U}) and the spurions $Y_{U,D}$. In Ref. [71] the invariance under CP was additionally assumed by restraining all operator coefficients to be real; no genuine CP-odd operator stems at leading order of the linear expansion (the sibling of \mathcal{O}_4 would appear in it only at higher order). In our approach we will keep the new source of CP violation naturally present at leading order only for the non-linear expansion, for its theoretical and phenomenological interest.

$d_\chi = 5$. In consequence, the phenomenological signals of MFV is expected to exhibit notable differences between the two scenarios.

So far only fermion-gauge interactions have been described in the set of Eq. (3.1). A more general and realistic scenario would account for a light Higgs contribution in those interactions. Indeed, letting the operators \mathcal{O}_i be coupled to a corresponding light Higgs expansion as

$$\mathcal{O}_i(h) \equiv \mathcal{O}_i \mathcal{F}_i(h), \quad (3.2)$$

fermion-gauge- h interacting vertexes are obtained at tree level in the unitary gauge. Again the functions $\mathcal{F}_i(h)$ are $(h + \langle h \rangle)$ -dependent³. The operators coefficients of $\mathcal{O}_1 - \mathcal{O}_4$ are bounded from analysing $\Delta F = 1$ and $\Delta F = 2$ observables in Ref. [171], and commented in Appendix C. Bounds obtained there are not sensitive to a light scalar h contribution and the overall operator coefficients in Eq. (3.2) may differ from their Higgsless counterparts in Eqs. (A.12) only through a (negligible) loop contribution.

To realize now to which linear siblings the operators in Eq. (A.12) correspond to, consider the effective Lagrangian expansion

$$\mathcal{L}_{eff}^f = \xi \sum_{i=1}^3 \hat{a}_i \mathcal{O}_i(h) + \xi^2 \hat{a}_4 \mathcal{O}_4(h) \quad (3.3)$$

where a redefinition by powers of ξ of the operators coefficients defined in Ref. [171] has been implemented, $a_i \equiv \xi \hat{a}_i$ for $i = 1, 2, 3$, while $a_4 \equiv \xi^2 \hat{a}_4$. Notice that the lowest-dimension siblings of \mathcal{O}_1 and \mathcal{O}_2 arise at $d = 6$, whereas for \mathcal{O}_4 is at $d = 8$ [171]. For \mathcal{O}_3 the situation is indeed special, as it corresponds to a combination of $d = 6$ and $d = 8$ operators in the linear expansion [171]. In fact, for $\xi \ll 1$, the functions $\mathcal{F}_i(h)$ can be expanded into combinations of $F(h)$ similar as that in Eq. (2.20), such that

$$\begin{aligned} \mathcal{O}_1(h) &\equiv \mathcal{O}_1 F(h) (1 + \alpha_1 \xi F(h)) , & \mathcal{O}_2(h) &\equiv \mathcal{O}_2 F(h) (1 + \alpha_2 \xi F(h)) , \\ \mathcal{O}_3(h) &\equiv \mathcal{O}_3 F(h) (1 + \alpha_3 \xi F(h)) , & \mathcal{O}_4(h) &\equiv \mathcal{O}_4 F^2(h) , \end{aligned} \quad (3.4)$$

the contribution from siblings up to $d = 8$ have been accounted for \mathcal{O}_3 (further contributions will arise considering higher-dimension siblings), but not only for \mathcal{O}_3 , also possible $d = 8$ -siblings contributions for \mathcal{O}_1 and \mathcal{O}_2 .

The $\xi \ll 1$ -limit keeps linear terms in ξ , being negligible contributions from $\mathcal{O}_4(h)$ ⁴

³Only terms linear in h should be retained in Eq. (3.3); for the same reason it is neither pertinent to consider couplings containing $\partial_\mu h$ (that is, derivatives of $\mathcal{F}(h)$).

⁴ $\mathcal{O}_3(h)$ coincides with $-\mathcal{O}_2(h)$ [171], then only two linearly-independent flavoured operators remain (e.g. $\mathcal{O}_1(h)$ and $\mathcal{O}_2(h)$), as previously studied in the literature.

For the $\xi \sim 1$ limit all four operators are relevant and higher order terms in ξ may contribute. And one recognizes the need of a QCD-like resummation. In particular any chiral operator is made up by an infinite combination of linear ones, an effect represented by the generic $\mathcal{F}_i(h)$ functions, which admit in general an expansion in powers of ξ as discussed previously.

Finally, the low-energy effective flavour Lagrangian induced by $\mathcal{O}_1(h)–\mathcal{O}_4(h)$ operators in Eq. (3.3), in the unitary gauge reads

$$\begin{aligned} \mathcal{L}_{eff}^f = & -\frac{g}{\sqrt{2}} W_\mu^+ \bar{U}_L \gamma^\mu \left[a_W \left(1 + \beta_W \frac{h}{v} \right) + i a_{CP} \left(1 + \beta_{CP} \frac{h}{v} \right) \right] (\mathbf{y}_U^2 V + V \mathbf{y}_D^2) D_L + \text{h.c.} + \\ & - \frac{g}{2 \cos \theta_W} Z_\mu \left[a_Z^u \bar{U}_L \gamma^\mu (\mathbf{y}_U^2 + V \mathbf{y}_D^2 V^\dagger) U_L \left(1 + \beta_Z^u \frac{h}{v} \right) + \right. \\ & \left. + a_Z^d \bar{D}_L \gamma^\mu (\mathbf{y}_D^2 + V^\dagger \mathbf{y}_U^2 V) D_L \left(1 + \beta_Z^d \frac{h}{v} \right) \right], \end{aligned} \quad (3.5)$$

where

$$\begin{aligned} a_Z^u & \equiv a_1 + a_2 + a_3, & a_Z^d & \equiv a_1 - a_2 - a_3, \\ a_W & \equiv a_2 - a_3, & a_{CP} & \equiv -a_4. \end{aligned} \quad (3.6)$$

Coefficients β_i in Eq. (3.5) are similarly defined as the coefficients a_i in Eq. (3.6), once the $\mathcal{F}(h)$ functions are expanded to first order in h , $\mathcal{F}_i(h) \sim (1 + \beta_i h + \dots)$; in general each β_i may receive contributions from all orders in ξ for large ξ . In Eq. (3.5) are present at low-energies vertices with additional external h -legs, differing with respect to the strongly interacting heavy Higgs scenarios, and implying interesting phenomenological consequences illustrated later on. Coefficients a_Z^d , a_W and a_{CP} are bounded in Ref. [171] from tree-level contributions to observables.

When considering loop-level impact from these coefficients to radiative processes such as the $b \rightarrow s\gamma$ decay, possible bounds are also obtained and the effective next to leading order operators in the expansion, i.e. those operators suppressed by the strong dynamics scale Λ_s , have to be considered in the analysis as they contribute at tree-level to that process. Such operators and their phenomenological consequences are considered in the next section.

3.2 Operators suppressed by Λ_s

Gauge invariant operators suppressed by Λ_s and relevant for flavour must have a bilinear structure in the quark fields of the type $\bar{Q}_L(\dots) \mathbf{U}(x) Q_R$, where dots stand for objects that transform in the trivial or in the adjoint representation of $SU(2)_L$. Besides the vector and scalar chiral fields \mathbf{V}_μ and \mathbf{T} , they can contain either the rank-2 antisymmetric tensor $\sigma_{\mu\nu}$ or the strength tensors $B_{\mu\nu}$, $W_{\mu\nu}$ and $G_{\mu\nu}$. Moreover, operators constructed from the antisymmetric rank 2 chiral tensor, transforming in the adjoint of $SU(2)_L$ and defined as

$$\mathbf{V}_{\mu\nu} \equiv \mathcal{D}_\mu \mathbf{V}_\nu - \mathcal{D}_\nu \mathbf{V}_\mu = i g \mathbf{W}_{\mu\nu} - i \frac{g}{2} B_{\mu\nu} \mathbf{T} + [\mathbf{V}_\mu, \mathbf{V}_\nu]. \quad (3.7)$$

are not linearly independent from those listed in Eqs. (3.8)-(3.9), as the second equality in Eq. (3.7) shows.

According to their Lorentz structure, the resulting independent chiral couplings can be classified in three main groups:

i) **dipole-type operators:**

$$\begin{aligned} \mathcal{X}_1 &= g' \bar{Q}_L \sigma^{\mu\nu} \mathbf{U} Q_R B_{\mu\nu}, & \mathcal{X}_2 &= g' \bar{Q}_L \sigma^{\mu\nu} \mathbf{T} \mathbf{U} Q_R B_{\mu\nu}, \\ \mathcal{X}_3 &= g \bar{Q}_L \sigma^{\mu\nu} \sigma_i \mathbf{U} Q_R W_{\mu\nu}^i, & \mathcal{X}_4 &= g \bar{Q}_L \sigma^{\mu\nu} \sigma_i \mathbf{T} \mathbf{U} Q_R W_{\mu\nu}^i, \\ \mathcal{X}_5 &= g_s \bar{Q}_L \sigma^{\mu\nu} \mathbf{U} Q_R G_{\mu\nu}, & \mathcal{X}_6 &= g_s \bar{Q}_L \sigma^{\mu\nu} \mathbf{T} \mathbf{U} Q_R G_{\mu\nu}, \\ \mathcal{X}_7 &= g \bar{Q}_L \sigma^{\mu\nu} \mathbf{T} \sigma_i \mathbf{U} Q_R W_{\mu\nu}^i, & \mathcal{X}_8 &= g \bar{Q}_L \sigma^{\mu\nu} \mathbf{T} \sigma_i \mathbf{T} \mathbf{U} Q_R W_{\mu\nu}^i; \end{aligned} \quad (3.8)$$

ii) **operators containing the rank-2 antisymmetric tensor $\sigma^{\mu\nu}$:**

$$\begin{aligned} \mathcal{X}_9 &= \bar{Q}_L \sigma^{\mu\nu} [\mathbf{V}_\mu, \mathbf{V}_\nu] \mathbf{U} Q_R, & \mathcal{X}_{10} &= \bar{Q}_L \sigma^{\mu\nu} [\mathbf{V}_\mu, \mathbf{V}_\nu] \mathbf{T} \mathbf{U} Q_R, \\ \mathcal{X}_{11} &= \bar{Q}_L \sigma^{\mu\nu} [\mathbf{V}_\mu \mathbf{T}, \mathbf{V}_\nu \mathbf{T}] \mathbf{U} Q_R, & \mathcal{X}_{12} &= \bar{Q}_L \sigma^{\mu\nu} [\mathbf{V}_\mu \mathbf{T}, \mathbf{V}_\nu \mathbf{T}] \mathbf{T} \mathbf{U} Q_R; \end{aligned} \quad (3.9)$$

iii) **other operators containing the chiral vector fields \mathbf{V}_μ :**

$$\begin{aligned} \mathcal{X}_{13} &= \bar{Q}_L \mathbf{V}_\mu \mathbf{V}^\mu \mathbf{U} Q_R, & \mathcal{X}_{14} &= \bar{Q}_L \mathbf{V}_\mu \mathbf{V}^\mu \mathbf{T} \mathbf{U} Q_R, \\ \mathcal{X}_{15} &= \bar{Q}_L \mathbf{V}_\mu \mathbf{T} \mathbf{V}^\mu \mathbf{U} Q_R, & \mathcal{X}_{16} &= \bar{Q}_L \mathbf{V}_\mu \mathbf{T} \mathbf{V}^\mu \mathbf{T} \mathbf{U} Q_R, \\ \mathcal{X}_{17} &= \bar{Q}_L \mathbf{T} \mathbf{V}_\mu \mathbf{T} \mathbf{V}^\mu \mathbf{U} Q_R, & \mathcal{X}_{18} &= \bar{Q}_L \mathbf{T} \mathbf{V}_\mu \mathbf{T} \mathbf{V}^\mu \mathbf{T} \mathbf{U} Q_R. \end{aligned} \quad (3.10)$$

The effective chiral Lagrangian contribution from these fermion-gauge flavour-changing operators turns out to be

$$\Delta \mathcal{L}_\mathcal{X} = \sum_{i=1}^{18} b_i \frac{\mathcal{X}_i}{\Lambda_s}, \quad (3.11)$$

with all the operators suppressed by the strong dynamics scale⁵ Λ_s , and b_i arbitrary $\mathcal{O}(1)$ operator coefficients. Redefining the latter it is possible to link them to their lowest-dimension siblings in the linear expansion

$$\Delta\mathcal{L}_{\mathcal{X}} = \sqrt{\xi} \sum_{i=1}^8 \hat{b}_i \frac{\mathcal{X}_i}{\Lambda_s} + \xi \sqrt{\xi} \sum_{i=9}^{18} \hat{b}_i \frac{\mathcal{X}_i}{\Lambda_s}. \quad (3.12)$$

\mathcal{X}_{1-6} correspond to $d = 6$ operators in the linear expansion, while \mathcal{X}_7 and \mathcal{X}_8 to combinations from $d = 6$ and $d = 8$ siblings. Furthermore, \mathcal{X}_{9-18} will have linear siblings of $d = 8$, but \mathcal{X}_{17} and \mathcal{X}_{18} that are combinations of $d = 8$ and $d = 10$ operators in the linear regime. For the small ξ limit the lowest siblings are retained in Eq. (3.12), all them being listed in Appendix C.

Interactions encoded in $\Delta\mathcal{L}_{\mathcal{X}}$ of Eq. (3.11) can be split in the unitary gauge as

$$\delta\mathcal{L}_{\mathcal{X}} = \Delta\mathcal{L}_{\mathcal{X}}^u + \Delta\mathcal{L}_{\mathcal{X}}^d + \Delta\mathcal{L}_{\mathcal{X}}^{u-d}, \quad (3.13)$$

where

$$\begin{aligned} \Delta\mathcal{L}_{\mathcal{X}}^d = & \frac{g^2}{4 \cos \theta_W^2 \Lambda_s} \frac{b_Z^d}{\Lambda_s} \bar{D}_L D_R Z_\mu Z^\mu + \frac{g^2}{2 \Lambda_s} \frac{b_W^d}{\Lambda_s} \bar{D}_L D_R W_\mu^+ W^{-\mu} + g^2 \frac{c_W^d}{\Lambda_s} \bar{D}_L \sigma^{\mu\nu} D_R W_\mu^+ W_\nu^- + \\ & + e \frac{d_F^d}{\Lambda_s} \bar{D}_L \sigma^{\mu\nu} D_R F_{\mu\nu} + \frac{g}{2 \cos \theta_W} \frac{d_Z^d}{\Lambda_s} \bar{D}_L \sigma^{\mu\nu} D_R Z_{\mu\nu} + g_s \frac{d_G^d}{\Lambda_s} \bar{D}_L \sigma^{\mu\nu} D_R G_{\mu\nu} + \text{h.c.}, \end{aligned} \quad (3.14)$$

$$\begin{aligned} \Delta\mathcal{L}_{\mathcal{X}}^{u-d} = & \frac{g^2}{2\sqrt{2} \cos \theta_W} \left(\frac{b_{WZ}^+}{\Lambda_s} \bar{U}_L D_R W_\mu^+ Z^\mu + \frac{b_{WZ}^-}{\Lambda_s} \bar{D}_L U_R W_\mu^- Z^\mu \right) + \\ & + \frac{g^2}{2\sqrt{2} \cos \theta_W} \left(\frac{c_{WZ}^+}{\Lambda_s} \bar{U}_L \sigma^{\mu\nu} D_R W_\mu^+ Z_\nu + \frac{c_{WZ}^-}{\Lambda_s} \bar{D}_L \sigma^{\mu\nu} U_R W_\mu^- Z_\nu \right) + \\ & + \frac{g}{\sqrt{2}} \left(\frac{d_W^+}{\Lambda_s} \bar{U}_L \sigma^{\mu\nu} D_R W_{\mu\nu}^+ + \frac{d_W^-}{\Lambda_s} \bar{D}_L \sigma^{\mu\nu} U_R W_{\mu\nu}^- \right) + \text{h.c.}, \end{aligned} \quad (3.15)$$

and analogously for $\Delta\mathcal{L}_{\mathcal{X}}^u$ as in $\Delta\mathcal{L}_{\mathcal{X}}^d$ interchanging $d \leftrightarrow u$ and $D_{L,R} \leftrightarrow U_{L,R}$. In these equations $W_{\mu\nu}^\pm = \partial_\mu W_\nu^\pm - \partial_\nu W_\mu^\pm \pm i g (W_\mu^3 W_\nu^\pm - W_\nu^3 W_\mu^\pm)$, while the photon and Z field strengths are defined as $F_{\mu\nu} = \partial_\mu A_\nu - \partial_\nu A_\mu$ and $Z_{\mu\nu} = \partial_\mu Z_\nu - \partial_\nu Z_\mu$, respectively. Coefficients in Eqs. (3.14) and (3.15) are related to those defined in Eq. (3.11) and reported in Appendix D.

⁵It is worth to underline that for the analysis of the non-linear operators \mathcal{X}_i , the relevant scale is Λ_s and not f as for the analysis in the previous section. Indeed, f is associated to light Higgs insertions, while Λ_s refers to the characteristic scale of the strong resonances that, once integrated out, give rise to the operators listed in Eqs. (3.8)-(3.10).

Tree level impact to $b \rightarrow s\gamma$ decay from these fermion-gauge chiral operators \mathcal{X}_i are possible, in addition to the loop-level contributions from the leading order operators \mathcal{O}_i in Eqs. (A.12), (3.5) and (3.6). Before dealing with the bounds from both of the contributions, let us recall the bounds existing in the literature [171] on the coefficients in Eq. (3.6) from $\Delta F = 1$ and $\Delta F = 2$ observables.

3.3 Phenomenological analysis

The phenomenological impact from the effective operators, encoded in the expansions of Eq. (3.5) and (3.13)-(3.15) are analysed in this section, where bounds existing in the literature [171] on the coefficients of the flavour-changing chiral operators are resumed and updated, and then discussed new bounds and other phenomenological considerations with and without a light Higgs:

- Loop level impact of fermion-gauge chiral operators (\mathcal{O}_1 to \mathcal{O}_4) on those same radiative decays;
- Tree-level bounds on the fermion-gauge chiral operators \mathcal{X}_i , from radiative decays;
- Light Higgs to fermions couplings, from operators $\mathcal{O}_1(h)$ to $\mathcal{O}_4(h)$.

3.3.1 $\Delta F = 1$ and $\Delta F = 2$ observables

Operator coefficients in Eq. (3.5) have been bounded from $\Delta F = 1$ and $\Delta F = 2$ observables, in a MFV ansatz within a strong Higgs dynamics approach in Ref. [171], and can be straightforwardly applied to non-linear regimes with a light h scalar. In fact, tree-level Z -mediated FCNC (Fig. 3.1) induced from \mathcal{O}_{1-3} in Eq. (3.5), together with the MFV structure playing role there, allow sizeable flavour-changing effects that, for the down quark sector⁶ turns out to be constraining a_Z^d as

$$-0.044 < a_Z^d < 0.009 \quad \text{at 95\% of C.L.} \quad (3.16)$$

from $K^+ \rightarrow \pi^+ \bar{\nu}\nu$, $B \rightarrow X_s \ell^+ \ell^-$ and $B \rightarrow \mu^+ \mu^-$ data providing the strongest constraints. Appendix C summarizes another similar bounds, as well as the set of tree level Wilson coefficients modifications from \mathcal{O}_{1-3} employed for bounding the coefficient a_Z^d .

⁶For the purposes of the present work, only $\Delta F = 1$ processes involving K and B mesons need to be considered. New up-type tree-level FCNC contributions in Eq. (3.5) neglected in here as being strengthened by a non-diagonal spurion combination $V \mathbf{y}_D^2 V^\dagger$, subleading with respect to that one in the down sector, $V^\dagger \mathbf{y}_U^2 V$, by at least a factor y_b^2/y_t^2 .

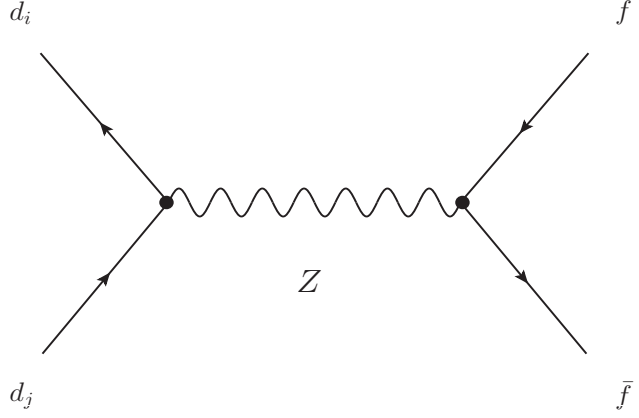


Figure 3.1: Tree-level Z -mediated FCNC from \mathcal{O}_{1-3} . f accounts for any SM fermion field.

In addition, W -mediated box diagrams (Fig. 3.2) suffer from couplings modifications in Eq. (3.5) from \mathcal{O}_{2-4} contributions, and consequently $\Delta F = 2$ transitions are sensitive too⁷. Regarding these transitions, in Ref. [171] have been analysed

- The CP-violating parameter ϵ_K of the $K^0 - \bar{K}^0$ system and the mixing-induced CP asymmetries $S_{\psi K_S}$ and $S_{\psi \phi}$ in the decays $B_d^0 \rightarrow \psi K_S$ and $B_s^0 \rightarrow \psi \phi$. Induced corrections to ϵ_K are proportional to y_t^2 , whereas those to $S_{\psi K_S}$ and $S_{\psi \phi}$ are proportional to y_b^2 . Consequently, possible large deviations from the predicted SM values are only allowed in the K system.
- The ratio among the meson mass differences in the B_d and B_s systems, $R_{\Delta M_B} \equiv \Delta M_{B_d}/\Delta M_{B_s}$. The NP contributions on the mass differences almost cancel in this ratio and therefore departures with respect to the SM prediction for this observable are negligible.
- The ratio among the $B^+ \rightarrow \tau^+ \nu$ branching ratio and the B_d mass difference, $R_{BR/\Delta M} \equiv BR(B^+ \rightarrow \tau^+ \nu)/\Delta M_{B_d}$. This observable is clean from theoretical hadronic uncertainties and the constraints on the NP parameters are therefore potentially strong.

⁷Tree-level FCNC Z diagrams can be relevant also and considered later soon, while Z -mediated boxes and weak penguin diagrams are safely neglected as being suppressed wrt tree-level Z contributions.

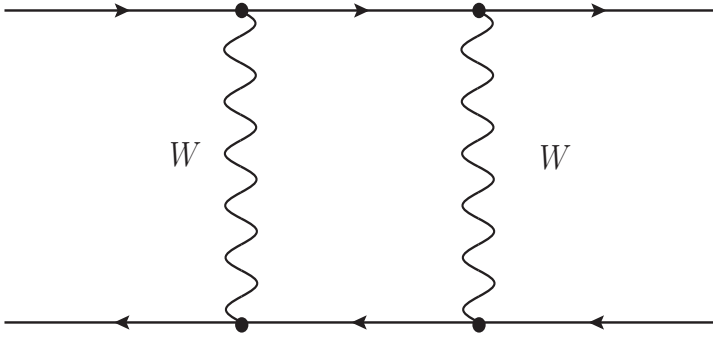


Figure 3.2: W -mediated box diagrams sensitive to couplings modifications in Eq. (3.5) from \mathcal{O}_{2-4} contributions, impacting thus in $\Delta F = 2$ transitions. f accounts for any SM fermion field.

Small and slight departures with respect to the SM prediction for $S_{\psi K_S}$ are allowed, and then only values close to the exclusive determination for $|V_{ub}|$ are favoured (Appendix C summarizes this, Ref. [171] discusses it in detail.). A $|V_{ub}| - \gamma$ parameter space, with γ being one of the angles of the unitary triangle, is bounded by requiring that both $S_{\psi K_S}$ and $R_{\Delta M_B}$ observables are inside the 3σ experimental determination. Choosing, as an example, the reference point $(|V_{ub}|, \gamma) = (3.5 \times 10^{-3}, 66^\circ)$ from the parameter space, is possible to predict SM values for ϵ_K and $R_{BR/\Delta M}$ as⁸

$$\epsilon_K = 1.88 \times 10^{-3}, \quad R_{BR/\Delta M} = 1.62 \times 10^{-4}, \quad (3.17)$$

that should be compared to the corresponding experimental determinations⁹. The errors on these quantities are $\sim 15\%$ and $\sim 8\%$, estimated considering the uncertainties on the input parameters and the analysis performed in Ref. [177].

A correlation between ϵ_K and $R_{BR/\Delta M}$, and therefore a $a_{CP} - a_W$ parameter space are obtained by requiring that ϵ_K and $R_{BR/\Delta M}$ lie inside their own 3σ experimental de-

⁸The predicted SM value for ϵ_K differs from that in Ref. [171] due to the new input parameters used: in particular $\hat{B}_K = 0.7643 \pm 0.0097$ has sensibly increased [179].

⁹ $(R_{BR/\Delta M})_{exp}$ has been computed considering the recent world average $BR(B^+ \rightarrow \tau^+ \nu) = (0.99 \pm 0.25) \times 10^{-4}$ from Ref. [180].

$$(\epsilon_K)_{exp} = (2.228 \pm 0.011) \times 10^{-3}, \quad (R_{BR/\Delta M})_{exp} = (1.95 \pm 0.49) \times 10^{-4}, \quad (3.18)$$

termination, as it can be seen in Fig. B.3 from Ref. [171]. Finally, the allowed $a_{CP} - a_W$ parameter space leads to the mixing-induced CP-asymmetry $S_{\psi\phi}$ and the B semileptonic CP-asymmetry to be near the SM prediction, in agreement with the recent LHCb measurements [178].

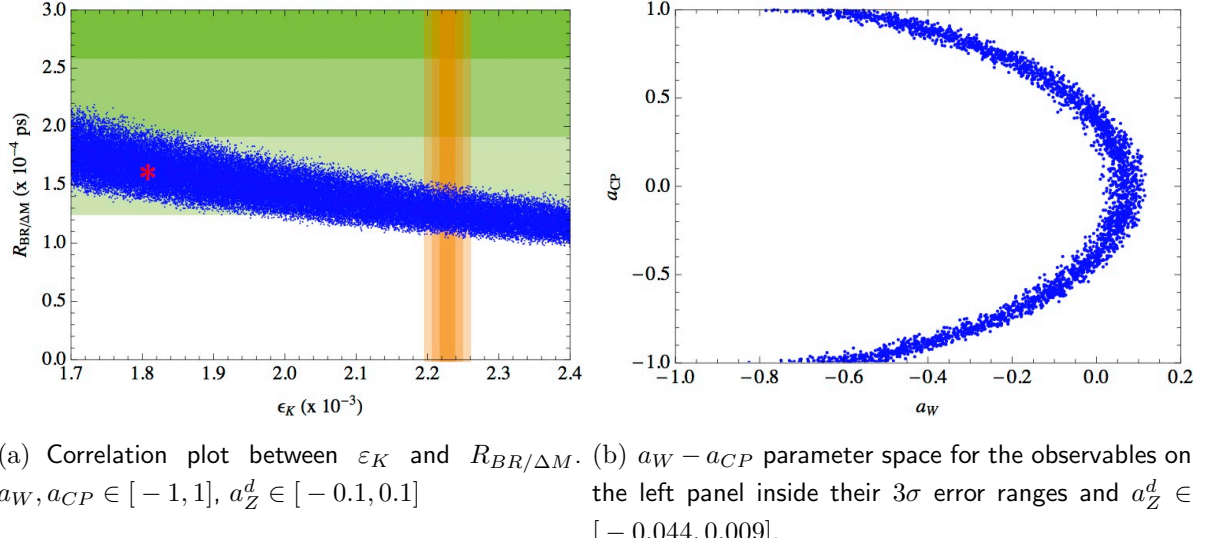


Figure 3.3: Results for the reference point $(|V_{ub}|, \gamma) = (3.5 \times 10^{-3}, 66^\circ)$. Left panel: in red the SM prediction and its 1σ theoretical error bands for ϵ_K and $R_{BR/\Delta M}$ for this reference point; in orange (green) the 1σ , 2σ and 3σ (from the darker to the lighter) experimental error ranges for ϵ_K ($R_{BR/\Delta M}$), in blue the correlation between ϵ_K and $R_{BR/\Delta M}$ induced by NP contributions. Right panel: allowed values for a_W and a_{CP} upon the setup of the left panel. See Ref. [171] for further details.

In Appendix C are summarized all the bounds from the implemented $\Delta F = 1$ and $\Delta F = 2$ observables in the framework. More specifically, the set of Wilson coefficients departures with respect to the SM value and the limits obtained from $\Delta F = 1$ constraints are provided, whilst the corresponding box diagrams modifications contributing to the corresponding $\Delta F = 2$ observables are analysed together with the allowed bounds, correlations and parameter space therein.

Additionally to the aforementioned $a_{CP} - a_W$ parameter space from ϵ_K - $R_{BR/\Delta M}$ correlations, new limits on a_W and a_{CP} are possible from their loop-level impact on radiative B decays. Processes that also receive tree level contributions from the set of chiral operators \mathcal{X}_i in Sect. 3.2¹⁰ Next section focus on the former contributions.

¹⁰They are expected a priori to be all of comparable strength, the most powerful experimental constraints should result from the tree-level impact of dipole operators \mathcal{X}_1 to \mathcal{X}_8 , as they include vertices

3.3.2 $\bar{B} \rightarrow X_s \gamma$ branching ratio

The current experimental value of the $\bar{B} \rightarrow X_s \gamma$ branching ratio [181] is

$$Br(\bar{B} \rightarrow X_s \gamma) = (3.31 \pm 0.16 \pm 0.30 \pm 0.10) \times 10^{-4}, \quad (3.19)$$

for a photon-energy cut-off $E_\gamma > 1.6$ GeV. On the other hand, its NNLO SM prediction for that same energy cut-off and in the \bar{B} -meson rest frame, reads [182–184]

$$Br(\bar{B} \rightarrow X_s \gamma) = (3.15 \pm 0.23) \times 10^{-4}. \quad (3.20)$$

NP can impact on this SM prediction and can also be bounded by the precision from the experimental measure. SM contribution to the $b \rightarrow s\gamma$ decay can be accounted by the effective Lagrangian at the $\mu_b = \mathcal{O}(m_b)$ scale as

$$\mathcal{L}_{eff} = \frac{4G_F}{\sqrt{2}} V_{ts}^* V_{tb} \left[\sum_{i=1}^6 C_i(\mu_b) Q_i(\mu_b) + C_{7\gamma}(\mu_b) Q_{7\gamma}(\mu_b) + C_{8G}(\mu_b) Q_{8G}(\mu_b) \right], \quad (3.21)$$

with $Q_{1,2}$, $Q_{3,\dots,6}$ and $Q_{7\gamma,8G}$ current-current, QCD penguin and magnetic dipole operators, respectively, and terms proportional to $V_{us}^* V_{ub}$ have been neglected¹¹.

Wilson coefficients $C_i(\mu_b)$ at the scale μ_b are derived via QCD renormalisation group (RG) running of the corresponding Wilson coefficients at the higher effective scale μ of the underlying theory, which is the matching scale linking the effective and full descriptions, and turning out to be the electroweak scale $\mu = \mathcal{O}(M_W)$ for the SM case. RG effects are in general non-negligible, enhancing at the end the SM $b \rightarrow s\gamma$ decay rate by a factor of $2 - 3$ [183] after including those effects, sourced dominantly by the mixing of charged current-current operators with the dipole operators, and to a smaller extent from the mixing with QCD-penguin operators. These QCD effects can be formally encoded as

$$C_i(\mu_b) = U_{ij}(\mu_b, \mu) C_j(\mu), \quad (3.22)$$

where $U_{ij}(\mu_b, \mu)$ are the RG evolution matrix elements running from the effective scale μ down to μ_b [185].

The expression for the $\bar{B} \rightarrow X_s \gamma$ branching ratio can be compactly written as

$$Br(\bar{B} \rightarrow X_s \gamma) = R (|C_{7\gamma}(\mu_b)|^2 + N(E_\gamma)), \quad (3.23)$$

involving just three fields, one of them being a light gauge boson. Photonic penguins and also gluonic penguins and tree-level four-fermion diagrams (through renormalization group mixing effects) will be explored below and contrasted with radiative B decays.

¹¹The same applies to the contributions from the so-called primed operators, similar to those appearing in Eq. (3.21) although with opposite chirality structure, which are suppressed by the m_s/m_b ratio.

where $R = 2.47 \times 10^{-3}$ is simply an overall factor as discussed in Refs. [182, 184] and $N(E_\gamma) = (3.6 \pm 0.6) \times 10^{-3}$ a non-perturbative contribution for the photon-energy cut-off $E_\gamma > 1.6$ GeV. $C_{7\gamma}(\mu_b)$ can be split into SM and NP contributions as

$$C_{7\gamma}(\mu_b) = C_{7\gamma}^{SM}(\mu_b) + \Delta C_{7\gamma}(\mu_b), \quad (3.24)$$

where, for $\mu_b = 2.5$ GeV, the SM contribution at the NNLO level, is given by [182–184] $C_{7\gamma}^{SM}(\mu_b) = -0.3523$.

Non-unitarity CKM matrix modifications and flavour violating Z -fermion couplings induced by the chiral operators \mathcal{O}_{1-4} , as well as direct contributions from the chiral operators \mathcal{X}_{1-8} will be the source for NP impact in $\Delta C_{7\gamma}(\mu_b)$. Focus first in the former effects.

\mathcal{O}_{1-4} impact

The effective scale of the chiral operators is $f \geq v$, but no contributions to the Wilson coefficients relevant for $b \rightarrow s\gamma$ arise at scales above the electroweak one. As a result, the analysis of these contributions is alike to that in the SM, except for the fact that the NP operators modify the initial conditions at μ_W . The Wilson coefficients at the scale μ_W can be written as

$$C_i(\mu_W) = C_i^{SM}(\mu_W) + \Delta C_i(\mu_W), \quad (3.25)$$

with the SM coefficients at the LO given by [186]

$$\begin{aligned} C_2^{SM}(\mu_W) &= 1, \\ C_{7\gamma}^{SM}(\mu_W) &= \frac{7x_t - 5x_t^2 - 8x_t^3}{24(x_t - 1)^3} + \frac{-2x_t^2 + 3x_t^3}{4(x_t - 1)^4} \log x_t, \\ C_{8G}^{SM}(\mu_W) &= \frac{2x_t + 5x_t^2 - x_t^3}{8(x_t - 1)^3} + \frac{-3x_t^2}{4(x_t - 1)^4} \log x_t, \end{aligned} \quad (3.26)$$

where $x_t \equiv m_t^2/M_W^2$. Non-unitarity CKM matrix modifications induce corrections to all the three Wilson coefficients encoded [68] as

$$\begin{aligned} \Delta C_2(\mu_W) &= (a_W - i a_{CP}) y_b^2 + (a_W^2 + a_{CP}^2) y_b^2 y_c^2, \\ \Delta C_{7\gamma}(\mu_W) &= (2a_W y_t^2 + (a_W^2 + a_{CP}^2) y_t^4) \left(\frac{23}{36} + C_{7\gamma}^{SM}(\mu_W) \right), \\ \Delta C_{8G}(\mu_W) &= (2a_W y_t^2 + (a_W^2 + a_{CP}^2) y_t^4) \left(\frac{1}{3} + C_{8G}^{SM}(\mu_W) \right). \end{aligned} \quad (3.27)$$

Contributions through W boson exchange are proportional to a_W and a_{CP} , modifying tree-level vertex couplings for Q_2 as well as vertexes for the 1-loop penguin diagrams giving rise to $Q_{7\gamma}$ and Q_{8G} (more details in Appendix C). On the other hand, the new flavour-changing Z -fermion vertices participate in penguin diagrams contributing to the $b \rightarrow s\gamma$ decay amplitude, with a Z boson running in the loop [187]. These contributions can be safely neglected, though, because they are proportional to the $a_Z^{u,d}$ parameters, which are already severely constrained from their tree-level impact on other FCNC processes.

Including the QCD RG corrections, the NP contributions at LO to the Wilson coefficients are given by:

$$\Delta C_{7\gamma}(\mu_b) = \eta^{\frac{16}{23}} \Delta C_{7\gamma}(\mu_W) + \frac{8}{3} \left(\eta^{\frac{14}{23}} - \eta^{\frac{16}{23}} \right) \Delta C_{8G}(\mu_W) + \Delta C_2(\mu_W) \sum_{i=1}^8 \kappa_i \eta^{\sigma_i}, \quad (3.28)$$

with

$$\eta \equiv \frac{\alpha_s(\mu_W)}{\alpha_s(\mu_b)} = 0.45. \quad (3.29)$$

Here κ 's and σ 's are the magic numbers listed in Tab. 3.1, while η has been calculated taking $\alpha_s(M_Z = 91.1876 \text{ GeV}) = 0.118$. Due to the simple additive structure of the NP contributions in Eq. (3.25), these magic numbers are the same as in the SM context.

i	1	2	3	4	5	6	7	8
σ_i	$\frac{14}{23}$	$\frac{16}{23}$	$\frac{6}{23}$	$-\frac{12}{23}$	0.4086	-0.4230	-0.8994	0.1456
κ_i	2.2996	-1.0880	$-\frac{3}{7}$	$-\frac{1}{14}$	-0.6494	-0.0380	-0.0185	-0.0057

Table 3.1: The magic numbers for $\Delta C_{7\gamma}(\mu_b)$ defined in Eq. (3.28).

The NP parameter space from the set \mathcal{O}_{1-4} is bounded by the experimental value for $BR(\bar{B} \rightarrow X_s \gamma)$ in Fig. 3.4. Shadowed (grey) exclusion regions from the present loop-level impact on $BR(\bar{B} \rightarrow X_s \gamma)$ are superimposed with Fig. B.3b, based on the analysis of $\Delta F = 2$ observables for the reference point $(|V_{ub}|, \gamma) = (3.5 \times 10^{-3}, 66^\circ)$. Combining both of the analysis is possible to reduce the allowed parameter space in the scatter plot of Fig. B.3b, by eliminating about half of the points as it is shown in Fig. 3.4.

Fig. 3.4 shows that a_{CP} , the overall coefficient of the genuinely CP-odd coupling \mathcal{O}_4 , and thus of $\mathcal{O}_4(h)$ in Eq. (3.2), is still loosely constrained by low-energy data. This has an interesting phenomenological consequence on Higgs physics prospects, since it translates

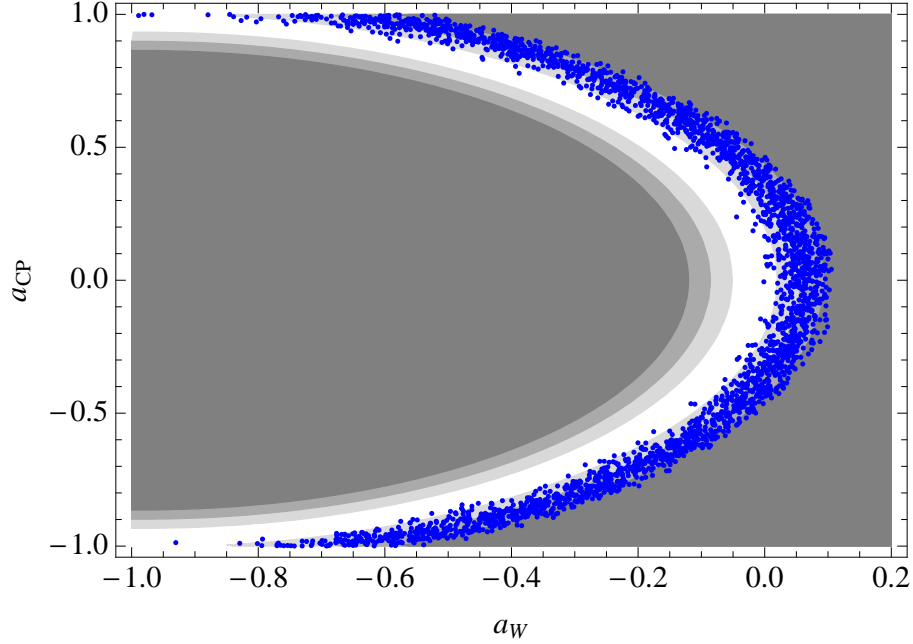


Figure 3.4: $a_W - a_{CP}$ parameter space for ε_K and $BR(B^+ \rightarrow \sigma^+ \nu)/\Delta M_{B_d}$ observables inside their 3σ error ranges and $a_Z^d \in [-0.044, 0.009]$ (see [171] for details). The gray areas correspond to the bounds from the $BR(\bar{B} \rightarrow X_s \gamma)$ at 1σ , 2σ , and 3σ , from the lighter to the darker, respectively.

into correlated exotic Higgs-fermion couplings, which for instance at leading order in h read:

$$\delta \mathcal{L}_{\chi=4}^h \supset a_{CP} \left(1 + \beta_{CP} \frac{h}{v} \right) \mathcal{O}_4 . \quad (3.30)$$

For intermediate values of ξ (for which the linear expansion could be an acceptable guideline), the relative weight of the couplings with and without an external Higgs particle reduces to -see Eq. (3.4)-

$$\beta_{CP} \sim 4 . \quad (3.31)$$

These are encouraging results in the sense of allowing short-term observability. In a conservative perspective, the operator coefficients of the non-linear expansion should be expected to be $\mathcal{O}(1)$. Would this be the case, the possibility of NP detection would be delayed until both low-energy flavour experiments and LHC precision on h -fermion couplings nears the $\mathcal{O}(10^{-2})$ level, which for LHC means to reach at least its 3000 fb^{-1} running regime. Notwithstanding this, a steady improvement of the above bounds should be sought.

\mathcal{X}_i -contributions

For the chiral operators \mathcal{X}_i considered, the effective scale weighting their overall strength is $\Lambda_s \leq 4\pi f$. In the numerical analysis that follows, we will consider for Λ_s the smallest value possible, i.e. $\Lambda_s = 4\pi v$. For this value, the effects due to the operators \mathcal{X}_i are maximized: indeed, for higher scales, the initial conditions for the Wilson coefficients are suppressed with the increasing of Λ_s . This effect is only slightly softened, but not cancelled, by the enhancement due to the QCD running from a higher initial scale. For the analytical expressions, we will keep the discussion at a more general level and the high scale will be denoted by μ_s , $\mu_s \gg v$. At this scale the top and W bosons are still dynamical and therefore they do not contribute yet to any Wilson coefficients. The only operators relevant for $b \rightarrow s\gamma$ decay and with non-vanishing initial conditions are thus $Q_{7\gamma}$ and Q_{8G} , whose contributions arise from the dipole chiral operators \mathcal{X}_i . At the scale μ_s the Wilson coefficients can thus be written as

$$C_i(\mu_s) \equiv C_i^{SM}(\mu_s) + \Delta C_i^{\mathcal{X}}(\mu_s), \quad (3.32)$$

where the only non-vanishing contributions are

$$\Delta C_{7\gamma}^{\mathcal{X}}(\mu_s) = d_F^d \frac{(4\pi)^2 v y_t^2}{\sqrt{2}\mu_s}, \quad \Delta C_{8G}^{\mathcal{X}}(\mu_s) = d_G^d \frac{(4\pi)^2 v y_t^2}{\sqrt{2}\mu_s}, \quad (3.33)$$

with d_F^d and d_G^d denoting the relevant photonic and gluonic dipole operator coefficients in Eq. (3.14), respectively.

The QCD RG analysis from μ_s down to μ_b should be performed in two distinct steps:

- i) A six flavour RG running from the scale μ_s down to μ_W . Focusing on the Wilson coefficients corresponding to the SM and to the \mathcal{X}_i -couplings as well, at the scale μ_W the coefficients read

$$C_i(\mu_W) \equiv C_i^{SM}(\mu_W) + \Delta C_i^{\mathcal{X}}(\mu_W), \quad (3.34)$$

where the only non-vanishing contributions from the set \mathcal{X}_i are those given by

$$\begin{aligned} C_{7\gamma}^{\mathcal{X}}(\mu_W) &= \frac{8}{3} (1 - \eta_{\mu_s}^{2/21}) \eta_{\mu_s}^{2/3} \Delta C_{8G}^{\mathcal{X}}(\mu_s) + \eta_{\mu_s}^{16/21} \Delta C_{7\gamma}^{\mathcal{X}}(\mu_s), \\ C_{8G}^{\mathcal{X}}(\mu_W) &= \eta_{\mu_s}^{2/3} \Delta C_{8G}^{\mathcal{X}}(\mu_s), \end{aligned} \quad (3.35)$$

with

$$\eta_{\mu_s} \equiv \frac{\alpha_s(\mu_s)}{\alpha_s(\mu_W)}. \quad (3.36)$$

In the numerical analysis $\eta_{\mu_s} = 0.67$ will be taken.

ii) A five-flavour RG running from μ_W down to μ_b . This analysis is alike to that described in the previous section, substituting the initial conditions for the Wilson coefficients in Eq. (3.25)-Eq. (3.27) for those in Eqs. (3.34)-(3.36).

It is interesting to focus on the final numerical result for the $BR(\bar{B} \rightarrow X_s \gamma)$, leaving unspecified only the parameters $b_{F,G}^d$:

$$BR(b \rightarrow s\gamma) = 0.000315 - 0.00175 b_{eff}^d + 0.00247 (b_{eff}^d)^2, \quad (3.37)$$

where

$$b_{eff}^d \equiv 3.8 b_F^d + 1.2 b_G^d. \quad (3.38)$$

The corresponding plot is shown on the left-hand side of Fig. 3.5, which depicts the dependence of the branching ratio on b_{eff}^d , together with the experimental 3σ regions. Two distinct ranges for b_{eff}^d are allowed:

$$-0.07 \lesssim b_{eff}^d \lesssim 0.04 \quad \text{or} \quad 0.67 \lesssim b_{eff}^d \lesssim 0.78. \quad (3.39)$$

Using the expression for b_{eff}^d in Eq. (3.38), it is possible to translate these bounds onto the $b_F^d - b_G^d$ parameter space, as shown on the right-hand side of Fig. 3.5. The two narrow bands depict the two allowed regions.

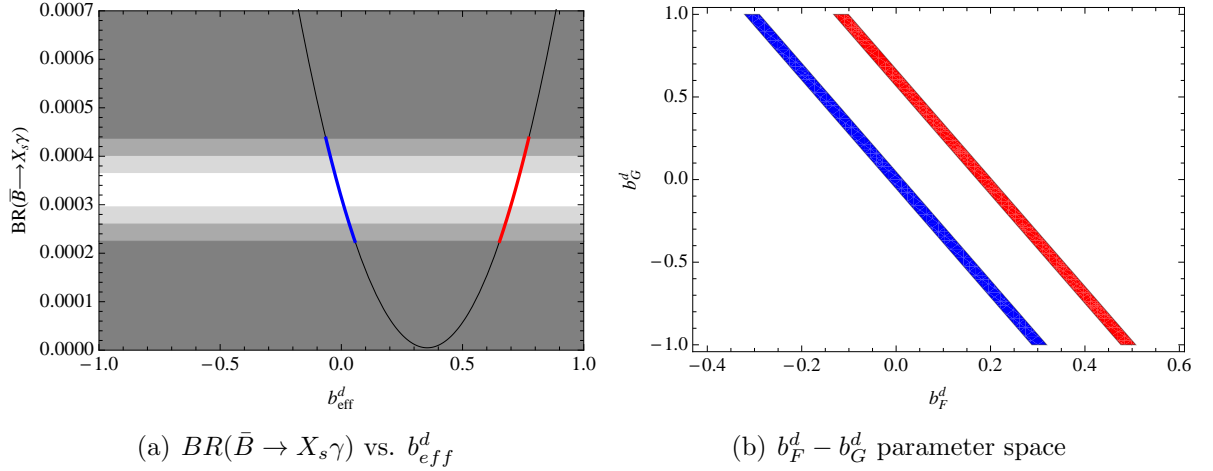


Figure 3.5: $BR(\bar{B} \rightarrow X_s \gamma)$ vs. b_{eff}^d (left panel) and $b_F^d - b_G^d$ parameter space (right panel). Horizontal bands in the left panel are the experimentally excluded regions at 1σ , 2σ , and 3σ , from the lighter to the darker, respectively. The 3σ corresponding allowed $b_F^d - b_G^d$ parameter space is depicted as two separate narrow bands in the right panel.

Analogously to the case of $\mathcal{O}_1(h) \dots \mathcal{O}_4(h)$ operators discussed in the previous subsection, a correlation would hold between a low-energy signal from these \mathcal{X}_i -couplings and

the detection of exotic fermionic couplings at LHC, upon considering their extension to include h -dependent insertions. Nevertheless, a consistent analysis would require in this case to consider $d = 6$ couplings of the non-linear expansion, which are outside the scope of the present work.

Chapter 4

Conclusions

The lack of indications of new resonances at LHC data other than a strong candidate to be the SM scalar boson h , together with the alignment of the couplings of the latter with SM expectations, draws a puzzling panorama with respect to the electroweak hierarchy problem. If the experimental pattern persists, either the extended prejudice against fine-tunings of the SM parameters should be dropped, or the new physics scale is still awaiting discovery and may be associated for instance to a dynamical origin of the SM scalar boson. This thesis work has been inspired by the generic scenario in which a strong dynamics lies behind the origin of a light Higgs particle h , such as in the so-called composite Higgs scenarios, within an effective Lagrangian framework. In fact, it has derived the most general effective couplings in the presence of one light scalar particle h , be it linked to the origin of EWSB or a generic scalar unrelated to it.

The results generalize the operator basis for the bosonic sector of the electroweak non-linear EFT in Refs. [21–25] (which assumed no light scalar in the low-energy spectrum other than the longitudinal components of the W and Z bosons) to the case in which a light scalar h particle is present, up to four-derivatives in the chiral expansion. The basis of independent bosonic operators is now larger, with new couplings present. Furthermore, the functional dependence on h is no more expected to follow in general the pattern in powers of $(v + h)$ characteristic of the SM and of BSM linear-realizations of EWSB, and has been parametrized by generic $\mathcal{F}(h)$ functions, see Eqs. (2.20) and (2.21). The complete set of four-derivative chiral CP-even and CP-odd effective operators has been given in Eqs. (2.27)–(2.35), showing the existence of extra operators also with respect to those recently identified in the literature taking into account a light scalar h [26–29]. The construction of these bases is one of the main results of this work.

In specific composite Higgs models, in which the Higgs is a pseudo-Goldstone boson of a strong dynamics, the parameter describing the degree of non-linearity is the rate

$\xi = (v/f)^2$, where v denotes the EW scale and f the characteristic Goldstone boson scale. ξ must lie in the range $0 < \xi < 1$. Small values indicate a linear regime of EWSB and for $\xi \rightarrow 0$ lead to a low-energy theory undistinguishable from the SM, since all the effects of the strong interacting theory at the high scale become negligible. Larger values indicate a non-linear regime of the EWSB mechanism, and a chiral expansion describes then well the effects of the strong dynamics in a model-independent way. In an EFT approach ξ is not a physical observable, and the analysis of data should be implemented directly to measure/constraint the operator coefficients. Nevertheless, as that parameter allows an easy comparison between the leading correction expected in linear realizations of EWSB versus non-linear ones, we have often redefined the operator coefficients so as to extract and make explicit the ξ dependence expected for each type of coupling. The explicit dependence on ξ for each non-linear operator obtained can be found in Eqs. (2.25)-(2.34), which allowed to establish the correspondence of each non-linear operator with the lowest-dimension operator of the linear expansion that would lead to the same low-energy leading phenomenological couplings. This analysis showed that linear operators of dimensions 6, 8 and 12 are needed to encompass the leading four-derivative effects of the CP-even bosonic non-linear expansion, while linear operators of dimensions 6, 8 and 10 are required in the analogous comparison for CP-odd operators. Details are given in Appendix C.

A curious aspect of CP-violating basis in Eq. (2.35) is the presence among the leading two-derivative corrections of the operator $\mathcal{S}_{2D}(h)$, which impacts the renormalisation of the SM parameters, inducing finally a CP-odd component in the fermion- h and Z - h interactions, see Eqs. (2.41) and (2.42) respectively. No analogous effect is present at the leading order of the linear expansion, i.e. in the SM Lagrangian, as its would-be linear sibling turns out to be a $d = 6$ operator. Similar effects and physical impact stem as well from the four-derivative operator $\mathcal{S}_{13}(h)$. In addition, bounds on the CP-odd non-linear operator coefficients, mainly from anomalous triple vertices, have been established in Sects. 2.3.2-2.3.3. Specifically,

- * Bounds for the relevant non-linear operator coefficients contributing to the fermionic EDMs at 1-loop from the anomalous CP-odd $WW\gamma$ vertex have been obtained, see Eqs. (2.51) and (2.53).
- * Anomalous CP-odd WWZ vertices have been bounded from both CP-blind and from CP-sensitive observables. The strongest limits are still those resulting from LEP analyses, and we have translated them into bounds for the non-linear operator coefficients, see Eq. (2.56). The possible direct measurement of the CP-odd WWZ vertex through CP-blind signals in gauge boson single or pair production at colliders has been analyzed as well.

- * Bounds on the combinations of non-linear operators contributing to the $h\gamma\gamma$ vertex from their contribution to the fermionic EDMs have been determined, as illustrated in Eq. (2.75).
- * We have determined the bounds on combinations of CP-odd TGV couplings from the CMS study of the LHC Higgs boson data at 7 and 8 TeV on the leptonic channels induced by $h \rightarrow ZZ$, see Eq. (2.81). The future CMS sensitivity with the expected 14 TeV data on the same combination of coefficients has been explored, see Eq. (2.83).

By performing a realistic collider analysis of WZ pair production, the present and future potential of LHC to measure anomalous CP-odd TGVs have been estimated in Sec. 2.3.2, via the dependence on kinematic variables that traces the energy behaviour produced in the cross sections by the anomalous TGVs. As a conclusion, LEP bounds can be improved by using the 7 and 8 TeV collected LHC data sets, as shown in Table 2.2, whilst the precision reachable in the future 14 TeV run will approach the per cent level on the anomalous coefficients, proving thus the LHC potential. Furthermore, by means of CP-odd sensitive asymmetries defined in Eq. (2.66), it has been shown that the future LHC run will have the capability to establish the CP nature of the WWZ vertex for a large range of the parameter space that can be covered in that run, see Eqs. (2.69) and (2.70).

Concerning flavour effects in the assumed chiral effective framework, focus has also been given to possible implications for fermionic couplings of a strong interacting origin of electroweak symmetry breaking dynamics with a light scalar h , and with mass around 125 GeV. Flavour-changing operators \mathcal{O}_i for the non-linear regime, as well as those operators \mathcal{X}_i at the next to leading order in the expansion and suppressed by the strong dynamics scale Λ_s , have been identified in Chapter 3. Moreover, taking into account the QCD RG evolution, the coefficients of the latter have been constrained from a plethora of low-energy transitions. In particular we have analyzed in detail and in depth the constraints resulting from the data on $\bar{B} \rightarrow X_s \gamma$ branching ratio. Its impact is important on the global coefficients of the four relevant flavour-changing chiral couplings at the loop level, and on those of the dipole operators. The limits obtained constrain in turn the possible fermion- h exotic couplings to be explored at the LHC. A particularly interesting example is that of the intrinsically CP-odd operator \mathcal{O}_4 of the non-linear expansion, whose coefficient is loosely constrained by data: a correlation is established between the possible signals in low-energy searches of CP-violation and anomalous h -fermion couplings at the LHC. Their relative strength is explored for the case of a relatively small ξ . A similar correlation between low-energy flavour searches and LHC signals also follows for all other operators.

The complete set of independent CP-even and CP-odd leading effective bosonic operators identified here, together with the exploration of certain fermionic effective operators, the new bounds on the strength of the exotic interactions established, and the new phenomenological tools developed, should hopefully be useful in shedding light on the origin of the electroweak symmetry breaking mechanism underlying nature.

Chapter 5

Conclusiones

La no observación de nuevas resonancias en los datos del LHC aparte de la confirmación experimental de la existencia del bosón de Higgs del Modelo Estándar, junto con el alineamiento de los acoplos de dicho bosón con las predicciones teóricas del ME, plantean un panorama desafiante respecto al problema de la jerarquía electrodébil. Si los resultados experimentales persisten, entonces el prejuicio contra el ajuste de los parámetros del ME debe ser abandonado, o la escala de nueva física está aún por ser descubierta y podría estar asociada, por ejemplo, a un origen dinámico del bosón de Higgs. Este trabajo ha sido inspirado por el escenario genérico en el cual una dinámica fuerte subyace al origen de un Higgs liviano h , tal como en los escenarios de Higgs compuesto, y dentro de un marco de Lagrangiano efectivo. De hecho, han sido derivados los acoplos efectivos más generales en presencia de una partícula escalar h , ya sea vinculada al origen de la RSE o un escalar genérico no relacionada con ella.

Este trabajo generaliza la base de operadores para el sector bosónico de una TEC electrodébil no-lineal de las Refs. [21–25] (el cual asume la no presencia de escalares livianos en el espectro de bajas energías diferentes a las componentes longitudinales de los bosones W y Z) al caso en el cual un escalar liviano h está presente, hasta cuatro derivadas en la expansión quiral. La base de operadores bosónicos independientes es ahora más grande, con acoplos nuevos presentes. Además, la dependencia funcional en h no sigue más el patrón en potencias de $(v + h)$ característico del ME y de realizaciones lineales MME de RSE, y ha sido parametrizada mediante funciones genéricas $\mathcal{F}(h)$, ver Eqs. (2.20) and (2.21). La base completa de operadores quirales de cuatro derivadas que conservan y violan la simetría CP ha sido dadas en las Ecs. (2.27)-(2.35), exhibiendo la existencia de operadores extra respecto también a aquellos que dan cuenta de un escalar liviano h recientemente identificados en la literatura [26–29]. La construcción de estas bases es uno de los resultados principales de este trabajo.

En modelos específicos de Higgs compuesto, en el cual el Higgs es un bosón de pseudo-Goldstone de una dinámica fuerte, el parámetro que cuantifica el grado de no-linealidad es el cociente $\xi = (v/f)^2$, donde v denota la EE y f la escala característica de los bosones de Goldstone. ξ debe estar en el rango $0 < \xi < 1$. Valores pequeños de ξ describen regímenes lineales de RSE y para el caso $\xi \rightarrow 0$ se tienen teorías de bajas energías indistinguibles del ME, al ser despreciables todos los efectos de teorías fuertemente interactuantes a altas energías. Valores más grandes caracterizan un régimen no-lineal del mecanismo de RSE, y una expansión quiral describe bien entonces los efectos de dinámica fuerte de manera independiente del modelo. En un escenario de TEC, ξ no es un observable físico y el análisis de datos debería implementar directamente medidas y restricciones para los coeficientes de operadores. No obstante, puesto que el parámetro permite comparar fácilmente correcciones dominantes esperadas en realizaciones lineales de RSE versus no-lineales, hemos redefinido los coeficientes de operadores para extraer y hacer explícita la dependencia esperada en ξ para cada tipo de acople. Dicha dependencia para cada operador no-lineal puede ser vista en las Ecs. (2.25)-(2.34), la cual permite establecer la correspondencia de cada operador no-lineal con los operadores de más baja dimensión de la expansión lineal que conllevarían a los mismos acoplos fenomenológicos de bajas energías. Éste análisis ha mostrado que operadores lineales de dimensiones 6, 8 y 12 son necesarios para vincularlos con los efectos dominantes de cuatro derivadas de la expansión bosónica lineal que conserva CP, mientras operadores lineales de dimensión 6, 8 y 10 son necesarios análogamente para el caso de operadores que violan la simetría CP. Más detalles han sido dados en Apéndice C.

Un aspecto curioso de la base de operadores que no conserva CP en la Ec. (2.35) es la presencia del operador de dos derivadas $\mathcal{S}_{2D}(h)$, el cual afecta la renormalización de los parámetros del ME, induciendo finalmente una componente que viola CP en las interacciones fermión- h y $Z-h$, ver Ecs. (2.41) y (2.42) respectivamente. Efectos análogos en la expansión lineal al orden dominante, es decir en el ME, no están presentes al ser el correspondiente operador lineal de dimensión $d = 6$. Efectos e impacto físico similares provienen así mismo del operador de cuatro derivadas $\mathcal{S}_{13}(h)$. Adicionalmente, cotas para los coeficientes de los operadores no-lineales que violan CP, principalmente aquellos que contribuyen a los vértices cúbicos anómalos, han sido establecidos en las Secciones 2.3.2-2.3.3. Específicamente,

* Cotas para los coeficientes de los operadores no-lineales que contribuyen a 1-lazo al MDEs fermiónico proveniente del vértice anómalo $WW\gamma$ que viola CP, ver Ecs. (2.51) y (2.53).

* Vértices anómalos WWZ que violan CP han sido acotados mediante observables

sensibles a contribuciones de operadores que conservan y violan la simetría CP. Los límites más fuertes aún provienen de los análisis de LEP, y han sido implementados en cotas para los coeficientes de los operadores no-lineales, ver Ec. (2.56). La posible medición directa de vértices WWZ que violan CP mediante señales no sensibles a efectos de CP, en bosones de gauge o en producción de pares en colisionadores también han sido analizada.

- * Cotás en la combinación de operadores no-lineales que contribuyen al vértice $h\gamma\gamma$ han sido determinadas por su contribución al MDE fermiónico, ilustrado en Ec. (2.75).
- * Cotás en combinaciones de acoplos que violan CP han sido determinadas mediante estudios de CMS sobre propiedades del bosón de Higgs en el canal leptónico inducido por $h \rightarrow ZZ$, ver Ec. (2.81). La sensibilidad futura de CMS con los datos esperados a 14 TeV también ha sido explorada en la misma combinación de coeficientes, ver Ec. (2.83).

Realizando un análisis realista de producción de pares WZ en colisionadores, el potencial presente y futuro del LHC para medir acoplos anómalos TGV que violan CP han sido estimados en la Sección 2.3.2, mediante el uso de variables cinemáticas que dan cuenta del comportamiento en la energía producido en las secciones transversales debido a los efectos de acoplos anómalos TGV. Como conclusión, las cotas de LEP pueden ser mejoradas usando datos del LHC a 7 y 8 TeV, como se puede apreciar en las Tablas 2.2, mientras que la precisión alcanzable en el futuro a 14 TeV se acercará al nivel del 1% en los coeficientes anómalos, demostrando así el potencial del LHC. Además, mediante la asimetría definida en Ec. (2.66), ha sido mostrado que el futuro del LHC tendrá la capacidad de establecer la naturaleza CP de los vértices WWZ para un gran rango del espacio de parámetros que puede ser cubierto por los datos del LHC, ver Ecs. (2.69) y (2.70).

En lo que a efectos de sabor en el escenario efectivo quiral asumido se refiere, se ha centrado la atención en posibles implicaciones para los acoplos fermiónicos de un origen interactuante fuerte de RSE con un escalar liviano h , y masa cercana a 125 GeV. Operadores no-lineales que cambian el sabor \mathcal{O}_i , así como también aquellos operadores \mathcal{X}_i subdominantes en la expansión y suprimidos por la escala de dinámica fuerte Λ_s , han sido identificados en el Capítulo 3. Además, al tener en cuenta la evolución de QCD con la energía, los coeficientes provenientes de los operadores \mathcal{X}_i han sido constreñidos de diversas transiciones a bajas energías. En particular, han sido analizados en detalle cotas resultantes de la intensidad del proceso $\bar{B} \rightarrow X_s\gamma$. Su impacto es relevante en los coeficientes globales de los acoplos quirales que cambian el sabor a 1-lazo en las correcciones readiativas, y en aquellos de los operadores dipolares. Los límites obtenidos constriñen los

posibles acoplos exóticos fermiones- h explorables en el LHC. Un ejemplo particularmente interesante es el operador que viola CP \mathcal{O}_4 de la expansión no-lineal, cuyos coeficientes están ligeramente constreñidos por los datos: una correlación es establecida entre las posibles señales de violación de CP a bajas energías y acoplos anómalos h -fermión en el LHC. Su intensidad relativa es explorada para el caso de valores pequeños de ξ . Similar correlación entre búsquedas de sabor a bajas energías y señales del LHC también se aplica al resto de operadores.

El conjunto completo de operadores bosónicos efectivos que conservan y violan CP identificados aquí, junto con la exploración de ciertos operadores fermiónicos, las nuevas cotas en la intensidad de las interacciones exóticas establecidas, y las herramientas fenomenológicas desarrolladas, deberían ser útiles para esclarecer el origen del mecanismo de rompimiento de la simetría electrodébil subyacente a la naturaleza.

APPENDIXES

Appendix A

Useful Formulas for non-linear $d_\chi = 4$ basis

In this appendix, only operators involving fermions and the strong Higgs sector are analyzed. For the complete basis of operators, including all the gauge-strong Higgs interactions, one can refer to [21–23, 172, 173, 188–190].

The main quantities needed in the construction are the basic “covariant” quantities under the SM gauge group are \mathbf{T} and \mathbf{V}_μ in Eq. (2.15). All these quantities are traceless $\text{Tr}(\mathbf{T}) = \text{Tr}(\mathbf{V}_\mu) = 0$, and decomposable via generic 2×2 matrix properties, one can therefore decompose them as $\mathbf{T} = \frac{1}{2}\text{Tr}(\mathbf{T}\tau^i)\tau_i$ and $\mathbf{V}_\mu = \frac{1}{2}\text{Tr}(\mathbf{V}_\mu\tau^i)\tau_i$. Relevant traces in the unitary gauge are

$$\text{Tr}(\mathbf{T}\tau^i)_U = 2\delta_{i3}, \quad \text{Tr}(\mathbf{V}_\mu\tau^a)_U = igW_\mu^a, \quad \text{Tr}(\mathbf{TV}_\mu)_U = i\frac{g}{c_W}Z_\mu, \quad (\text{A.1})$$

for $i = 1, 2, 3$ and $a = 1, 2$ and the suffix index U standing for unitary gauge expressions.

Additionally one has the relations

$$\begin{aligned} \mathbf{V}_\mu &= \frac{1}{2}\text{Tr}(\mathbf{V}_\mu\tau^i)\tau_i, \\ (\mathbf{TV}^\mu + \mathbf{V}^\mu\mathbf{T}) &= \text{Tr}(\mathbf{TV}_\mu)\mathbb{I}_{2 \times 2}, \\ (\mathbf{TV}^\mu - \mathbf{V}^\mu\mathbf{T}) &= \frac{i}{2}\epsilon^{ijk}\text{Tr}(\mathbf{T}\tau_i)\text{Tr}(\mathbf{V}^\mu\tau_j)\tau_k, \\ \mathbf{TV}_\mu\mathbf{T} &= \frac{1}{2}[\text{Tr}(\mathbf{TV}_\mu)\text{Tr}(\mathbf{T}\tau^i) - \text{Tr}(\mathbf{V}_\mu\tau^i)]\tau_i. \end{aligned} \quad (\text{A.2})$$

Employing previous relations operators defined in Eqs. (A.12) can be written alternatively

as

$$\begin{aligned}\mathcal{O}_1 &= \frac{1}{2} J^\mu \text{Tr}(\mathbf{T} \mathbf{V}_\mu) , & \mathcal{O}_2 &= \frac{1}{2} J_i^\mu \text{Tr}(\mathbf{V}_\mu \tau^i) , \\ \mathcal{O}_3 &= \frac{1}{2} J_i^\mu [\text{Tr}(\mathbf{T} \mathbf{V}_\mu) \text{Tr}(\mathbf{T} \tau^i) - \text{Tr}(\mathbf{V}_\mu \tau^i)] , & \mathcal{O}_4 &= \frac{i}{4} \varepsilon^{ijk} \text{Tr}(\mathbf{T} \tau_i) \text{Tr}(\mathbf{V}_\mu \tau_j) J_k^\mu ,\end{aligned}\quad (\text{A.3})$$

with J^μ and J_i^μ the $SU(2)_L$ singlet and triplet currents, respectively:

$$J^\mu = i \bar{Q}_L \lambda_F \gamma^\mu Q_L , \quad J_i^\mu = i \bar{Q}_L \lambda_F \gamma^\mu \tau_i Q_L . \quad (\text{A.4})$$

A.1 CP transformation properties

Under charge (C) and parity (P) symmetries, \mathbf{T} and \mathbf{V}_μ will behave as [23]

$$\mathbf{T}(t, x) \xrightarrow{\mathcal{CP}} -\tau_2 \mathbf{T}(t, -x) \tau_2 , \quad (\text{A.5})$$

$$\mathbf{V}_\mu(t, x) \xrightarrow{\mathcal{CP}} \tau_2 \mathbf{V}^\mu(t, -x) \tau_2 . \quad (\text{A.6})$$

By means of Eqs.(A.5) and (A.6) it is straightforward to recover the transformation properties of the traces:

$$\text{Tr}(\mathbf{T} \tau_i) \xrightarrow{\mathcal{CP}} \text{Tr}(\mathbf{T} \tau_i^*) , \quad (\text{A.7})$$

$$\text{Tr}(\mathbf{V}_\mu \tau_i) \xrightarrow{\mathcal{CP}} -\text{Tr}(\mathbf{V}_\mu \tau_i^*) , \quad (\text{A.8})$$

$$\text{Tr}(\mathbf{T} \mathbf{V}_\mu) \xrightarrow{\mathcal{CP}} -\text{Tr}(\mathbf{T} \mathbf{V}_\mu) . \quad (\text{A.9})$$

Using in addition the transformation properties of the singlet and triplet $SU(2)_L$ fermionic currents:

$$\bar{Q}_L \gamma^\mu Q_L \xrightarrow{\mathcal{CP}} -\bar{Q}_L \gamma_\mu Q_L , \quad (\text{A.10})$$

$$\bar{Q}_L \gamma^\mu \tau_i Q_L \xrightarrow{\mathcal{CP}} -\bar{Q}_L \gamma_\mu \tau_i^* Q_L , \quad (\text{A.11})$$

one can easily verify that $\mathcal{O}_{1,2,3}$ are CP-even, while \mathcal{O}_4 is CP-odd.

One of the most relevant differences of the strong interacting Higgs scenario, with respect to the linear case, is the presence of a new source of CP violation at chiral dimension $d_\chi = 4$.

A.2 Relation with the linear representation

Linking the operators in the non-linear basis with the corresponding ones in the linear realization one has

$$\begin{aligned} \mathcal{O}_1 &\longleftrightarrow -\frac{1}{v^2} \mathcal{O}_{\Phi 1}, & \mathcal{O}_2 &\longleftrightarrow \frac{1}{v^2} \mathcal{O}_{\Phi 2}, \\ \mathcal{O}_3 &\longleftrightarrow \frac{4}{v^4} \mathcal{O}_{\Phi 3} - \frac{1}{v^2} \mathcal{O}_{H2}, & \mathcal{O}_4 &\longleftrightarrow -\frac{2}{v^4} \mathcal{O}_{\Phi 4}, \end{aligned} \quad (\text{A.12})$$

with $\mathcal{O}_{\Phi i}$

$$\mathcal{O}_{\Phi 1} = i (\bar{Q}_L \lambda_{FC} \gamma^\mu Q_L) [\Phi^\dagger (D_\mu \Phi) - (D_\mu \Phi)^\dagger \Phi], \quad (\text{A.13})$$

$$\mathcal{O}_{\Phi 2} = i (\bar{Q}_L \lambda_{FC} \gamma^\mu \tau^i Q_L) [\Phi^\dagger \tau_i (D_\mu \Phi) - (D_\mu \Phi)^\dagger \tau_i \Phi], \quad (\text{A.14})$$

$$\mathcal{O}_{\Phi 3} = i (\bar{Q}_L \lambda_{FC} \gamma^\mu \tau^i Q_L) [\Phi^\dagger \tau_i \Phi] (\Phi^\dagger (D_\mu \Phi) - (D_\mu \Phi)^\dagger \Phi), \quad (\text{A.15})$$

$$\mathcal{O}_{\Phi 4} = i \varepsilon^{ijk} (\bar{Q}_L \lambda_{FC} \gamma^\mu \tau_i Q_L) [\Phi^\dagger \tau_j \Phi] (\Phi^\dagger \tau_k (D_\mu \Phi) - (D_\mu \Phi)^\dagger \tau_k \Phi), \quad (\text{A.16})$$

where the first two operators [71] appear in the linear expansion at dimension $d = 6$, while the last two appear only at dimension $d = 8$, and the following relations have been employed

$$\text{Tr}[\mathbf{T} \mathbf{V}_\mu] \longrightarrow -\frac{2}{v^2} [\Phi^\dagger (D_\mu \Phi) - (D_\mu \Phi)^\dagger \Phi] \quad (\text{A.17})$$

$$\text{Tr}[\mathbf{V}_\mu \tau^i] \longrightarrow \frac{2}{v^2} [\Phi^\dagger \tau^i (D_\mu \Phi) - (D_\mu \Phi)^\dagger \tau^i \Phi] \quad (\text{A.18})$$

$$\text{Tr}[\mathbf{T} \tau^i] \longrightarrow -\frac{4}{v^2} (\Phi^\dagger \tau^i \Phi). \quad (\text{A.19})$$

A.3 Formulae for the Phenomenological Analysis

In this appendix we provide details on the results presented in sects. B.3 and B.4.

A.3.1 $\Delta F = 2$ Wilson Coefficients

The Wilson coefficients of the $\Delta F = 2$ observables in presence of NP can be written separating the contributions from the box diagrams and the tree-level Z diagrams, so that

$$C^{(M)} = \Delta_{Box}^{(M)} C + \Delta_Z^{(M)} C, \quad (\text{A.20})$$

where $M = K, B_d, B_s$. Taking into account only the corrections to the W -quark vertices, we find the following contributions to the Wilson coefficient relevant for $M^0 - \bar{M}^0$ system at the matching scale $\mu_t \approx m_t(m_t)$ ($m_t(m_t)$ is the top quark mass m_t computed at the scale m_t in the $\overline{\text{MS}}$ scheme):

$$\Delta_{Box}^{(M)} C(\mu_t) = \sum_{i,j=u,c,t} \tilde{\lambda}_i \tilde{\lambda}_j F_{ij}, \quad (\text{A.21})$$

where for the K and B_q systems we have respectively

$$\tilde{\lambda}_i = \tilde{V}_{is}^* \tilde{V}_{id}, \quad \tilde{\lambda}_i = \tilde{V}_{ib}^* \tilde{V}_{iq}, \quad (\text{A.22})$$

with \tilde{V} the modified CKM matrix. The F_{ij} are the usual box functions with the exchange of W and up-type quarks (Fig. A.1) defined by

$$\begin{aligned} F_{ij} &\equiv F(x_i, x_j) = \frac{1}{4} \left[(4 + x_i x_j) I_2(x_i, x_j) - 8 x_i x_j I_1(x_i, x_j) \right] \\ I_1(x_i, x_j) &= \frac{1}{(1 - x_i)(1 - x_j)} + \left[\frac{x_i \log(x_i)}{(1 - x_i)^2(x_i - x_j)} + (i \leftrightarrow j) \right] \\ I_2(x_i, x_j) &= \frac{1}{(1 - x_i)(1 - x_j)} + \left[\frac{x_i^2 \log(x_i)}{(1 - x_i)^2(x_i - x_j)} + (i \leftrightarrow j) \right], \end{aligned} \quad (\text{A.23})$$

with $x_i = (m_i/M_W)^2$ (with m_i should be understood as $m_i(m_i)$).

In the SM limit, i.e. switching off the modifications of the W -quark couplings, $\tilde{V} \rightarrow V$ and therefore $\tilde{\lambda}_i \rightarrow \lambda$ and it is possible to rewrite the previous expression in eq. (A.21) in terms of the usual Inami-Lim functions $S_0(x_t)$, $S_0(x_c)$ and $S_0(x_c, x_t)$, using the unitarity relations of the CKM matrix:

$$\begin{aligned} S_0(x_t) &\equiv \frac{4 x_t - 11 x_t^2 + x_t^3}{4(1 - x_t)^2} - \frac{3 x_t^3 \log x_t}{2(1 - x_t)^3} \\ S_0(x_c) &\equiv x_c \\ S_0(x_c, x_t) &\equiv x_c \left[\log \frac{x_t}{x_c} - \frac{3 x_t}{4(1 - x_t)} - \frac{3 x_t^2 \log x_t}{4(1 - x_t)^2} \right]. \end{aligned} \quad (\text{A.24})$$

When the NP contributions are switch on, the modification of the CKM factors λ_i are, for instance for the K system,

$$\tilde{\lambda}_i \equiv \tilde{V}_{id_2}^* \tilde{V}_{id_1} = \lambda_i \left[1 + i a_{CP} \Delta_{12}^d + a_W (\Sigma_{1i}^d + \Sigma_{2i}^d) + (a_W^2 + a_{CP}^2) \Sigma_{1i}^d \Sigma_{2i}^d \right], \quad (\text{A.25})$$

$$\tilde{\lambda}'_i \equiv \tilde{V}_{u2i}^* \tilde{V}_{u1i} = \lambda'_i \left[1 + i a_{CP} \Delta_{12}^u + a_W (\Sigma_{1i}^u + \Sigma_{2i}^u) + (a_W^2 + a_{CP}^2) \Sigma_{1i}^u \Sigma_{2i}^u \right], \quad (\text{A.26})$$

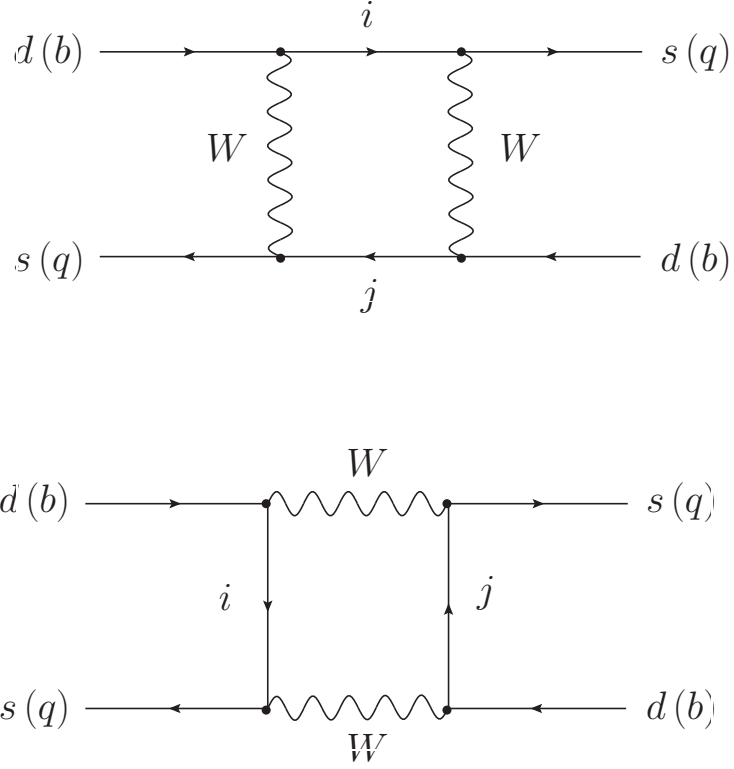


Figure A.1: W -mediated box diagrams contributing to the neutral kaon system (d and s quarks in the external legs) and meson system B_q as well (b and $q = d, s$ quarks in the external legs)

with $\lambda_i = V_{id_2}^* V_{id_1}$, $\lambda'_i = V_{u_2 i}^* V_{u_1 i}$ and

$$\Delta_{12}^x = y_{x_1}^2 - y_{x_2}^2, \quad \Sigma_{1i}^x = y_{x_1}^2 + y_i^2, \quad \Sigma_{2i}^x = y_{x_2}^2 + y_i^2. \quad (\text{A.27})$$

For the B_s and B_d one has to replace accordingly the quark labels. Deviations of $\tilde{\lambda}_i \tilde{\lambda}_j$ with respect to the SM expression can be parametrized as follows:

$$\tilde{\lambda}_i \tilde{\lambda}_j = \lambda_i \lambda_j (1 + \delta \lambda_{ij}) \quad (\text{A.28})$$

where for the K system

$$\begin{aligned} \delta \lambda_{ij} = & 2i a_{CP} \Delta_{12}^x + a_W A_{ij}^x + a_{CP}^2 B_{ij}^x + a_W^2 C_{ij}^x + i a_{CP} a_W \Delta_{12}^x B_{ij}^x + \\ & + (a_{CP}^2 + a_W^2)(i a_{CP} D_{ij}^x + a_W E_{ij}^x) + (a_{CP}^2 + a_W^2)^2 L_{ij}^x, \end{aligned} \quad (\text{A.29})$$

with

$$\begin{aligned}
A_{ij}^x &= \Sigma_{1i}^x + \Sigma_{1j}^x + \Sigma_{2i}^x + \Sigma_{2j}^x, \\
B_{ij}^x &= \Sigma_{1i}^x \Sigma_{2i}^x + \Sigma_{1j}^x \Sigma_{2j}^x - (\Delta_{12}^x)^2, \\
C_{ij}^x &= \Sigma_{1i}^x \Sigma_{1j}^x + \Sigma_{2i}^x \Sigma_{2j}^x + \Sigma_{1i}^x (\Sigma_{2i}^x + \Sigma_{2j}^x) + \Sigma_{1j}^x (\Sigma_{2i}^x + \Sigma_{2j}^x), \\
D_{ij}^x &= \Delta_{12}^x (\Sigma_{1i}^x \Sigma_{2i}^x + \Sigma_{1j}^x \Sigma_{2j}^x), \\
E_{ij}^x &= (\Sigma_{1i}^x + \Sigma_{2i}^x) \Sigma_{1j}^x \Sigma_{2j}^x + (\Sigma_{1j}^x + \Sigma_{2j}^x) \Sigma_{1i}^x \Sigma_{2i}^x, \\
L_{ij}^x &= \Sigma_{1i}^x \Sigma_{1j}^x \Sigma_{2i}^x \Sigma_{2j}^x.
\end{aligned} \tag{A.30}$$

Previous expressions hold for both of the K and the for B_q systems, only Δ_{12}^x , Σ_{1i}^x and Σ_{2i}^x distinguish the different systems. With such notation, we can write the expression in eq. (A.21) as follows:

$$\begin{aligned}
\Delta_{Box}^{(K)} C(\mu_t) &= \lambda_t^2 S'_0(x_t) + \lambda_c^2 S'_0(x_c) + 2 \lambda_t \lambda_c S'_0(x_c, x_t), \\
\Delta_{Box}^{(B_q)} C(\mu_t) &= \lambda_t^2 S'_0(x_t),
\end{aligned} \tag{A.31}$$

where

$$\begin{aligned}
S'_0(x_t) &\equiv (1 + \delta \lambda_{tt}) F_{tt} + (1 + \delta \lambda_{uu}) F_{uu} - 2 (1 + \delta \lambda_{ut}) F_{ut}, \\
S'_0(x_c) &\equiv (1 + \delta \lambda_{cc}) F_{cc} + (1 + \delta \lambda_{uu}) F_{uu} - 2 (1 + \delta \lambda_{uc}) F_{uc}, \\
S'_0(x_c, x_t) &\equiv (1 + \delta \lambda_{ct}) F_{ct} + (1 + \delta \lambda_{uu}) F_{uu} - (1 + \delta \lambda_{uc}) F_{uc} - (1 + \delta \lambda_{ut}) F_{ut}.
\end{aligned} \tag{A.32}$$

Integrating the Z boson at the μ_t scale¹, the following contributions to the Wilson coefficients are obtained

$$\Delta C_Z^{(K)}(\mu_t) = \frac{4 \pi^2}{G_F^2 M_W^2} \frac{1}{2 M_Z^2} (C^{d,s})^2, \quad \Delta C_Z^{(B_q)}(\mu_t) = \frac{4 \pi^2}{G_F^2 M_W^2} \frac{1}{2 M_Z^2} (C^{q,b})^2, \tag{A.33}$$

with

$$C^{d,s} = \frac{g}{2 \cos \theta_W} a_Z^d (\lambda_{FC})_{12}^*, \quad C^{d,b} = \frac{g}{2 \cos \theta_W} a_Z^d (\lambda_{FC})_{13}^*, \quad C^{s,b} = \frac{g}{2 \cos \theta_W} a_Z^d (\lambda_{FC})_{23}^*. \tag{A.34}$$

The Wilson coefficients given above are evaluated at the μ_t scale and therefore the complete analysis requires the inclusion of the renormalisation group (RG) QCD evolution down to low energy scales, at which the hadronic matrix elements are evaluated by lattice methods.

In our model we can apply the same RG QCD analysis as in the SM context: indeed, both the effective operator, that arises from the modified box diagrams and the tree-level

¹Integrating out the Z boson at μ_t or at M_Z introduces a subleading error in our computation, that can be safely neglected.

Z diagrams by integrating out the heavier degrees of freedom, and the matching scale are the same as in the SM. In particular no new effective operators with different chiral structure from that one in eq. (B.12) and no higher scales than μ_t are present. All the NP effects are encoded into the Wilson coefficients.

By the use of the Wilson coefficients reported in this appendix and having in mind the previous discussion on the QCD evolution, we find the following full expressions for the mixing amplitudes:

$$\begin{aligned} M_{12}^K &= R_K \left[\eta_2 \lambda_t^2 S'_0(x_t) + \eta_1 \lambda_c^2 S'_0(x_c) + 2 \eta_3 \lambda_t \lambda_c S'_0(x_c, x_t) + \eta_2 \Delta C_Z^{(K)}(\mu_t) \right]^*, \\ M_{12}^q &= R_{B_q} \left[\lambda_t^2 S'_0(x_t) + \Delta C_Z^{(B_q)}(\mu_t) \right]^*. \end{aligned} \quad (\text{A.35})$$

A.3.2 Approximate Analytical Expressions

Expanding in a_W and a_{CP} up to the first terms, the relevant parameters $\delta\lambda_{ij}$ are simplified, for the K system, as

$$\begin{aligned} \delta\lambda_{uu} &= 2(a_W - i a_{CP}) y_s^2, & \delta\lambda_{cc} &= 4 a_W y_c^2 - 2 i a_{CP} y_s^2, \\ \delta\lambda_{tt} &= 4 a_W y_t^2 - 2 i a_{CP} y_s^2, & \delta\lambda_{uc} &= 2 a_W y_c^2 - 2 i a_{CP} y_s^2. \\ \delta\lambda_{ut} &= \delta\lambda_{ct} = 2 a_W y_t^2 - 2 i a_{CP} y_s^2, \end{aligned} \quad (\text{A.36})$$

while for the B_q systems

$$\begin{aligned} \delta\lambda_{uu} &= \delta\lambda_{cc} = \delta\lambda_{uc} = 2(a_W - i a_{CP}) y_b^2, \\ \delta\lambda_{tt} &= 2 a_W (2 y_t^2 + y_b^2) - 2 i a_{CP} y_b^2 (1 + 2 a_W y_t^2), \\ \delta\lambda_{ut} &= \delta\lambda_{ct} = 2 a_W (y_t^2 + y_b^2) - 2 i a_{CP} y_b^2 (1 + a_W y_t^2), \end{aligned} \quad (\text{A.37})$$

where the terms of order $\mathcal{O}(a_W^2, a_{CP}^2, a_W a_{CP})$ have been neglected. The coefficients $C^{d,s}$, $C^{d,b}$ and $C^{s,b}$ that enter the tree level Z contributions are now

$$C^{d,s} = \frac{g}{2 \cos \theta_W} a_Z^d y_t^2 V_{ts}^* V_{td}, \quad C^{d,b} = \frac{g}{2 \cos \theta_W} a_Z^d y_t^2 V_{tb}^* V_{td}, \quad C^{s,b} = \frac{g}{2 \cos \theta_W} a_Z^d y_t^2 V_{tb}^* V_{ts}. \quad (\text{A.38})$$

Finally we report the explicit expressions for $G(x_i)$ and $H(x_i, x_j)$ appearing in the ex-

pressions in sect. B.3:

$$\begin{aligned}
 G(x_t) &= 2(F_{tt} - F_{ut}) = \frac{4x_t + 2x_t \log x_t}{1 - x_t} - \frac{7x_t^2 - x_t^3}{2(1 - x_t)^2} + \frac{2x_t^2 - 5x_t^3}{(1 - x_t)^3} \log x_t, \\
 G(x_c) &= 2(F_{cc} - F_{uc}) = 2x_c(2 + \log x_c) \\
 H(x_t, x_c) &= F_{tc} - F_{ut} = x_c \left(\frac{4 - 11x_t + 7x_t^2}{4(1 - x_t)^2} + \frac{4 - 8x_t + x_t^2}{4(1 - x_t)^2} \log x_t \right), \\
 H(x_c, x_t) &= F_{ct} - F_{uc} = -x_c \log x_c + x_t \frac{4 - 3x_c}{4(1 - x_t)} + \frac{4x_t + x_c(4 - 8x_t + x_t^2)}{4(1 - x_t)^2} \log x_t.
 \end{aligned}$$

Appendix B

MFV in a Strong Higgs Dynamics scenario

Implementing a MFV hypothesis in a Strong Higgs Dynamics framework, as in Ref. [171], non-unitarity effects for the CKM matrix are allowed from the modified W -fermion couplings in Eq. (3.5), and limits for them are obtained from $\Delta F = 1$ and $\Delta F = 2$ observables as well. Let us analyse first the CKM matrix modifications.

B.1 Non Unitarity and CP Violation

CKM matrix unitarity is dropped off in the Lagrangian of Eq. (3.5) by

$$\tilde{V}_{ij} = V_{ij} \left[1 + (a_W + ia_{CP})(y_{u_i}^2 + y_{d_j}^2) \right], \quad (\text{B.1})$$

and keeping top Yukawa coupling as the most relevant contribution¹, unitarity deviations are driven by²,

$$\sum_k \tilde{V}_{ik}^* \tilde{V}_{jk} \simeq \delta_{ij} + [2a_W y_t^2 + (a_W^2 + a_{CP}^2) y_t^4] \delta_{it} \delta_{jt}, \quad (\text{B.2})$$

$$\sum_k \tilde{V}_{ki}^* \tilde{V}_{kj} \simeq \delta_{ij} + [2a_W y_t^2 + (a_W^2 + a_{CP}^2) y_t^4] V_{ti}^* V_{tj}. \quad (\text{B.3})$$

¹These relations should be modified if one works in a framework in which $y_b \approx y_t$.

²3rd quarks family mediated transitions present sizable unitarity corrections as expected from Eq. (1.45) and still not severely constrained by experiments, whilst those on the first two family sectors, as being Yukawa and mixing angles-suppressed, are $\mathcal{O}(10^{-4})$, perfectly in agreement with present bounds. Notice from Eqs. (B.2) and (B.3) the quadratic a_{CP} -dependence for non-unitarity corrections.

and the parametrization-invariant definition of the angles of the unitarity triangles is

$$\begin{aligned} \arg \left(-\frac{\tilde{V}_{ik}^* \tilde{V}_{il}}{\tilde{V}_{jk}^* \tilde{V}_{jl}} \right) = & \arg \left(-\frac{V_{ik}^* V_{il}}{V_{jk}^* V_{jl}} \right) + a_{CP} \left[2 a_W \left(y_{u_j}^2 - y_{u_i}^2 \right) \left(y_{d_l}^2 - y_{d_k}^2 \right) + \right. \\ & \left. - \left(3 a_W^2 - a_{CP}^2 \right) \left(y_{u_j}^2 - y_{u_i}^2 \right) \left(y_{d_l}^2 - y_{d_k}^2 \right) \left(y_{u_i}^2 + y_{u_j}^2 + y_{d_k}^2 + y_{d_l}^2 \right) \right] + \mathcal{O}(a^4), \end{aligned} \quad (\text{B.4})$$

remarking that

- a_{CP} -dependent corrections, as expected from the fact that the SM source of CP-violation is the only one remaining in the absence of \mathcal{O}_4 ;
- Non-degenerate up and down sectors for the two quark families case necessary and sufficient to induce a_{CP} -dependent physical CP-odd effects that are not present in the one-family case;
- CP-odd effects playing role at quadratic order $\mathcal{O}(a_{CP} a_W)$. \mathcal{O}_4 solely (e.g. $a_W = a_Z^u = a_Z^d = 0$ in Eq. (3.5)) leads to cubic correction $\mathcal{O}(a_{CP}^3)$ or higher.

Operator coefficients in Eq. (3.5) can be bounded from $\Delta F = 1$ and $\Delta F = 2$ observables data. Focus first on the former observables.

B.2 $\Delta F = 1$ Observables

Tree-level Z -mediated FCNC induced from \mathcal{O}_{1-3} in Eq. (3.5), diagrammatically sketched in Fig. B.1, are encoded in the low-energy effective Lagrangian³ as

$$\frac{G_F \alpha}{2\sqrt{2}\pi s_W^2} V_{ti}^* V_{tj} \sum_n C_n \mathcal{Q}_n + \text{h.c.}, \quad C_n = C_n^{SM} + C_n^{NP}, \quad (\text{B.5})$$

with C_n the Wilson coefficient corresponding to the FCNC operators \mathcal{Q}_n ⁴

$$\begin{aligned} \mathcal{Q}_{\bar{\nu}\nu} &= \bar{d}_i \gamma_\mu (1 - \gamma_5) d_j \bar{\nu} \gamma^\mu (1 - \gamma_5) \nu, & \mathcal{Q}_7 &= e_q \bar{d}_i \gamma_\mu (1 - \gamma_5) d_j \bar{q} \gamma^\mu (1 + \gamma_5) q, \\ \mathcal{Q}_{9V} &= \bar{d}_i \gamma_\mu (1 - \gamma_5) d_j \bar{\ell} \gamma^\mu \ell, & \mathcal{Q}_9 &= e_q \bar{d}_i \gamma_\mu (1 - \gamma_5) d_j \bar{q} \gamma^\mu (1 - \gamma_5) q, \\ \mathcal{Q}_{10A} &= \bar{d}_i \gamma_\mu (1 - \gamma_5) d_j \bar{\ell} \gamma^\mu \gamma_5 \ell, \end{aligned} \quad (\text{B.6})$$

³Only $\Delta F = 1$ processes involving K and B mesons are considered. New up-type tree-level FCNC contributions in Eq. (3.5) are neglected in here as being strengthened by a non-diagonal spurion combination $V \mathbf{y}_D^2 V^\dagger$, subleading with respect to that one in the down sector, $V^\dagger \mathbf{y}_U^2 V$, by at least a factor y_b^2/y_t^2 .

⁴All quark species are summed in $\mathcal{Q}_{7,9}$, with their corresponding e_q quark electric charge.

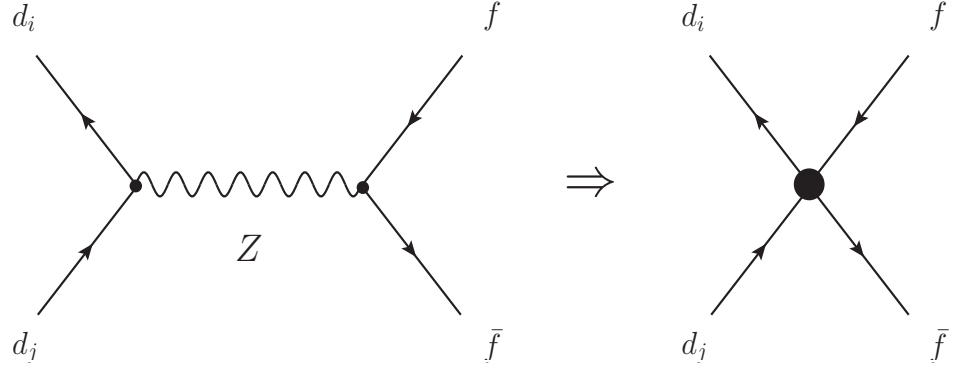


Figure B.1: Tree-level Z -mediated currents (left) contributing to the FCNC operators Q_n (right). Black dot vertex in the right figure symbolizes the non-zero contributions C_n^{NP} to the Wilson coefficient C_n for the corresponding effective operator Q_n .

Operator	Observable	Bound (@ 95% C.L.)
\mathcal{O}_{9V}	$B \rightarrow X_s l^+ l^-$	$-0.811 < a_Z^d < 0.232$
\mathcal{O}_{10A}	$B \rightarrow X_s l^+ l^-$, $B \rightarrow \mu^+ \mu^-$	$-0.050 < a_Z^d < 0.009$
$\mathcal{O}_{\bar{\nu}\nu}$	$K^+ \rightarrow \pi^+ \bar{\nu}\nu$	$-0.044 < a_Z^d < 0.133$

Table B.1: FCNC bounds [191] on the combination of the operator coefficients a_Z^d , obtained from a tree-level analysis.

receiving NP contributions contained in C_n^{NP} as

$$\begin{aligned}
 C_{\nu\bar{\nu}}^{NP} &= -\kappa y_t^2 a_Z^d, & C_7^{NP} &= +2\kappa s_W^2 y_t^2 a_Z^d, \\
 C_{9V}^{NP} &= \kappa (1 - 4s_W^2) y_t^2 a_Z^d, & C_9^{NP} &= -2\kappa c_W^2 y_t^2 a_Z^d. \\
 C_{10A}^{NP} &= -\kappa y_t^2 a_Z^d,
 \end{aligned} \tag{B.7}$$

where $\kappa \equiv \pi s_W^2 / (2\alpha)$ reflects the relative strength of the NP tree-level contribution with respect to the loop-suppressed SM one. Different mesons rare decays can constrain [191] to a_Z^d , those with less hadronic uncertainties are reported in Table B.1 with the overall range $-0.044 < a_Z^d < 0.009$ at 95% of CL⁵.

Concerning tree level W -mediated CC, the branching ratio for $B^+ \rightarrow \tau^+ \nu$ is sensitive

⁵Likewise a_Z^u can be limited from $\Delta F = 1$ FCNC transitions among up-type quarks, turning out to be of order $\mathcal{O}(a_Z^d y_b^2 / y_t^2)$ and consequently are negligible.

to their contributions and from the modified CKM matrix element \tilde{V}_{ub} in Eq. (B.1):

$$BR(B^+ \rightarrow \tau^+ \nu) = \frac{G_F^2 m_{B^+} m_\tau^2}{8\pi} \left(1 - \frac{m_\tau^2}{m_{B^+}^2}\right)^2 F_{B^+}^2 |V_{ub}|^2 \left|1 + (a_W + i a_{CP}) y_b^2\right|^2 \tau_{B^+}, \quad (\text{B.8})$$

with F_{B^+} the B decay constant⁶. Z -mediated FCNC contributions to this process appear at one-loop level and can be safely neglected.

B.3 $\Delta F = 2$ Observables

Neutral kaon oscillations

W -mediated box diagrams suffer from couplings modifications in the effective low-energy Lagrangian of Eq. (3.5) and consequently $\Delta F = 2$ transitions get modified too. Furthermore, tree-level FCNC Z diagrams can be relevant also for $\Delta F = 2$ transitions⁷. In particular, neutral kaon and meson oscillations mixing amplitudes M_{12}^K and M_{12}^q ($q = d, s$) respectively defined as

$$M_{12}^K = \frac{\langle \bar{K}^0 | \mathcal{H}_{\text{eff}}^{\Delta S=2} | K^0 \rangle^*}{2 m_K}, \quad M_{12}^q = \frac{\langle \bar{B}_q^0 | \mathcal{H}_{\text{eff}}^{\Delta B=2} | B_q^0 \rangle^*}{2 m_{B_q}}, \quad (\text{B.9})$$

are sensitive to those modifications, and therefore, the $K_L - K_S$ mass difference and the CP-violating parameter ε_K

$$\Delta M_K = 2 \text{Re}(M_{12}^K), \quad \varepsilon_K = \frac{\kappa_\epsilon e^{i\varphi_\epsilon}}{\sqrt{2} (\Delta M_K)_{\text{exp}}} \text{Im}(M_{12}^K), \quad (\text{B.10})$$

are also affected, with φ_ϵ and κ_ϵ (see these used input values in Table 2 of Ref. [171]) accounting for $\varphi_\epsilon \neq \pi/4$ and including long-distance contributions to $\text{Im}(\Gamma_{12})$ and $\text{Im}(M_{12})$. The effective Hamiltonian in Eq. (B.9) accounting for $\Delta F = 2$ processes is usually written as

$$\mathcal{H}_{\text{eff}}^{\Delta F=2} = \frac{G_F^2 M_W^2}{4\pi^2} C(\mu) Q, \quad (\text{B.11})$$

⁶The SM lepton- W couplings have been assumed in writing Eq. (B.8). Even if we are not considering the lepton sector in our scenario, those couplings are strongly constrained by the SM electroweak analysis and therefore any analogous NP modification in the lepton sector should be safely negligible.

⁷ Z -mediated boxes and weak penguin diagrams are safely neglected as being suppressed wrt tree-level Z contributions.

with $C(\mu)$ Wilson coefficient at the scale μ , corresponding to the effective operator Q describing neutral meson mixing as

$$Q = (\bar{d}_i^\alpha \gamma_\mu P_L d_j^\alpha)(\bar{d}_i^\beta \gamma^\mu P_L d_j^\beta). \quad (\text{B.12})$$

NP contributions can be distinguished in M_{12}^K by splitting it into its SM and NP contributions⁸ $M_{12}^K = (M_{12}^K)_{SM} + (M_{12}^K)_{NP}$, and neglecting all contributions proportional to $y_{u,d,s}$ and y_c^n with $n > 2$

$$\begin{aligned} (M_{12}^K)_{SM} &= R_K \left[\eta_2 \lambda_t^2 S_0(x_t) + \eta_1 \lambda_c^2 S_0(x_c) + 2 \eta_3 \lambda_t \lambda_c S_0(x_c, x_t) \right]^*, \\ (M_{12}^K)_{NP} &= R_K \left[\eta_2 \lambda_t^2 \tilde{S}_0(x_t) + \eta_1 \lambda_c^2 \tilde{S}_0(x_c) + 2 \eta_3 \lambda_t \lambda_c \tilde{S}_0(x_c, x_t) \right]^*, \\ R_K &\equiv \frac{G_F^2 M_W^2}{12 \pi^2} F_K^2 m_K \hat{B}_K, \end{aligned} \quad (\text{B.13})$$

with η_i containing QCD higher order effects, $\lambda_i = \tilde{V}_{is}^* \tilde{V}_{id}$, \hat{B}_K the scale-independent hadronic B-mixing matrix element [179], and

$$\begin{aligned} \tilde{S}_0(x_t) &= y_t^2 (2 a_W + y_t^2 a_{CP}^2) G(x_t) + \frac{(4 \pi y_t^2 a_Z^d)^2}{g^2}, \\ \tilde{S}_0(x_c) &= 2 a_W y_c^2 G(x_c) \\ \tilde{S}_0(x_c, x_t) &= y_t^2 (2 a_W + a_{CP}^2 y_t^2) H(x_t, x_c) + 2 a_W y_c^2 H(x_c, x_t) \end{aligned} \quad (\text{B.14})$$

with S_0 , G and H loop functions defined in Appendix A. Notice the tree-level FCNC Z diagrams contribution in $\tilde{S}_0(x_t)$. Other contributions are negligible because of the Yukawa suppression.

Neutral meson oscillations

$B_{d,s}$ systems have different SM and NP contribution distinction for the mixing amplitude⁹ M_{12}^q

$$\begin{aligned} (M_{12}^q)_{SM} &= R_{B_q} [\lambda_t^2 S_0(x_t)]^*, \\ (M_{12}^q)_{NP} &= (M_{12}^q)_{SM} \mathcal{C}_{B_q} e^{2i\varphi_{B_q}}, \\ R_{B_q} &\equiv \frac{G_F^2 M_W^2}{12 \pi^2} F_{B_q}^2 m_{B_q} \hat{B}_{B_q} \eta_B, \end{aligned} \quad (\text{B.15})$$

⁸The expression for M_{12}^K is phase-convention dependent. In the following we will give all the results in the convention in which the phase of the $K \rightarrow \pi\pi$ decay amplitude is vanishing.

⁹The expression for M_{12}^q is phase-convention dependent and we adopt the convention in which the decay amplitudes of the corresponding processes, $B_d^0 \rightarrow \psi K_S$ and $B_s^0 \rightarrow \psi\phi$, have a vanishing phase.

where $\mathcal{C}_{B_{d,s}}$ and $\varphi_{B_{d,s}}$ parametrize NP effects, and F_{B_q} and \hat{B}_{B_q} denote neutral B decay constant and mixing hadronic matrix elements, respectively. The mass differences in the $B_{d,s}$ systems are given by

$$\Delta M_q = 2 |M_{12}^q| \equiv (\Delta M_q)_{\text{SM}} \mathcal{C}_{B_q}, \quad (\text{B.16})$$

with

$$\mathcal{C}_{B_d} = \mathcal{C}_{B_s} = \left| 1 + 2 a_W \left(y_t^2 \frac{G(x_t)}{S_0(x_t)} + y_b^2 \right) + \frac{(4\pi y_t^2 a_Z^d)^2}{g^2 S_0(x_t)} + 2 i a_W a_{CP} y_t^2 y_b^2 \frac{G(x_t)}{S_0(x_t)} \right|. \quad (\text{B.17})$$

φ_{B_q} enters in the mixing-induced CP asymmetries $S_{\psi K_S}$ and $S_{\psi\phi}$ for the decays $B_d^0 \rightarrow \psi K_S$ and $B_s^0 \rightarrow \psi\phi$, respectively as

$$S_{\psi K_S} = \sin(2\beta + 2\varphi_{B_d}), \quad S_{\psi\phi} = \sin(2\beta_s - 2\varphi_{B_s}), \quad (\text{B.18})$$

where β and β_s are angles in the unitary triangles,

$$\beta \equiv \arg \left(-\frac{V_{cb}^* V_{cd}}{V_{tb}^* V_{td}} \right), \quad \beta_s \equiv \arg \left(-\frac{V_{tb}^* V_{ts}}{V_{cb}^* V_{cs}} \right), \quad (\text{B.19})$$

and the new phases are given by

$$\varphi_{B_d} = \varphi_{B_s} = 2 a_W a_{CP} y_t^2 y_b^2 \frac{G(x_t)}{S_0(x_t)}. \quad (\text{B.20})$$

In looking for clean observables affected by NP contributions, the ratio $R_{\Delta M_B} \equiv \Delta M_{B_d}/\Delta M_{B_s}$ suffers no modification as ΔM_{B_d} and ΔM_{B_s} are equal (see Eq. (B.17)), then any deviation from the SM value of this observable is then negligible in our framework. Another observable is the ratio between ΔM_{B_d} and the $B^+ \rightarrow \tau^+ \nu$ branching ratio [192]:

$$R_{BR/\Delta M} = \frac{3\pi\tau_{B^+}}{4\eta_B \hat{B}_{B_d} S_0(x_t)} \frac{m_\tau^2}{M_W^2} \frac{|V_{ub}|^2}{|V_{tb}^* V_{td}|^2} \left(1 - \frac{m_\tau^2}{m_{B_d}^2} \right)^2 \frac{|1 + (a_W + i a_{CP}) y_b^2|^2}{\mathcal{C}_{B_d}}, \quad (\text{B.21})$$

where we took $m_{B^+} \approx m_{B_d}$, well justified considering the errors in the other quantities in this formula.

B Semileptonic CP-Asymmetry

Finally, a fourth observable provides rich information on meson mixing, the like-sign dimuon charge asymmetry of semileptonic b decays A_{sl}^b

$$A_{sl}^b \equiv \frac{N_b^{++} - N_b^{--}}{N_b^{++} + N_b^{--}}, \quad (\text{B.22})$$

with N_b^{++} and N_b^{--} denoting the number of events containing two positively or negatively charged muons, respectively. In $p\bar{p}$ colliders, such events can only arise through $B_d^0 - \bar{B}_d^0$ or $B_s^0 - \bar{B}_s^0$ mixings. Due to the intimate link with meson oscillations, A_{sl}^b is also called semileptonic CP-asymmetry and gets contributions from both B_d and B_s systems [193, 194]:

$$A_{sl}^b = (0.594 \pm 0.022) a_{sl}^d + (0.406 \pm 0.022) a_{sl}^s, \quad (\text{B.23})$$

where

$$\begin{aligned} a_{sl}^d &\equiv \left| \frac{(\Gamma_{12}^d)_{SM}}{(M_{12}^d)_{SM}} \right| \sin \phi_d = (5.4 \pm 1.0) \times 10^{-3} \sin \phi_d, \\ a_{sl}^s &\equiv \left| \frac{(\Gamma_{12}^s)_{SM}}{(M_{12}^s)_{SM}} \right| \sin \phi_s = (5.0 \pm 1.1) \times 10^{-3} \sin \phi_s, \end{aligned} \quad (\text{B.24})$$

with

$$\phi_d \equiv \arg \left\{ - \frac{(M_{12}^d)_{SM}}{(\Gamma_{12}^d)_{SM}} \right\} = -4.3^\circ \pm 1.4^\circ, \quad \phi_s \equiv \arg \left\{ - \frac{(M_{12}^s)_{SM}}{(\Gamma_{12}^s)_{SM}} \right\} = 0.22^\circ \pm 0.06^\circ. \quad (\text{B.25})$$

NP contributions are parametrized analogously as for Γ_{12}^q in M_{12}^q ,

$$\Gamma_{12}^q = (\Gamma_{12}^q)_{SM} \tilde{\mathcal{C}}_{B_q} \quad \text{with} \quad \tilde{\mathcal{C}}_{B_q} = 1 + 2 a_W y_b^2, \quad (\text{B.26})$$

in the approximation used here. With such a notation, it follows that

$$a_{sl}^q = \left| \frac{(\Gamma_{12}^q)_{SM}}{(M_{12}^q)_{SM}} \right| \frac{\tilde{\mathcal{C}}_{B_q}}{\mathcal{C}_{B_q}} \sin (\phi_q + 2\varphi_{B_q}), \quad (\text{B.27})$$

with \mathcal{C}_{B_q} given in Eq. (B.17).

B.4 Phenomenological analysis

A more detailed phenomenological discussion completing the analysis done in Sect. 3.3.1 can be found in Ref. [171]. The physical parameters we considered in the analysis and their present experimental values are summarized in there. Additionally the tension between the exclusive and the inclusive experimental determinations for $|V_{ub}|$ and the well known $\varepsilon_K - S_{\psi K_S}$ and $BR(B^+ \rightarrow \tau^+ \nu)$ anomalies were also discussed there. The exclusive determination for $|V_{ub}|$ was assumed in Ref. [171], due to the negligible NP contributions to $S_{\psi K_S}$ through φ_{B_d} (suppressed by y_b^2), while NP contributions to ε_K are sizable, as it can be seen in Eq. (B.18) of Sect. B.3. The $|V_{ub}| - \gamma$ parameter space was also constrained

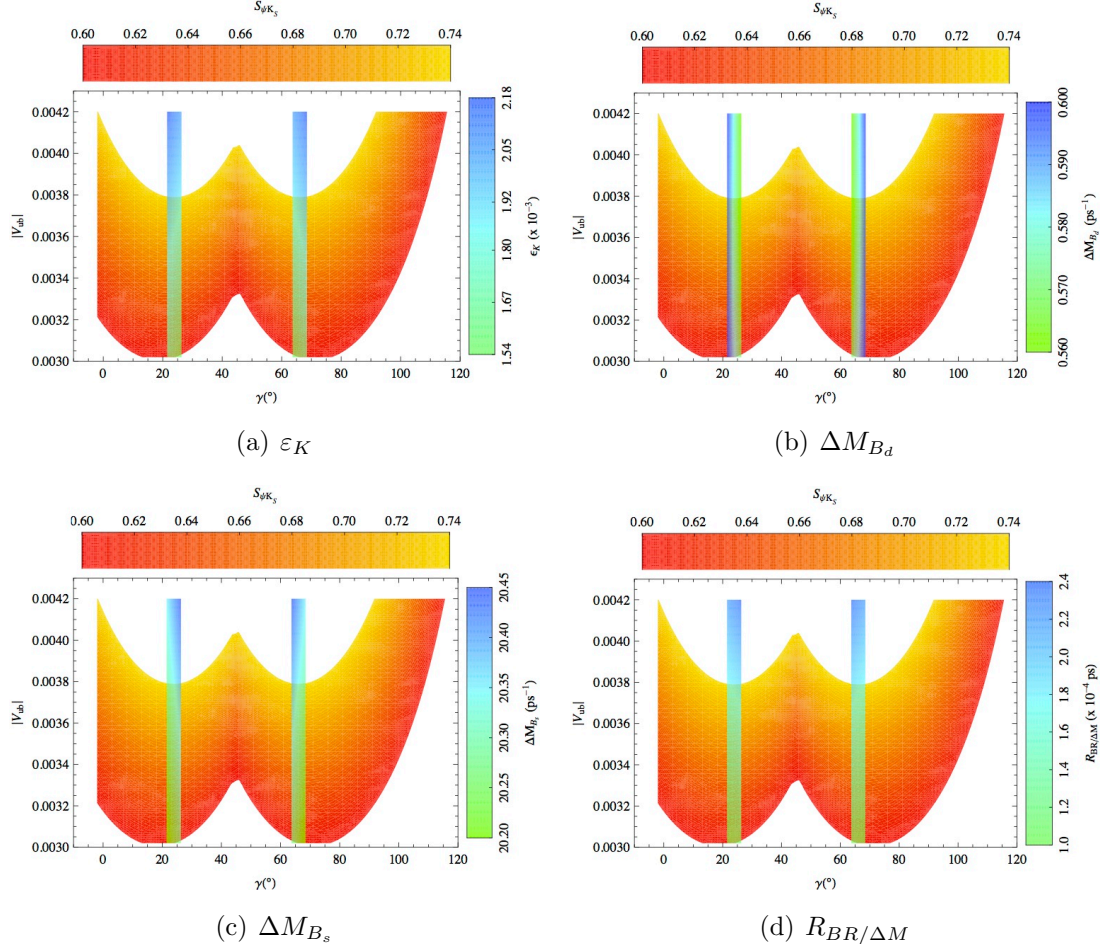


Figure B.2: SM predictions for ε_K , $\Delta M_{B_{d,s}}$ and $R_{BR}/\Delta M$ in the reduced $|V_{ub}| - \gamma$ parameter space. See [171] for more details.

in Ref. [171] from independent measurements of $R_{\Delta M_B}$ and $S_{\psi K_S}$. Fig. B.2 shows the SM predictions for ε_K , $\Delta M_{B_{d,s}}$ and $R_{BR}/\Delta M$ in such $|V_{ub}| - \gamma$ parameter space, where $R_{BR/\Delta M} \equiv BR(B^+ \rightarrow \tau^+ \nu)/\Delta M_{B_d}$, useful in order to reduce most of the theoretical uncertainties on ΔM_{B_d} . These particular patterns of the SM predictions are going to be relevant when discussing NP effects, because it is a common feature of all the points in the “reduced” $|V_{ub}| - \gamma$ parameter space.

FCNC Constraints on a_{CP} , a_W and a_Z^d

None of the observables considered here get contributions from a_Z^u , the analysis will be restricted only to the constraints on a_{CP} , a_W and a_Z^d from ε_K and $R_{BR/\Delta M}$ in Fig. B.3. The analytic expressions for the NP contributions were considered in previous sections.

Observables $S_{\psi\phi}$ and A_{sl}^b are also presented separately in Fig. B.4. See [171] for a more complete and detailed discussion.

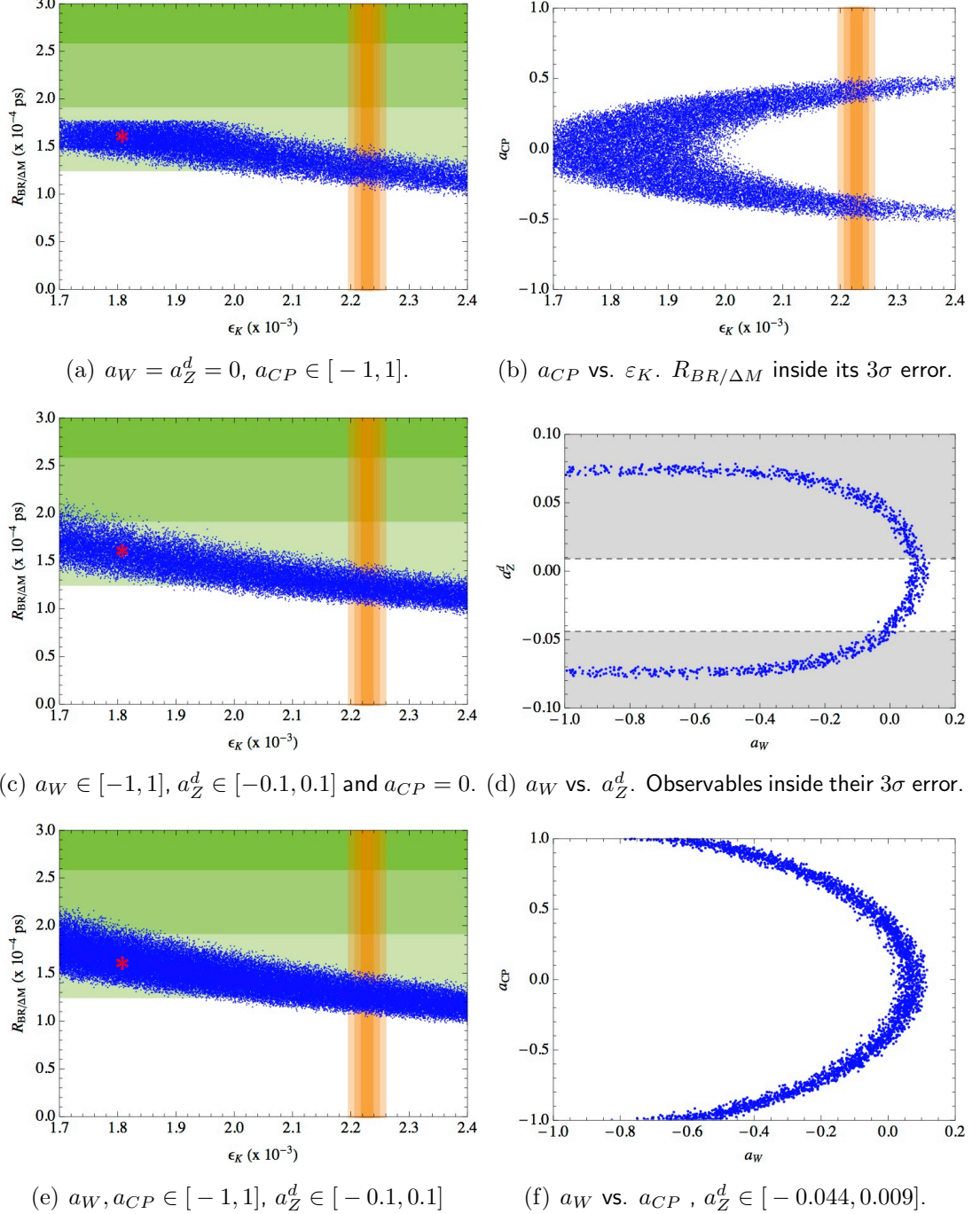


Figure B.3: ϵ_K vs. $R_{BR/\Delta M}$ for different values of a_W , a_{CP} and a_Z^d (left), and $a_W - a_{CP}$ parameter space (right) for ϵ_K and $R_{BR/\Delta M}$ inside their 3σ error ranges. Results for the reference point ($|V_{ub}|$, γ) = $(3.5 \times 10^{-3}, 66^\circ)$. More details in Ref. [171].

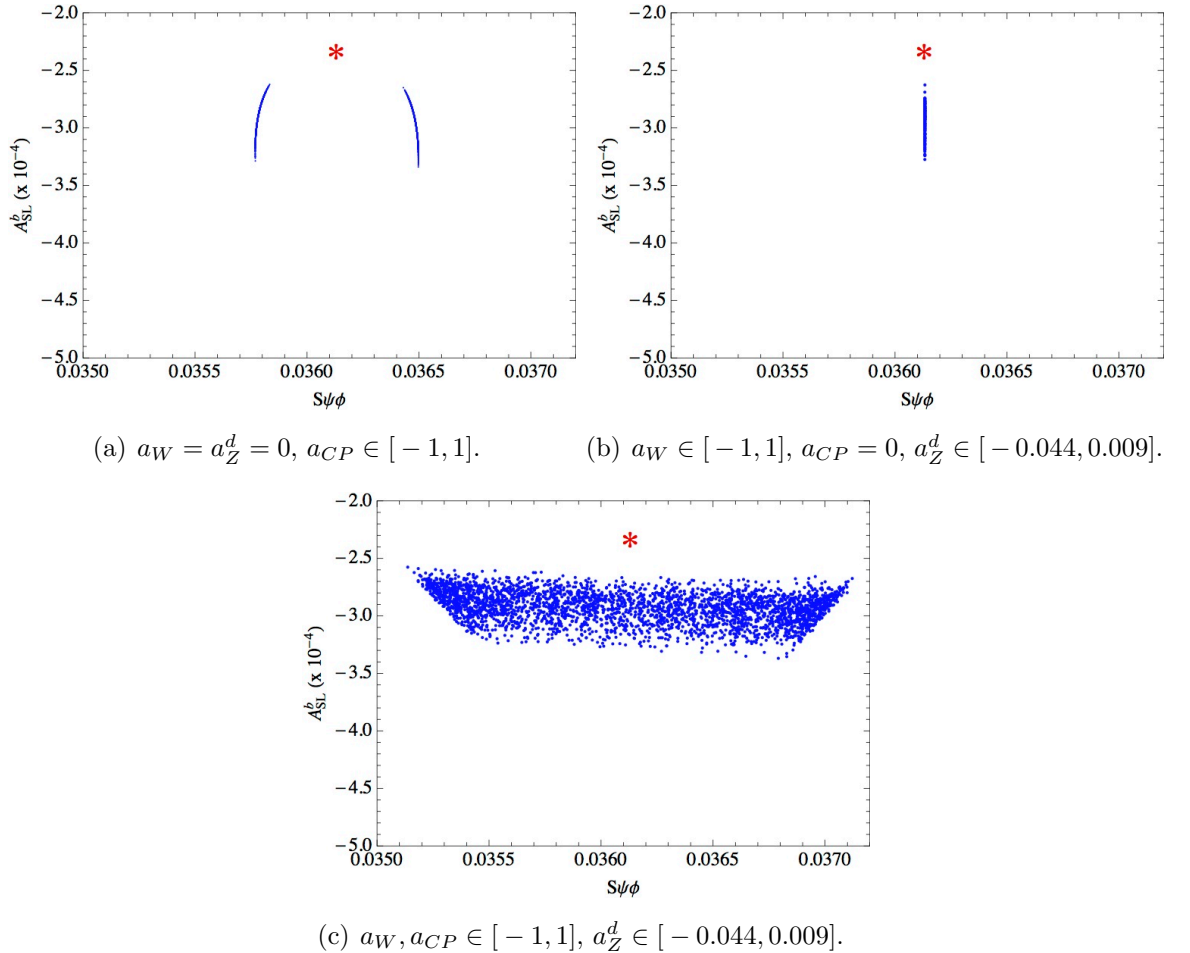


Figure B.4: Correlation between A_{sl}^b and $S_{\psi\phi}$. For all points, ε_K and $R_{BR/\Delta M}$ are inside their 3σ error ranges. See [171] for a detailed description.

Appendix C

Linear siblings of the CP-odd chiral operators $\mathcal{S}_i(h)$

The interactions described by the chiral operators in Eq. (2.35) can also be described in the context of a linearly realised EWSB, through linear operators built in terms of the SM Higgs doublet. In this Appendix, the connection between the two expansions is discussed¹. In the following some useful relations involving the Higgs doublet Φ are used to establish the connection.

Useful relations

$$\Phi^\dagger \tau_i \overleftrightarrow{D}_\mu \Phi = (D_\mu \Phi)^\dagger \tau_i \Phi - \Phi^\dagger \tau_i (D_\mu \Phi) \quad (\text{C.1})$$

$$\sum_i^3 (\tau^i)_{\alpha\beta} (\tau_i)_{\gamma\delta} = 2 \left(\delta_{\alpha\delta} \delta_{\beta\gamma} - \frac{1}{2} \delta_{\alpha\beta} \delta_{\gamma\delta} \right) \quad (\text{C.2})$$

¹As the number and nature of the leading order operators in the chiral and linear expansions are not the same, an exact correspondence between the two kind of operators can be found only in the cases when $d = 6$ linear operators are involved, as only for them complete bases of independent terms have been defined. Otherwise, it will be indicated which chiral operators should be combined in order to generate the gauge interactions contained in specific $d > 6$ linear operators.

$$\epsilon_{ijk} \left(\Phi^\dagger \tau^i \overleftrightarrow{D}_\mu \Phi \right) \left(\Phi^\dagger \tau^j \overleftrightarrow{D}_\nu \Phi \right) \left(\Phi^\dagger \tau_k \Phi \right)$$

$$= i 2 \left[(D_\mu \Phi^\dagger) (D_\nu \Phi) (\Phi^\dagger \Phi) (\Phi^\dagger \Phi) - (D_\mu \Phi^\dagger) \Phi \Phi^\dagger (D_\nu \Phi) (\Phi^\dagger \Phi) \right] - \{\mu \leftrightarrow \nu\} \quad (\text{C.3})$$

$$\epsilon_{ijk} \left(\Phi^\dagger \tau^i \overleftrightarrow{D}_\mu \Phi \right) \left(\Phi^\dagger \tau^j \overleftrightarrow{D}_\nu \Phi \right)$$

$$= i \left[(D_\mu \Phi^\dagger) (D_\nu \Phi) (\Phi^\dagger \tau^k \Phi) - (D_\mu \Phi^\dagger) \tau^k (D_\nu \Phi) (\Phi^\dagger \Phi) \right] +$$

$$- i \left[(D_\mu \Phi^\dagger) \Phi (D_\nu \Phi^\dagger) \tau^k \Phi - \Phi^\dagger (D_\mu \Phi) \Phi^\dagger \tau^k (D_\nu \Phi) \right] - \{\mu \leftrightarrow \nu\} \quad (\text{C.4})$$

$$\left(\Phi^\dagger \tau_i \overleftrightarrow{D}_\mu \Phi \right) \left(\Phi^\dagger \tau^i \Phi \right) = \left(\Phi^\dagger \overleftrightarrow{D}_\mu \Phi \right) \left(\Phi^\dagger \Phi \right)$$

$$\left(\Phi^\dagger \tau^i \overleftrightarrow{D}_\mu \Phi \right)^2$$

$$= \left[(D_\mu \Phi^\dagger) \Phi \right]^2 + \left[\Phi^\dagger (D_\mu \Phi) \right]^2 - 4 (D_\mu \Phi^\dagger) (D^\mu \Phi) (\Phi^\dagger \Phi) + 2 (D_\mu \Phi^\dagger) \Phi \Phi^\dagger (D^\mu \Phi) \quad (\text{C.5})$$

$$\left(\Phi^\dagger \tau_i \overleftrightarrow{D}_\mu \Phi \right) \left(\Phi^\dagger \tau_i \overleftrightarrow{D}_\nu \Phi \right)$$

$$= (D_\mu \Phi^\dagger) \Phi (D_\nu \Phi^\dagger) \Phi + \Phi^\dagger (D_\mu \Phi) \Phi^\dagger (D_\nu \Phi) - 2 (D_\mu \Phi^\dagger) (D_\nu \Phi) (\Phi^\dagger \Phi) +$$

$$- 2 (D_\nu \Phi^\dagger) (D_\mu \Phi) (\Phi^\dagger \Phi) + (D_\mu \Phi^\dagger) \Phi \Phi^\dagger (D_\nu \Phi) + (D_\nu \Phi^\dagger) \Phi \Phi^\dagger (D_\mu \Phi) \quad (\text{C.6})$$

For chiral operators connected to $d = 6$ linear operators:

$$\begin{aligned}
\mathcal{S}_{\tilde{B}}(h) &\rightarrow g'^2 \epsilon^{\mu\nu\rho\sigma} B_{\mu\nu} B_{\rho\sigma} (\Phi^\dagger \Phi) \\
\mathcal{S}_{\tilde{W}}(h) &\rightarrow g^2 \epsilon^{\mu\nu\rho\sigma} \text{Tr} (W_{\mu\nu} W_{\rho\sigma}) (\Phi^\dagger \Phi) \\
\mathcal{S}_{\tilde{G}}(h) &\rightarrow g_s^2 \epsilon^{\mu\nu\rho\sigma} G_{\mu\nu}^a G_{\rho\sigma}^a (\Phi^\dagger \Phi) \\
\mathcal{S}_{2D}(h) &\rightarrow \left(\Phi^\dagger \overleftrightarrow{D^\mu} D_\mu \Phi \right) (\Phi^\dagger \Phi) \\
\mathcal{S}_1(h) &\rightarrow g g' \epsilon^{\mu\nu\rho\sigma} B_{\mu\nu} W_{\rho\sigma}^j (\Phi^\dagger \tau_j \Phi) \\
\mathcal{S}_2(h) &\rightarrow g' \epsilon^{\mu\nu\rho\sigma} B_{\mu\nu} \left[\left(\Phi^\dagger \overleftrightarrow{D_\sigma} D_\rho \Phi \right) + 2 (D_\rho \Phi)^\dagger D_\sigma \Phi \right] \\
\mathcal{S}_3(h) &\rightarrow g \epsilon^{\mu\nu\rho\sigma} W_{\mu\nu}^i \left[\left(\Phi^\dagger \tau_i \overleftrightarrow{D_\sigma} D_\rho \Phi \right) + 2 (D_\rho \Phi)^\dagger \tau_i D_\sigma \Phi \right]
\end{aligned} \tag{C.7}$$

For chiral operators connected to $d > 6$ linear operators:

$$\begin{aligned}
\mathcal{S}_4(h) &\rightarrow g W_i^{\mu\nu} \left(\Phi^\dagger \tau^i \overleftrightarrow{D_\mu} \Phi \right) \left(\Phi^\dagger \overleftrightarrow{D_\nu} \Phi \right) \quad (d = 8) \\
\mathcal{S}_5(h), \mathcal{S}_{10}(h) &\rightarrow (D^\mu \Phi)^\dagger (D^\nu \Phi) \left(\Phi^\dagger \overleftrightarrow{D_\mu} D_\nu \Phi \right) \quad (d = 8) \\
\mathcal{S}_6(h), \mathcal{S}_{11}(h) &\rightarrow (D^\mu \Phi)^\dagger (D_\mu \Phi) \left(\Phi^\dagger \overleftrightarrow{D^\nu} D_\nu \Phi \right) \quad (d = 8) \\
\mathcal{S}_7(h) &\rightarrow \epsilon_{ijk} W_{\mu\nu}^i \left(\Phi^\dagger \tau^j \overleftrightarrow{D^\mu} D^\nu \Phi \right) \left(\Phi^\dagger \tau^k \Phi \right) \quad (d = 8) \\
\mathcal{S}_8(h) &\rightarrow g^2 \epsilon^{\mu\nu\rho\sigma} W_{\mu\nu}^i W_{\rho\sigma}^j (\Phi^\dagger \tau_i \Phi) (\Phi^\dagger \tau_j \Phi) \quad (d = 8) \\
\mathcal{S}_9(h) &\rightarrow g \epsilon^{\mu\nu\rho\sigma} W_{\mu\nu}^i (\Phi^\dagger \tau^i \Phi) \left(\Phi^\dagger \overleftrightarrow{D_\rho} D_\sigma \Phi \right) \quad (d = 8) \\
\mathcal{S}_{12}(h), \mathcal{S}_{13}(h), \mathcal{S}_{14}(h) &\rightarrow \left(\Phi^\dagger \overleftrightarrow{D^\mu} D_\mu \Phi \right) D^\nu D_\nu (\Phi^\dagger \Phi) \quad (d = 8) \\
\mathcal{S}_{15}(h), \mathcal{S}_{16}(h) &\rightarrow \left(\Phi^\dagger \overleftrightarrow{D^\mu} \Phi \right) \left(\Phi^\dagger \overleftrightarrow{D_\mu} \Phi \right) \left(\Phi^\dagger \overleftrightarrow{D^\nu} D_\nu \Phi \right) \quad (d = 10)
\end{aligned} \tag{C.8}$$

where in the brackets the dimension of the specific linear operator is explicitly reported.

Appendix D

Linear siblings of the operators \mathcal{X}_i

The first set of non-linear operators listed in Eq. (3.8) corresponds to the following eight linear operators containing fermions, the Higgs doublet Φ , the rank-2 antisymmetric tensor $\sigma^{\mu\nu}$ and the field strengths $B_{\mu\nu}$, $W_{\mu\nu}$ and $G_{\mu\nu}$:

$$\begin{aligned}
\mathcal{X}_{\Phi 1} &= g' \bar{Q}_L \sigma^{\mu\nu} \Phi D_R B_{\mu\nu} \\
\mathcal{X}_{\Phi 2} &= g' \bar{Q}_L \sigma^{\mu\nu} \tilde{\Phi} U_R B_{\mu\nu} \\
\mathcal{X}_{\Phi 3} &= g \bar{Q}_L \sigma^{\mu\nu} W_{\mu\nu} \Phi D_R \\
\mathcal{X}_{\Phi 4} &= g \bar{Q}_L \sigma^{\mu\nu} W_{\mu\nu} \tilde{\Phi} U_R \\
\mathcal{X}_{\Phi 5} &= g_s \bar{Q}_L \sigma^{\mu\nu} \Phi D_R G_{\mu\nu} \\
\mathcal{X}_{\Phi 6} &= g_s \bar{Q}_L \sigma^{\mu\nu} \tilde{\Phi} U_R G_{\mu\nu}, \\
\mathcal{X}_{\Phi 7} &= g \bar{Q}_L \sigma^{\mu\nu} \sigma_i \Phi D_R \Phi^\dagger W_{\mu\nu} \sigma^i \Phi \\
\mathcal{X}_{\Phi 8} &= g \bar{Q}_L \sigma^{\mu\nu} \sigma_i \tilde{\Phi} U_R \Phi^\dagger \sigma^i W_{\mu\nu} \Phi.
\end{aligned} \tag{D.1}$$

The operators $\mathcal{X}_{\Phi 7, \Phi 8}$ have mass dimension $d = 8$, while all the others have (linear) mass dimension $d = 6$. The correspondence among these linear operators and those non-linear listed in Eq. (3.8) is the following: for $i = 1, \dots, 8$,

$$\mathcal{X}_i \leftrightarrow \sum_{j=1}^8 \mathcal{C}_{ij} \mathcal{X}_{\Phi j} \quad \text{with} \quad \mathcal{C} = \frac{\sqrt{2}}{f} \begin{pmatrix} 1 & 1 & 0 & 0 & 0 & 0 & 0 & 0 \\ -1 & 1 & 0 & 0 & 0 & 0 & 0 & 0 \\ 0 & 0 & 1 & 1 & 0 & 0 & 0 & 0 \\ 0 & 0 & -1 & 1 & 0 & 0 & 0 & 0 \\ 0 & 0 & 0 & 0 & 1 & 1 & 0 & 0 \\ 0 & 0 & 0 & 0 & -1 & 1 & 0 & 0 \\ 0 & 0 & 1 & -1 & 0 & 0 & -4/f^2 & 4/f^2 \\ 0 & 0 & -1 & -1 & 0 & 0 & 4/f^2 & 4/f^2 \end{pmatrix} \tag{D.2}$$

The second set of non-linear operators listed in Eq. (3.9) corresponds to the following four linear operators containing fermions, the Higgs doublet Φ and the rank-2 antisymmetric tensor $\sigma^{\mu\nu}$:

$$\begin{aligned}\mathcal{X}_{\Phi 9} &= \bar{Q}_L \sigma^{\mu\nu} \Phi D_R \left[(D_\mu \Phi)^\dagger D_\nu \Phi - (\mu \leftrightarrow \nu) \right], \\ \mathcal{X}_{\Phi 10} &= \bar{Q}_L \sigma^{\mu\nu} \tilde{\Phi} U_R \left[(D_\mu \Phi)^\dagger D_\nu \Phi - (\mu \leftrightarrow \nu) \right], \\ \mathcal{X}_{\Phi 11} &= \bar{Q}_L \sigma_i \sigma^{\mu\nu} \Phi D_R \left[(D_\mu \Phi)^\dagger \sigma^i D_\nu \Phi - (\mu \leftrightarrow \nu) \right], \\ \mathcal{X}_{\Phi 12} &= \bar{Q}_L \sigma_i \sigma^{\mu\nu} \tilde{\Phi} U_R \left[(D_\mu \Phi)^\dagger \sigma^i D_\nu \Phi - (\mu \leftrightarrow \nu) \right],\end{aligned}\tag{D.3}$$

all of them of mass dimension $d = 8$. The correspondence among these linear operators and those non-linear listed in Eq. (3.9) is the following

$$\mathcal{X}_i \leftrightarrow \sum_{j=9}^{12} \mathcal{C}_{ij} \mathcal{X}_{\Phi j} \quad \text{with} \quad \mathcal{C} = \frac{2\sqrt{2}}{f^3} \begin{pmatrix} 0 & 0 & 1 & 1 \\ 0 & 0 & -1 & 1 \\ 1 & -1 & 0 & 0 \\ -1 & -1 & 0 & 0 \end{pmatrix} \tag{D.4}$$

for $i = 9, \dots, 12$. For the third set in Eq. (3.10), we consider the following six linear operators involving fermions and the Higgs doublet Φ :

$$\begin{aligned}\mathcal{X}_{\Phi 13} &= \bar{Q}_L \Phi D_R (D_\mu \Phi)^\dagger D^\mu \Phi, \\ \mathcal{X}_{\Phi 14} &= \bar{Q}_L \tilde{\Phi} U_R (D_\mu \Phi)^\dagger D^\mu \Phi, \\ \mathcal{X}_{\Phi 15} &= \bar{Q}_L \sigma_i \Phi D_R (D_\mu \Phi)^\dagger \sigma^i D^\mu \Phi, \\ \mathcal{X}_{\Phi 16} &= \bar{Q}_L \sigma_i \tilde{\Phi} U_R (D_\mu \Phi)^\dagger \sigma^i D^\mu \Phi, \\ \mathcal{X}_{\Phi 17} &= \bar{Q}_L \Phi D_R (D_\mu \Phi)^\dagger \Phi \Phi^\dagger D^\mu \Phi, \\ \mathcal{X}_{\Phi 18} &= \bar{Q}_L \tilde{\Phi} U_R (D_\mu \Phi)^\dagger \Phi \Phi^\dagger D^\mu \Phi,\end{aligned}\tag{D.5}$$

where $\mathcal{X}_{\Phi 13\text{--}\Phi 16}$ have mass dimension $d = 8$, while $\mathcal{X}_{\Phi 17\text{--}\Phi 18}$ have mass dimension $d = 10$. The correspondence between these linear operators and those non-linear listed in Eq. (3.10) for $i = 13, \dots, 18$, is

$$\mathcal{X}_i \leftrightarrow \sum_{j=13}^{18} \mathcal{C}_{ij} \mathcal{X}_{Hj} \quad \text{with} \quad \mathcal{C} = \frac{2\sqrt{2}}{f^3} \begin{pmatrix} -1 & -1 & 0 & 0 & 0 & 0 \\ 1 & -1 & 0 & 0 & 0 & 0 \\ 0 & 0 & 1 & 1 & 0 & 0 \\ 0 & 0 & -1 & 1 & 0 & 0 \\ 2 & 2 & 1 & -1 & -8/f^2 & -8/f^2 \\ -2 & 2 & -1 & -1 & 8/f^2 & -8/f^2 \end{pmatrix}. \tag{D.6}$$

Operator coefficients in the unitary basis

The relations between the coefficients appearing in the Lagrangians Eq. (3.14)-(3.15) and the ones defined in Eq. (3.11) for the effective Lagrangian in the unitary basis

$$\begin{pmatrix} c_W^u \\ c_W^d \\ c_{WZ}^+ \\ c_{WZ}^- \\ d_F^u \\ d_F^d \\ d_Z^u \\ d_Z^d \\ d_W^+ \\ d_W^- \\ d_G^u \\ d_G^d \end{pmatrix} = \mathcal{A} \begin{pmatrix} b_1 \\ \dots \\ b_{12} \end{pmatrix}, \quad \begin{pmatrix} b_Z^u \\ b_Z^d \\ b_W^u \\ b_W^d \\ b_{WZ}^+ \\ b_{WZ}^- \end{pmatrix} = \mathcal{B} \begin{pmatrix} b_{13} \\ \dots \\ b_{18} \end{pmatrix} \quad (\text{D.7})$$

$$\mathcal{A} = \begin{pmatrix} 0 & 0 & 2i & 2i & 0 & 0 & 2i & 2i & -1 & -1 & 1 & 1 \\ 0 & 0 & -2i & 2i & 0 & 0 & 2i & -2i & 1 & -1 & -1 & 1 \\ 0 & 0 & 0 & 0 & 0 & 0 & 0 & 0 & 4 & -4 & 0 & 0 \\ 0 & 0 & 0 & 0 & 0 & 0 & 0 & 0 & -4 & -4 & 0 & 0 \\ 1 & 1 & 1 & 1 & 0 & 0 & 1 & 1 & 0 & 0 & 0 & 0 \\ 1 & -1 & -1 & 1 & 0 & 0 & 1 & -1 & 0 & 0 & 0 & 0 \\ -2s_W^2 & -2s_W^2 & 2c_W^2 & 2c_W^2 & 0 & 0 & 2c_W^2 & 2c_W^2 & 0 & 0 & 0 & 0 \\ -2s_W^2 & 2s_W^2 & -2c_W^2 & 2c_W^2 & 0 & 0 & 2c_W^2 & -2c_W^2 & 0 & 0 & 0 & 0 \\ 0 & 0 & 2 & -2 & 0 & 0 & 2 & -2 & 0 & 0 & 0 & 0 \\ 0 & 0 & 2 & 2 & 0 & 0 & -2 & -2 & 0 & 0 & 0 & 0 \\ 0 & 0 & 0 & 0 & 1 & 1 & 0 & 0 & 0 & 0 & 0 & 0 \\ 0 & 0 & 0 & 0 & 1 & -1 & 0 & 0 & 0 & 0 & 0 & 0 \end{pmatrix} \quad (\text{D.8})$$

$$\mathcal{B} = \begin{pmatrix} -1 & -1 & -1 & -1 & -1 & -1 \\ -1 & 1 & 1 & -1 & -1 & 1 \\ -1 & -1 & 1 & 1 & 1 & 1 \\ -1 & 1 & -1 & 1 & 1 & -1 \\ 0 & 0 & -2 & 2 & -2 & 2 \\ 0 & 0 & -2 & -2 & 2 & 2 \end{pmatrix} \quad (\text{D.9})$$

Appendix E

Feynman rules

This Appendix provides a complete list of all Feynman rules resulting from the CP-odd operators in the Lagrangian $\Delta\mathcal{L}_{\text{CP}}$ of Eqs. (2.34) and (2.35). Greek indexes denote the flavour of the fermionic legs and are assumed to be summed over when repeated; whenever they do not appear, it should be understood that the vertex is flavour diagonal. Moreover, y_f ($f = U, D, E$) denotes the eigenvalue of the corresponding Yukawa coupling matrix defined in Eq. (2.32). Chirality operators $P_{L,R}$ are defined as

$$P_L = \frac{1}{2} (1 - \gamma^5) , \quad P_R = \frac{1}{2} (1 + \gamma^5) . \quad (\text{E.1})$$

Flow in momentum convention is assumed in all diagrams. η -parameter in diagrams Eq. (FR.1)-(FR.4) stands for the gauge fixing parameter. Only diagrams with up to four legs are shown and the expansion for $\mathcal{F}_i(h)$ in Eq. (2.30) has been adopted, together with the definitions of the \hat{a}_i coefficients in Eq. (2.37) and $\hat{b}_i = c_i b_i$. Vertices cubic in h have been omitted below, but for Eq. (FR.26) which results from the product of two $F_i(h)$ functions, see Footnote 5 in Chapter 2. Finally, the SM and BSM Lorentz structures are reported in two distinct columns, on the left and on the right, respectively. Notice that all the pure gauge and gauge- h interactions have no SM contribution. All quantities entering in the Feynman rules below have resulted after the Z -renormalization scheme has been implemented.

$$(FR.1) \quad \begin{array}{c} A_\mu(p) \end{array} \quad \text{wavy line} \quad \begin{array}{c} A_\nu(p) \end{array} \quad \frac{-i}{p^2} \left[g^{\mu\nu} - (1 - \eta) \frac{p^\mu p^\nu}{p^2} \right]$$

$$(FR.2) \quad \begin{array}{c} Z_\mu(p) \end{array} \quad \text{wavy line} \quad \begin{array}{c} Z_\nu(p) \end{array} \quad \frac{-i}{p^2 - m_Z^2} \left[g^{\mu\nu} - (1 - \eta) \frac{p^\mu p^\nu}{p^2 - \eta m_Z^2} \right]$$

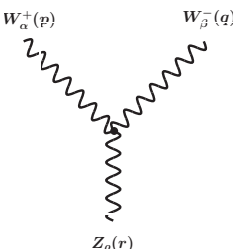
$$(FR.3) \quad \begin{array}{c} W_\mu^+(p) \end{array} \quad \text{wavy line} \quad \begin{array}{c} W_\nu^-(p) \end{array} \quad \frac{-i}{p^2 - m_W^2} \left[g^{\mu\nu} - (1 - \eta) \frac{p^\mu p^\nu}{p^2 - \eta m_W^2} \right]$$

$$(FR.4) \quad \begin{array}{c} G_\mu^a(p) \end{array} \quad \text{double wavy line} \quad \begin{array}{c} G_\nu^b(p) \end{array} \quad \frac{-ig^{\mu\nu}}{p^2} \left[g^{\mu\nu} - (1 - \eta) \frac{p^\mu p^\nu}{p^2} \right]$$

$$(FR.5) \quad \begin{array}{c} h(p) \end{array} \quad \text{dashed line} \quad \begin{array}{c} h(p) \end{array} \quad \frac{-i}{p^2 - m_h^2}$$

$$(FR.6) \quad \begin{array}{c} f(p) \end{array} \quad \text{solid line} \quad \begin{array}{c} f(p) \end{array} \quad \frac{i(\not{p} + m_f)}{p^2 - m_f^2}; \quad m_f = -\frac{v \mathbf{y}_f}{\sqrt{2}}, \quad f = U, D, E$$

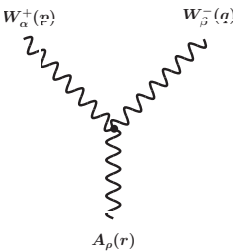
(FR.7)



$$\begin{aligned} & \xi^2 e^3 \csc^2 \theta_W \csc (2 \theta_W) \left\{ -2 c_{11} g^{\alpha \beta} (p^\rho + q^\rho) + c_{10} (g^{\beta \rho} p^\alpha + g^{\alpha \rho} q^\beta) + \right. \\ & \left. + c_4 [g^{\beta \rho} (p^\alpha + r^\alpha) + g^{\alpha \rho} (q^\beta + r^\beta) + g^{\alpha \beta} (p^\rho + q^\rho)] \right\} + \end{aligned}$$

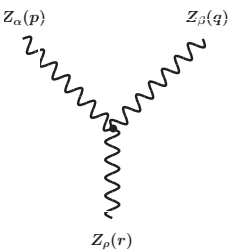
$$+ 8i \xi e^3 [\xi c_8 \cot \theta_W \csc^2 \theta_W - c_1 \csc (2 \theta_W)] (p_\sigma + q_\sigma) \epsilon^{\alpha \beta \rho \sigma}$$

(FR.8)



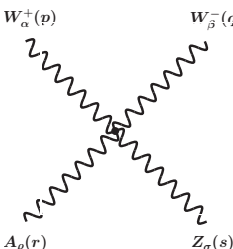
$$4i \xi e^3 \csc^2 \theta_W (2 \xi c_8 + c_1) (p_\sigma + q_\sigma) \epsilon^{\alpha \beta \rho \sigma}$$

(FR.9)



$$8 \xi^2 e^3 (2 \xi c_{16} + c_{10} + c_{11}) \csc^3 (2 \theta_W) [g^{\beta \rho} p^\alpha + g^{\alpha \rho} q^\beta - g^{\alpha \beta} (p^\rho + q^\rho)]$$

(FR.10)



$$\xi^2 (c_4 + c_{10}) e^4 \csc^2 \theta_W \csc (2 \theta_W) (g^{\alpha \sigma} g^{\beta \rho} - g^{\alpha \rho} g^{\beta \sigma})$$

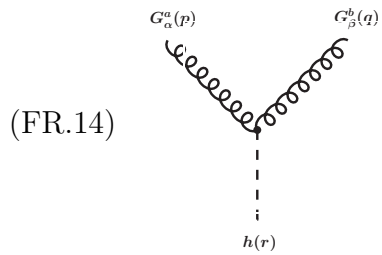


(FR.11)

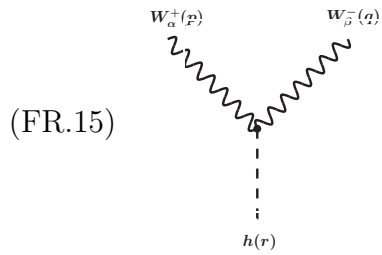
$$\frac{8i}{v} \xi e^2 \left[2 \left(-\frac{1}{4} \hat{a}_{\tilde{B}} + \xi \hat{a}_8 + \hat{a}_1 \right) - \frac{1}{4} \hat{a}_{\tilde{W}} \right] p_\mu q_\nu \epsilon^{\alpha\beta\mu\nu}$$

$$\begin{array}{c}
\text{Diagram: Two wavy lines meeting at a vertex labeled } Z_\alpha(r) \text{ and } Z_\beta(q) \text{, connected by a dashed line labeled } h(r) \text{.} \\
\text{Equation:} \\
\text{(FR.12)} \quad -\frac{4i}{v} \xi e^2 \left[4 \left(-\frac{1}{4} \hat{a}_{\tilde{B}} + \xi \hat{a}_8 + \hat{a}_1 \right) - 2 \left(-\frac{1}{2} \hat{a}_{\tilde{B}} + \hat{a}_2 \right) \sec^2 \theta_W + \right. \\
\left. + \csc^2 \theta_W \left(\frac{1}{2} \hat{a}_{\tilde{W}} - 4 \xi \hat{a}_8 + 2 \xi \hat{a}_9 + \hat{a}_3 \right) - \frac{1}{2} \hat{a}_{\tilde{W}} \right] p_\mu q_\nu \epsilon^{\alpha\beta\mu\nu}
\end{array}$$

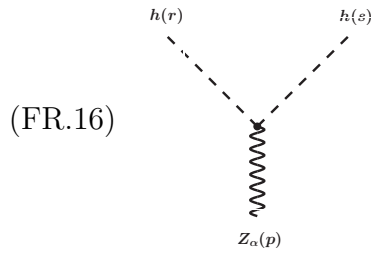
$$\begin{array}{c}
A_\alpha(p) \qquad \qquad Z_\beta(q) \\
\swarrow \qquad \qquad \searrow \\
\text{(FR.13)} \qquad \qquad \qquad -\frac{4i}{v} \xi e^2 \left[-\hat{a}_{\tilde{B}} \tan \theta_W - 2 \cot \theta_W \left(-\frac{1}{4} \hat{a}_{\tilde{W}} + 2 \xi \hat{a}_8 \right) + \right. \\
\qquad \qquad \qquad \left. + (2 \xi \hat{a}_9 + 2 \hat{a}_2 + \hat{a}_3) \csc(2\theta_W) - 4 \hat{a}_1 \cot(2\theta_W) \right] p_\mu q_\nu \epsilon^{\alpha\beta\mu\nu} \\
\text{---} \qquad \qquad \qquad \text{---} \\
h(r) \qquad \qquad \qquad \text{---}
\end{array}$$



$$-\frac{4i}{v} g_s^2 \delta^{ab} \xi \hat{a}_{\tilde{\Phi}} p_\mu q_\nu \epsilon^{\alpha\beta\mu\nu}$$



$$\begin{aligned} & \frac{2}{v} \xi^2 e^2 \csc^2 \theta_W [\hat{a}_7 g^{\alpha\beta} (p \cdot p - q \cdot q) - (\hat{a}_7 - \hat{a}_{12}) (p^\alpha p^\beta - q^\alpha q^\beta)] + \\ & - \frac{4i}{v} \xi e^2 \csc^2 \theta_W (\hat{a}_3 + \frac{1}{2} \hat{a}_{\tilde{W}}) p_\mu q_\nu \epsilon^{\alpha\beta\mu\nu} \end{aligned}$$

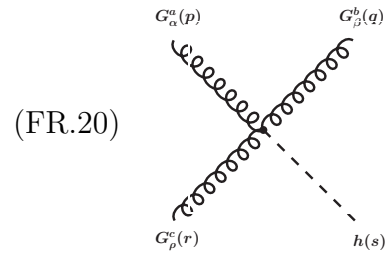


$$\begin{aligned} & \frac{2}{v^2} \xi e \csc(2\theta_W) \left\{ 8 \xi \hat{a}_{14} a'_{14} (r \cdot s) p^\alpha + v^2 \left[\left(\hat{a}_{2D} - \frac{\hat{b}_{2D}}{2} \right) p^\alpha + \right. \right. \\ & \left. \left. + \frac{4}{v^2} \xi \hat{a}_{13} (r^2 r^\alpha + s^2 s^\alpha) + \frac{2}{v^2} \xi \hat{b}_{13} p^2 p^\alpha \right] \right\} \end{aligned}$$

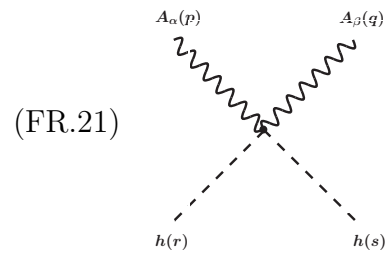
$$\begin{aligned}
 & \frac{1}{v} \xi^2 e^3 \csc^3 \theta_W \sec \theta_W \left\{ \hat{a}_{10} g^{\beta\rho} p^\alpha + \hat{a}_7 [g^{\beta\rho} (p^\alpha + q^\alpha + r^\alpha) + g^{\alpha\rho} (p^\beta + q^\beta + r^\beta)] + \hat{a}_{12} [g^{\beta\rho} (p^\alpha + q^\alpha + r^\alpha) + \right. \\
 & \left. + g^{\alpha\rho} (p^\beta + q^\beta + r^\beta)] + \hat{a}_{10} g^{\alpha\rho} q^\beta - 2 \hat{a}_6 g^{\alpha\beta} (p^\rho + q^\rho + r^\rho) - 2 \hat{a}_7 g^{\alpha\beta} (p^\rho + q^\rho + r^\rho) + 2 \hat{a}_{11} g^{\alpha\beta} r^\rho + \right. \\
 & \left. - \hat{a}_5 [g^{\beta\rho} (p^\alpha + q^\alpha + r^\alpha) + g^{\alpha\rho} (p^\beta + q^\beta + r^\beta)] - \hat{a}_4 [g^{\beta\rho} q^\alpha + g^{\alpha\rho} p^\beta - g^{\alpha\beta} (p^\rho + q^\rho)] + \right. \\
 & \left. + \cos(2\theta_W) \left[(\hat{a}_7 - \hat{a}_{12}) (g^{\beta\rho} (p^\alpha + q^\alpha + r^\alpha) + g^{\alpha\rho} (p^\beta + q^\beta + r^\beta)) - 2 \hat{a}_7 g^{\alpha\beta} (p^\rho + q^\rho + r^\rho) \right] \right\} + \\
 & \text{(FR.17)} \quad \begin{array}{c} W_\alpha^+(p) \quad \quad \quad W_\beta^-(q) \\ \text{---} \quad \quad \quad \text{---} \\ z_\rho(r) \quad \quad \quad h(s) \end{array}
 \end{aligned}$$

$$\begin{aligned}
 & \frac{2}{v} \xi^2 e^3 \csc^2 \theta_W \left\{ (\hat{a}_7 - \hat{a}_{12}) [g^{\beta\rho} (p^\alpha + q^\alpha + r^\alpha) + g^{\alpha\rho} (p^\beta + q^\beta + r^\beta)] - 2 \hat{a}_7 g^{\alpha\beta} (p^\rho + q^\rho + r^\rho) \right\} + \\
 & \text{(FR.18)} \quad \begin{array}{c} W_\alpha^+(p) \quad \quad \quad W_\beta^-(q) \\ \text{---} \quad \quad \quad \text{---} \\ z_\rho(r) \quad \quad \quad h(s) \end{array} \\
 & - \frac{4i}{v} \xi e^3 \csc^2 \theta_W \left[-\frac{1}{2} \hat{a}_{\tilde{W}} (p_\sigma + q_\sigma + r_\sigma) - \hat{a}_3 (p_\sigma + q_\sigma + r_\sigma) + 2 (2 \xi \hat{a}_8 + \hat{a}_1) r_\sigma \right] \epsilon^{\alpha\beta\rho\sigma}
 \end{aligned}$$

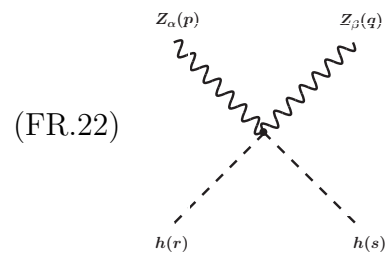
$$\begin{aligned}
 & \frac{16}{v} \xi^2 e^3 \csc^3 (2\theta_W) \left\{ (2 \xi \hat{a}_{16} + \hat{a}_{10} + \hat{a}_{11}) (g^{\beta\rho} p^\alpha + g^{\alpha\rho} q^\beta + g^{\alpha\beta} r^\rho) + \right. \\
 & \left. - (2 \xi \hat{a}_{15} + \hat{a}_5 + \hat{a}_6) [g^{\beta\rho} (p^\alpha + q^\alpha + r^\alpha) + g^{\alpha\rho} (p^\beta + q^\beta + r^\beta) + \right. \\
 & \left. + g^{\alpha\beta} (p^\rho + q^\rho + r^\rho)] \right\}
 \end{aligned}$$



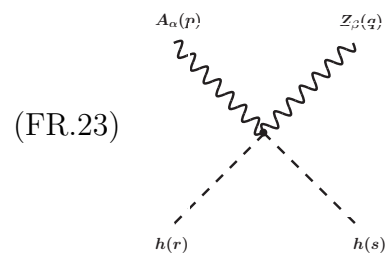
$$\frac{4}{v} f^{abc} g_s^3 \xi \hat{a}_{\tilde{\mathfrak{G}}} (p_\mu + q_\mu + r_\mu) \epsilon^{\alpha\beta\mu\rho}$$



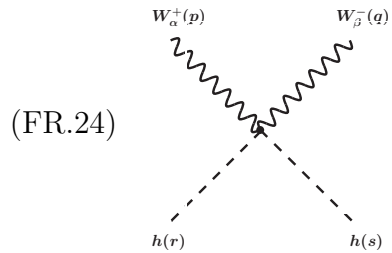
$$\frac{8i}{v^2} \xi e^2 \left[2 \left(-\frac{1}{4} \hat{b}_{\tilde{B}} + \xi \hat{b}_8 + \hat{b}_1 \right) - \frac{1}{4} \hat{b}_{\tilde{W}} \right] p_\mu q_\nu \epsilon^{\alpha\beta\mu\nu}$$



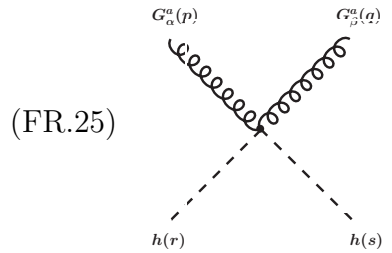
$$\begin{aligned} & -\frac{4i}{v^2} \xi e^2 \left[4 \left(-\frac{1}{4} \hat{b}_{\tilde{B}} + \xi \hat{b}_8 + \hat{b}_1 \right) - 2 \left(-\frac{1}{2} \hat{b}_{\tilde{B}} + \hat{b}_2 \right) \sec^2 \theta_W + \right. \\ & \left. + \csc^2 \theta_W \left(\frac{1}{2} \hat{b}_{\tilde{W}} - 4 \xi \hat{b}_8 + 2 \xi \hat{b}_9 + \hat{b}_3 \right) - \frac{1}{2} \hat{b}_{\tilde{W}} \right] p_\mu q_\nu \epsilon^{\alpha\beta\mu\nu} \end{aligned}$$



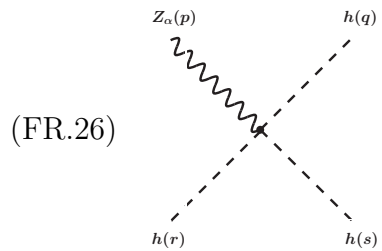
$$\begin{aligned} & -\frac{4i}{v^2} \xi e^2 \left[-\hat{b}_{\tilde{B}} \tan \theta_W - 2 \cot \theta_W \left(-\frac{1}{4} \hat{b}_{\tilde{W}} + 2 \xi \hat{b}_8 \right) + \right. \\ & \left. + \left(2 \xi \hat{b}_9 + 2 \hat{b}_2 + \hat{b}_3 \right) \csc (2\theta_W) - 4 \hat{b}_1 \cot (2\theta_W) \right] p_\mu q_\nu \epsilon^{\alpha\beta\mu\nu} \end{aligned}$$



$$\begin{aligned}
 & \frac{2}{v^2} \xi^2 e^2 \csc^2 \theta_W \left\{ \hat{b}_7 [g^{\alpha\beta}(q \cdot r - p \cdot r) + p^\beta r^\alpha - q^\alpha r^\beta] + \hat{b}_{12} (q^\beta r^\alpha - p^\alpha r^\beta) \right\} + \\
 & - \frac{2i}{v^2} \xi e^2 (\hat{b}_3 + \hat{b}_{\tilde{W}}) \csc^2 \theta_W p_\mu q_\nu \epsilon^{\alpha\beta\mu\nu}
 \end{aligned}$$



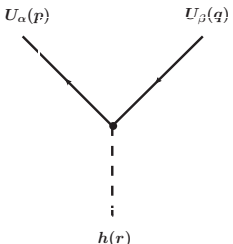
$$- \frac{4i}{v^2} g_s^2 \delta^{ab} \xi \hat{b}_{\tilde{Q}} p_\mu q_\nu \epsilon^{\alpha\beta\mu\nu}$$



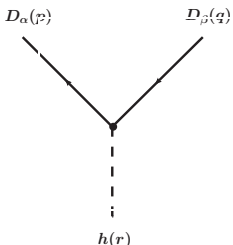
$$\begin{aligned}
 & \frac{2}{v^3} \xi e \csc(2\theta_W) \left\{ 8 \xi p^\alpha (r \cdot q + q \cdot s + r \cdot s) (\hat{a}_{14} b'_{14} + \hat{b}_{14} a'_{14}) + \right. \\
 & \left. + v^2 [\hat{a}_{2D} p^\alpha + \frac{4}{v^2} \xi \hat{a}_{13} (q^2 q^\alpha + r^2 r^\alpha + s^2 s^\alpha)] \right\}
 \end{aligned}$$

SM**Non-SM**

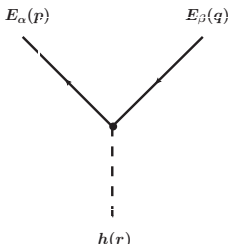
(FR.27)


$$-\frac{i}{\sqrt{2}} \left[P_L \left(Y_U^\dagger \right)_{\alpha\beta} + P_R (Y_U)_{\alpha\beta} \right] + \frac{1}{\sqrt{2}v^2} \xi (\hat{a}_{2D} v^2 - 4\xi \hat{a}_{13} r^2) \left[P_L \left(Y_U^\dagger \right)_{\alpha\beta} - P_R (Y_U)_{\alpha\beta} \right]$$

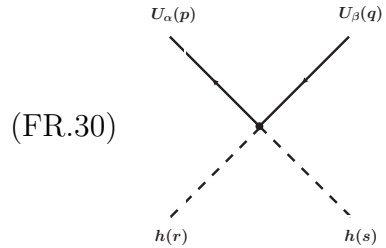
(FR.28)


$$-\frac{i}{\sqrt{2}} \left[P_L \left(Y_D^\dagger \right)_{\alpha\beta} + P_R (Y_D)_{\alpha\beta} \right] - \frac{1}{\sqrt{2}v^2} \xi (\hat{a}_{2D} v^2 - 4\xi \hat{a}_{13} r^2) \left[P_L \left(Y_D^\dagger \right)_{\alpha\beta} - P_R (Y_D)_{\alpha\beta} \right]$$

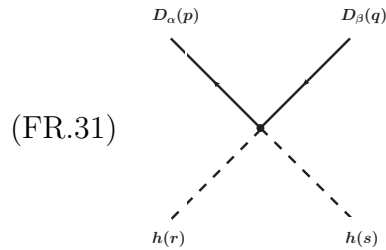
(FR.29)


$$-\frac{i}{\sqrt{2}} \left[P_L \left(Y_E^\dagger \right)_{\alpha\beta} + P_R (Y_E)_{\alpha\beta} \right] - \frac{1}{\sqrt{2}v^2} \xi (\hat{a}_{2D} v^2 - 4\xi \hat{a}_{13} r^2) \left[P_L \left(Y_E^\dagger \right)_{\alpha\beta} - P_R (Y_E)_{\alpha\beta} \right]$$

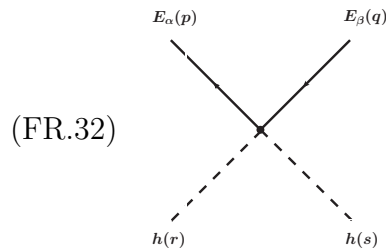
Non-SM



$$+ \frac{\sqrt{2}}{v^3} \xi [\hat{a}_{2D} v^2 - 2 \xi \hat{a}_{13} (r^2 + s^2)] \left[P_L \left(Y_U^\dagger \right)_{\alpha\beta} - P_R (Y_U)_{\alpha\beta} \right]$$



$$- \frac{\sqrt{2}}{v^3} \xi [\hat{a}_{2D} v^2 - 2 \xi \hat{a}_{13} (r^2 + s^2)] \left[P_L \left(Y_D^\dagger \right)_{\alpha\beta} - P_R (Y_D)_{\alpha\beta} \right]$$



$$- \frac{\sqrt{2}}{v^3} \xi [\hat{a}_{2D} v^2 - 2 \xi \hat{a}_{13} (r^2 + s^2)] \left[P_L \left(Y_E^\dagger \right)_{\alpha\beta} - P_R (Y_E)_{\alpha\beta} \right]$$

Bibliography

- [1] **ATLAS Collaboration** Collaboration, G. Aad *et. al.*, Phys.Lett. **B716** (2012) 1–29, [[arXiv:1207.7214](https://arxiv.org/abs/1207.7214)].
- [2] **CMS Collaboration** Collaboration, S. Chatrchyan *et. al.*, Phys.Lett. **B716** (2012) 30–61, [[arXiv:1207.7235](https://arxiv.org/abs/1207.7235)].
- [3] F. Englert and R. Brout, *Broken Symmetry and the Mass of Gauge Vector Mesons*, Phys.Rev.Lett. **13** (1964) 321–323.
- [4] P. W. Higgs, *Broken Symmetries, Massless Particles and Gauge Fields*, Phys.Lett. **12** (1964) 132–133.
- [5] P. W. Higgs, *Broken Symmetries and the Masses of Gauge Bosons*, Phys.Rev.Lett. **13** (1964) 508–509.
- [6] H. E. Haber and G. L. Kane, *The Search for Supersymmetry: Probing Physics Beyond the Standard Model*, Phys. Rept. **117** (1985) 75.
- [7] J. F. Gunion and H. E. Haber, *Higgs Bosons in Supersymmetric Models. 1.*, Nucl. Phys. B **272** (1986) 1 [Erratum-*ibid.* B **402** (1993) 567].
- [8] J. F. Gunion and H. E. Haber, *Higgs Bosons in Supersymmetric Models. 2. Implications for Phenomenology*, Nucl. Phys. B **278** (1986) 449.
- [9] L. Susskind, *Dynamics of Spontaneous Symmetry Breaking in the Weinberg- Salam Theory*, Phys. Rev. **D20** (1979) 2619–2625.
- [10] S. Dimopoulos and L. Susskind, *Mass without Scalars*, Nucl. Phys. **B155** (1979) 237–252.
- [11] S. Dimopoulos and J. Preskill, *Massless Composites with Massive Constituents*, Nucl.Phys. **B199** (1982) 206.

[12] A. Manohar and H. Georgi, *Chiral Quarks and the Nonrelativistic Quark Model*, Nucl.Phys. **B234** (1984) 189.

[13] D. B. Kaplan and H. Georgi, *$SU(2) \times U(1)$ Breaking by Vacuum Misalignment*, Phys.Lett. **B136** (1984) 183.

[14] D. B. Kaplan, H. Georgi, and S. Dimopoulos, *Composite Higgs Scalars*, Phys. Lett. **B136** (1984) 187.

[15] T. Banks, *Constraints on $SU(2) \times U(1)$ Breaking by Vacuum Misalignment*, Nucl.Phys. **B243** (1984) 125.

[16] H. Georgi, D. B. Kaplan, and P. Galison, *Calculation of the Composite Higgs Mass*, Phys.Lett. **B143** (1984) 152.

[17] H. Georgi and D. B. Kaplan, *Composite Higgs and Custodial $SU(2)$* , Phys.Lett. **B145** (1984) 216.

[18] M. J. Dugan, H. Georgi, and D. B. Kaplan, *Anatomy of a Composite Higgs Model*, Nucl. Phys. **B254** (1985) 299.

[19] R. Alonso, M. Gavela, L. Merlo, S. Rigolin, and J. Yepes, *The Effective Chiral Lagrangian for a Light Dynamical ‘Higgs’*, Phys.Lett. **B722** (2013) 330–335, [[arXiv:1212.3305](https://arxiv.org/abs/1212.3305)].

[20] M. B. Gavela, J. Gonzalez-Fraile, M. C. Gonzalez-Garcia, L. Merlo, S. Rigolin and J. Yepes, *CP violation with a dynamical Higgs*, arXiv:1406.6367 [hep-ph].

[21] T. Appelquist and C. W. Bernard, *Strongly Interacting Higgs Bosons*, Phys. Rev. **D22** (1980) 200.

[22] A. C. Longhitano, *Heavy Higgs Bosons in the Weinberg-Salam Model*, Phys. Rev. **D22** (1980) 1166.

[23] A. C. Longhitano, *Low-Energy Impact of a Heavy Higgs Boson Sector*, Nucl. Phys. **B188** (1981) 118.

[24] F. Feruglio, *The Chiral approach to the electroweak interactions*, Int.J.Mod.Phys. **A8** (1993) 4937–4972, [[hep-ph/9301281](https://arxiv.org/abs/hep-ph/9301281)].

[25] T. Appelquist and G.-H. Wu, *The Electroweak Chiral Lagrangian and New Precision Measurements*, Phys.Rev. **D48** (1993) 3235–3241, [[hep-ph/9304240](https://arxiv.org/abs/hep-ph/9304240)].

[26] R. Contino, C. Grojean, M. Moretti, F. Piccinini, and R. Rattazzi, *Strong Double Higgs Production at the Lhc*, JHEP **1005** (2010) 089, [[arXiv:1002.1011](https://arxiv.org/abs/1002.1011)].

[27] A. Azatov, R. Contino, and J. Galloway, *Model-Independent Bounds on a Light Higgs*, JHEP **1204** (2012) 127, [[arXiv:1202.3415](https://arxiv.org/abs/1202.3415)].

[28] G. F. Giudice, C. Grojean, A. Pomarol, and R. Rattazzi, *The Strongly-Interacting Light Higgs*, JHEP **06** (2007) 045, [[hep-ph/0703164](https://arxiv.org/abs/hep-ph/0703164)].

[29] I. Low, R. Rattazzi, and A. Vichi, JHEP **1004** (2010) 126, [[arXiv:0907.5413](https://arxiv.org/abs/0907.5413)].

[30] G. Buchalla, O. Catà, and C. Krause, *Complete Electroweak Chiral Lagrangian with a Light Higgs at NLO*, Nucl.Phys. **B880** (2014) 552–573, [[arXiv:1307.5017](https://arxiv.org/abs/1307.5017)].

[31] J. R. Dell’Aquila and C. A. Nelson, *P or CP Determination by Sequential Decays: V1 V2 Modes With Decays Into $\bar{\ell}(A) \ell(B)$ And/or $\bar{q}(A) q(B)$* , Phys.Rev. **D33** (1986) 80.

[32] J. R. Dell’Aquila and C. A. Nelson, *Distinguishing a Spin 0 Technipion and an Elementary Higgs Boson: V1 V2 Modes With Decays Into $\bar{\ell}(A) \ell(B)$ And/or $\bar{q}(A) q(B)$* , Phys.Rev. **D33** (1986) 93.

[33] J. R. Dell’Aquila and C. A. Nelson, *Simple Tests for CP or P Violation by Sequential Decays: V1 V2 Modes With Decays Into $\bar{\ell}(A) \ell(B)$ And/or $\bar{q}(A) q(B)$* , Phys.Rev. **D33** (1986) 101.

[34] A. Soni and R. Xu, *Probing CP violation via Higgs decays to four leptons*, Phys.Rev. **D48** (1993) 5259–5263, [[hep-ph/9301225](https://arxiv.org/abs/hep-ph/9301225)].

[35] D. Chang, W.-Y. Keung, and I. Phillips, *CP odd correlation in the decay of neutral Higgs boson into $Z Z$, $W+ W-$, or t anti- t* , Phys.Rev. **D48** (1993) 3225–3234, [[hep-ph/9303226](https://arxiv.org/abs/hep-ph/9303226)].

[36] T. Arens and L. Sehgal, *Energy spectra and energy correlations in the decay $H \rightarrow Z Z \rightarrow mu+ mu- mu+ mu-$* , Z.Phys. **C66** (1995) 89–94, [[hep-ph/9409396](https://arxiv.org/abs/hep-ph/9409396)].

[37] S. Choi, D. Miller, M. Muhlleitner, and P. Zerwas, *Identifying the Higgs spin and parity in decays to Z pairs*, Phys.Lett. **B553** (2003) 61–71, [[hep-ph/0210077](https://arxiv.org/abs/hep-ph/0210077)].

[38] C. Buszello, I. Fleck, P. Marquard, and J. van der Bij, *Prospective analysis of spin- and CP-sensitive variables in $H \rightarrow Z Z \rightarrow l(1)+ l(1)- l(2)+ l(2)-$ at the LHC*, Eur.Phys.J. **C32** (2004) 209–219, [[hep-ph/0212396](https://arxiv.org/abs/hep-ph/0212396)].

[39] R. M. Godbole, D. Miller, and M. M. Muhlleitner, *Aspects of CP violation in the $H ZZ$ coupling at the LHC*, JHEP **0712** (2007) 031, [[arXiv:0708.0458](https://arxiv.org/abs/0708.0458)].

[40] Q.-H. Cao, C. Jackson, W.-Y. Keung, I. Low, and J. Shu, *The Higgs Mechanism and Loop-induced Decays of a Scalar into Two Z Bosons*, Phys.Rev. **D81** (2010) 015010, [[arXiv:0911.3398](https://arxiv.org/abs/0911.3398)].

[41] Y. Gao, A. V. Gritsan, Z. Guo, K. Melnikov, M. Schulze, *et. al.*, *Spin determination of single-produced resonances at hadron colliders*, Phys.Rev. **D81** (2010) 075022, [[arXiv:1001.3396](https://arxiv.org/abs/1001.3396)].

[42] A. De Rujula, J. Lykken, M. Pierini, C. Rogan, and M. Spiropulu, *Higgs look-alikes at the LHC*, Phys.Rev. **D82** (2010) 013003, [[arXiv:1001.5300](https://arxiv.org/abs/1001.5300)].

[43] T. Plehn, D. L. Rainwater, and D. Zeppenfeld, *Determining the structure of Higgs couplings at the LHC*, Phys.Rev.Lett. **88** (2002) 051801, [[hep-ph/0105325](https://arxiv.org/abs/hep-ph/0105325)].

[44] C. Buszello and P. Marquard, *Determination of spin and CP of the Higgs boson from WBF*, [hep-ph/0603209](https://arxiv.org/abs/hep-ph/0603209).

[45] V. Hankele, G. Klamke, D. Zeppenfeld, and T. Figy, *Anomalous Higgs boson couplings in vector boson fusion at the CERN LHC*, Phys.Rev. **D74** (2006) 095001, [[hep-ph/0609075](https://arxiv.org/abs/hep-ph/0609075)].

[46] G. Klamke and D. Zeppenfeld, *Higgs plus two jet production via gluon fusion as a signal at the CERN LHC*, JHEP **0704** (2007) 052, [[hep-ph/0703202](https://arxiv.org/abs/hep-ph/0703202)].

[47] C. Englert, M. Spannowsky, and M. Takeuchi, *Measuring Higgs CP and couplings with hadronic event shapes*, JHEP **1206** (2012) 108, [[arXiv:1203.5788](https://arxiv.org/abs/1203.5788)].

[48] K. Odagiri, *On azimuthal spin correlations in Higgs plus jet events at LHC*, JHEP **0303** (2003) 009, [[hep-ph/0212215](https://arxiv.org/abs/hep-ph/0212215)].

[49] V. Del Duca, G. Klamke, D. Zeppenfeld, M. L. Mangano, M. Moretti, *et. al.*, *Monte Carlo studies of the jet activity in Higgs + 2 jet events*, JHEP **0610** (2006) 016, [[hep-ph/0608158](https://arxiv.org/abs/hep-ph/0608158)].

[50] J. R. Andersen, K. Arnold, and D. Zeppenfeld, *Azimuthal Angle Correlations for Higgs Boson plus Multi-Jet Events*, JHEP **1006** (2010) 091, [[arXiv:1001.3822](https://arxiv.org/abs/1001.3822)].

[51] C. Englert, D. Goncalves-Netto, K. Mawatari, and T. Plehn, *Higgs Quantum Numbers in Weak Boson Fusion*, JHEP **1301** (2013) 148, [[arXiv:1212.0843](https://arxiv.org/abs/1212.0843)].

[52] A. Djouadi, R. Godbole, B. Mellado, and K. Mohan, *Probing the spin-parity of the Higgs boson via jet kinematics in vector boson fusion*, Phys.Lett. **B723** (2013) 307–313, [[arXiv:1301.4965](https://arxiv.org/abs/1301.4965)].

[53] M. J. Dolan, P. Harris, M. Jankowiak, and M. Spannowsky, *Constraining CP-violating Higgs Sectors at the LHC using gluon fusion*, [arXiv:1406.3322](https://arxiv.org/abs/1406.3322).

[54] N. D. Christensen, T. Han, and Y. Li, *Testing CP Violation in ZZH Interactions at the LHC*, Phys.Lett. **B693** (2010) 28–35, [[arXiv:1005.5393](https://arxiv.org/abs/1005.5393)].

[55] N. Desai, D. K. Ghosh, and B. Mukhopadhyaya, *CP-violating HWW couplings at the Large Hadron Collider*, Phys.Rev. **D83** (2011) 113004, [[arXiv:1104.3327](https://arxiv.org/abs/1104.3327)].

[56] J. Ellis, D. S. Hwang, V. Sanz, and T. You, *A Fast Track towards the ‘Higgs’ Spin and Parity*, JHEP **1211** (2012) 134, [[arXiv:1208.6002](https://arxiv.org/abs/1208.6002)].

[57] R. Godbole, D. J. Miller, K. Mohan, and C. D. White, *Boosting Higgs CP properties via VH Production at the Large Hadron Collider*, Phys.Lett. **B730** (2014) 275–279, [[arXiv:1306.2573](https://arxiv.org/abs/1306.2573)].

[58] C. Delaunay, G. Perez, H. de Sandes, and W. Skiba, *Higgs Up-Down CP Asymmetry at the LHC*, Phys.Rev. **D89** (2014) 035004, [[arXiv:1308.4930](https://arxiv.org/abs/1308.4930)].

[59] M. Voloshin, *CP Violation in Higgs Diphoton Decay in Models with Vectorlike Heavy Fermions*, Phys.Rev. **D86** (2012) 093016, [[arXiv:1208.4303](https://arxiv.org/abs/1208.4303)].

[60] A. Y. Korchin and V. A. Kovalchuk, *Polarization effects in the Higgs boson decay to γZ and test of CP and CPT symmetries*, Phys.Rev. **D88** (2013), no. 3 036009, [[arXiv:1303.0365](https://arxiv.org/abs/1303.0365)].

[61] F. Bishara, Y. Grossman, R. Harnik, D. J. Robinson, J. Shu, *et. al.*, *Probing CP Violation in $h \rightarrow \gamma\gamma$ with Converted Photons*, JHEP **1404** (2014) 084, [[arXiv:1312.2955](https://arxiv.org/abs/1312.2955)].

[62] Y. Chen, A. Falkowski, I. Low, and R. Vega-Morales, *New Observables for CP Violation in Higgs Decays*, [arXiv:1405.6723](https://arxiv.org/abs/1405.6723).

[63] A. Freitas and P. Schwaller, *Higgs CP Properties From Early LHC Data*, Phys.Rev. **D87** (2013), no. 5 055014, [[arXiv:1211.1980](https://arxiv.org/abs/1211.1980)].

[64] A. Djouadi and G. Moreau, *The Couplings of the Higgs Boson and Its CP Properties from Fits of the Signal Strengths and Their Ratios at the 7+8 TeV LHC*, [arXiv:1303.6591](https://arxiv.org/abs/1303.6591).

[65] H. Belusca-Maito, *Effective Higgs Lagrangian and Constraints on Higgs Couplings*, [arXiv:1404.5343](https://arxiv.org/abs/1404.5343).

[66] J. Shu and Y. Zhang, *Impact of a CP Violating Higgs Sector: from Lhc to Baryogenesis*, Phys. Rev. Lett. **111** (2013) 9, 091801, [arXiv:1304.0773](https://arxiv.org/abs/1304.0773).

[67] K. Cheung, J. S. Lee and P. -Y. Tseng, *Higgs Precision (Higgcision) Era Begins*, JHEP **1305** (2013) 134 [arXiv:1302.3794](https://arxiv.org/abs/1302.3794).

[68] R. Alonso, M. Gavela, L. Merlo, S. Rigolin, and J. Yepes, *Flavor with a Light Dynamical "Higgs Particle"*, Phys. Rev. **D87** (2013) 055019, [[arXiv:1212.3307](https://arxiv.org/abs/1212.3307)].

[69] R. S. Chivukula and H. Georgi, *Composite Technicolor Standard Model*, Phys. Lett. **B188** (1987) 99.

[70] L. J. Hall and L. Randall, *Weak Scale Effective Supersymmetry*, Phys. Rev. Lett. **65** (1990) 2939–2942.

[71] G. D'Ambrosio, G. F. Giudice, G. Isidori, and A. Strumia, *Minimal Flavour Violation: an Effective Field Theory Approach*, Nucl. Phys. **B645** (2002) 155–187, [[hep-ph/0207036](https://arxiv.org/abs/hep-ph/0207036)].

[72] H. Fritzsch, M. Gell-Mann and H. Leutwyler, *Advantages of the Color Octet Gluon Picture*, Phys. Lett. B **47** (1973) 365.

[73] H. D. Politzer, *Reliable Perturbative Results for Strong Interactions*, Phys. Rev. Lett. **30** (1973) 1346.

[74] D. J. Gross and F. Wilczek, *Ultraviolet Behavior of Nonabelian Gauge Theories*, Phys. Rev. Lett. **30** (1973) 1343.

[75] S. L. Glashow, *Partial Symmetries of Weak Interactions*, Nucl. Phys. **22** (1961) 579.

[76] S. Weinberg, *A Model of Leptons*, Phys. Rev. Lett. **19** (1967) 1264.

[77] A. Salam, *Weak and Electromagnetic Interactions*, Conf. Proc. C **680519** (1968) 367.

[78] N. Cabibbo, *Unitary Symmetry and Leptonic Decays*, Phys. Rev. Lett. **10** (1963) 531.

[79] M. Kobayashi and T. Maskawa, *CP Violation in the Renormalizable Theory of Weak Interaction*, Prog. Theor. Phys. **49** (1973) 652.

[80] B. Pontecorvo, *Inverse beta processes and nonconservation of lepton charge*, Sov. Phys. JETP **7** (1958) 172 [Zh. Eksp. Teor. Fiz. **34** (1957) 247].

[81] Z. Maki, M. Nakagawa and S. Sakata, *Remarks on the unified model of elementary particles*, Prog. Theor. Phys. **28** (1962) 870.

[82] **Particle Data Group Collaboration**, J. Beringer *et al.*, *Review of Particle Physics (RPP)*, Phys. Rev. D **86** (2012) 010001.

[83] L. Wolfenstein, “Parametrization of the Kobayashi-Maskawa Matrix,” Phys. Rev. Lett. **51** (1983) 1945.

[84] W. Buchmuller and D. Wyler, *Effective Lagrangian Analysis of New Interactions and Flavor Conservation*, Nucl.Phys. **B268** (1986) 621.

[85] B. Grzadkowski, M. Iskrzynski, M. Misiak, and J. Rosiek, *Dimension-Six Terms in the Standard Model Lagrangian*, JHEP **1010** (2010) 085, [[arXiv:1008.4884](https://arxiv.org/abs/1008.4884)].

[86] G. Isidori, Y. Nir, and G. Perez, *Flavor Physics Constraints for Physics Beyond the Standard Model*, Ann. Rev. Nucl. Part. Sci. **60** (2010) 355, [[arXiv:1002.0900](https://arxiv.org/abs/1002.0900)].

[87] K. Hagiwara, R. Szalapski, and D. Zeppenfeld, *Anomalous Higgs boson production and decay*, Phys.Lett. **B318** (1993) 155–162, [[hep-ph/9308347](https://arxiv.org/abs/hep-ph/9308347)].

[88] M. Gonzalez-Garcia, *Anomalous Higgs couplings*, Int.J.Mod.Phys. **A14** (1999) 3121–3156, [[hep-ph/9902321](https://arxiv.org/abs/hep-ph/9902321)].

[89] T. Corbett, O. Eboli, J. Gonzalez-Fraile, and M. Gonzalez-Garcia, *Constraining anomalous Higgs interactions*, Phys.Rev. **D86** (2012) 075013, [[arXiv:1207.1344](https://arxiv.org/abs/1207.1344)].

[90] T. Corbett, O. Eboli, J. Gonzalez-Fraile, and M. Gonzalez-Garcia, *Robust Determination of the Higgs Couplings: Power to the Data*, Phys.Rev. **D87** (2013) 015022, [[arXiv:1211.4580](https://arxiv.org/abs/1211.4580)].

[91] **ATLAS** Collaboration, G. Aad *et. al.*, *Observation of a New Particle in the Search for the Standard Model Higgs Boson with the Atlas Detector at the LHC*, Phys.Lett. **B716** (2012) 1–29, [[arXiv:1207.7214](https://arxiv.org/abs/1207.7214)].

[92] **CMS** Collaboration, S. Chatrchyan *et. al.*, *Observation of a New Boson at a Mass of 125 GeV with the Cms Experiment at the LHC*, Phys.Lett. **B716** (2012) 30–61, [[arXiv:1207.7235](https://arxiv.org/abs/1207.7235)].

[93] I. Low, J. Lykken, and G. Shaughnessy, *Have We Observed the Higgs (Imposter)?*, Phys.Rev. **D86** (2012) 093012, [[arXiv:1207.1093](https://arxiv.org/abs/1207.1093)].

[94] J. Ellis and T. You, *Global Analysis of the Higgs Candidate with Mass 125 GeV*, JHEP **1209** (2012) 123, [[arXiv:1207.1693](https://arxiv.org/abs/1207.1693)].

[95] P. P. Giardino, K. Kannike, M. Raidal, and A. Strumia, *Is the Resonance at 125 GeV the Higgs Boson?*, Phys.Lett. **B718** (2012) 469–474, [[arXiv:1207.1347](https://arxiv.org/abs/1207.1347)].

[96] M. Montull and F. Riva, *Higgs Discovery: the Beginning Or the End of Natural Ewsb?*, JHEP **1211** (2012) 018, [[arXiv:1207.1716](https://arxiv.org/abs/1207.1716)].

[97] J. Espinosa, C. Grojean, M. Muhlleitner, and M. Trott, *First Glimpses at Higgs' Face*, JHEP **1212** (2012) 045, [[arXiv:1207.1717](https://arxiv.org/abs/1207.1717)].

[98] D. Carmi, A. Falkowski, E. Kuflik, T. Volansky, and J. Zupan, *Higgs After the Discovery: a Status Report*, JHEP **1210** (2012) 196, [[arXiv:1207.1718](https://arxiv.org/abs/1207.1718)].

[99] S. Banerjee, S. Mukhopadhyay, and B. Mukhopadhyaya, *New Higgs Interactions and Recent Data from the LHC and the Tevatron*, JHEP **1210** (2012) 062, [[arXiv:1207.3588](https://arxiv.org/abs/1207.3588)].

[100] F. Bonnet, T. Ota, M. Rauch, and W. Winter, *Interpretation of Precision Tests in the Higgs Sector in Terms of Physics Beyond the Standard Model*, Phys.Rev. **D86** (2012) 093014, [[arXiv:1207.4599](https://arxiv.org/abs/1207.4599)].

[101] T. Plehn and M. Rauch, *Higgs Couplings After the Discovery*, Europhys.Lett. **100** (2012) 11002, [[arXiv:1207.6108](https://arxiv.org/abs/1207.6108)].

[102] A. Djouadi, *Precision Higgs Coupling Measurements at the LHC Through Ratios of Production Cross Sections*, [arXiv:1208.3436](https://arxiv.org/abs/1208.3436).

[103] B. Batell, S. Gori, and L.-T. Wang, *Higgs Couplings and Precision Electroweak Data*, JHEP **1301** (2013) 139, [[arXiv:1209.6382](https://arxiv.org/abs/1209.6382)].

[104] G. Moreau, *Constraining Extra-Fermion(S) from the Higgs Boson Data*, Phys.Rev. **D87** (2013) 015027, [[arXiv:1210.3977](https://arxiv.org/abs/1210.3977)].

[105] G. Cacciapaglia, A. Deandrea, G. D. La Rochelle, and J.-B. Flament, *Higgs Couplings Beyond the Standard Model*, JHEP **1303** (2013) 029, [[arXiv:1210.8120](https://arxiv.org/abs/1210.8120)].

[106] A. Azatov and J. Galloway, *Electroweak Symmetry Breaking and the Higgs Boson: Confronting Theories at Colliders*, Int.J.Mod.Phys. **A28** (2013) 1330004, [[arXiv:1212.1380](https://arxiv.org/abs/1212.1380)].

[107] E. Masso and V. Sanz, *Limits on Anomalous Couplings of the Higgs to Electroweak Gauge Bosons from LEP and LHC*, Phys.Rev. **D87** (2013), no. 3 033001, [[arXiv:1211.1320](https://arxiv.org/abs/1211.1320)].

[108] G. Passarino, *NLO Inspired Effective Lagrangians for Higgs Physics*, Nucl.Phys. **B868** (2013) 416–458, [[arXiv:1209.5538](https://arxiv.org/abs/1209.5538)].

[109] A. Falkowski, F. Riva, and A. Urbano, *Higgs at Last*, [arXiv:1303.1812](https://arxiv.org/abs/1303.1812).

[110] P. P. Giardino, K. Kannike, I. Masina, M. Raidal, and A. Strumia, *The Universal Higgs Fit*, [arXiv:1303.3570](https://arxiv.org/abs/1303.3570).

[111] J. Ellis and T. You, *Updated Global Analysis of Higgs Couplings*, JHEP **1306** (2013) 103, [[arXiv:1303.3879](https://arxiv.org/abs/1303.3879)].

[112] R. Contino, M. Ghezzi, C. Grojean, M. Muhlleitner, and M. Spira, *Effective Lagrangian for a Light Higgs-Like Scalar*, JHEP **1307** (2013) 035, [[arXiv:1303.3876](https://arxiv.org/abs/1303.3876)].

[113] B. Dumont, S. Fichet, and G. von Gersdorff, *A Bayesian view of the Higgs sector with higher dimensional operators*, JHEP **1307** (2013) 065, [[arXiv:1304.3369](https://arxiv.org/abs/1304.3369)].

[114] J. Elias-Miro, J. Espinosa, E. Masso, and A. Pomarol, *Higgs Windows to New Physics Through $D = 6$ Operators: Constraints and One-Loop Anomalous Dimensions*, [arXiv:1308.1879](https://arxiv.org/abs/1308.1879).

[115] D. Lopez-Val, T. Plehn, and M. Rauch, *Measuring Extended Higgs Sectors as a Consistent Free Couplings Model*, JHEP **1310** (2013) 134, [[arXiv:1308.1979](https://arxiv.org/abs/1308.1979)].

[116] E. E. Jenkins, A. V. Manohar, and M. Trott, *Renormalization Group Evolution of the Standard Model Dimension Six Operators I: Formalism and lambda Dependence*, JHEP **1310** (2013) 087, [[arXiv:1308.2627](https://arxiv.org/abs/1308.2627)].

[117] A. Pomarol and F. Riva, *Towards the Ultimate Sm Fit to Close in on Higgs Physics*, [arXiv:1308.2803](https://arxiv.org/abs/1308.2803).

[118] S. Banerjee, S. Mukhopadhyay, and B. Mukhopadhyaya, *Higher dimensional operators and LHC Higgs data : the role of modified kinematics*, [arXiv:1308.4860](https://arxiv.org/abs/1308.4860).

[119] A. Alloul, B. Fuks, and V. Sanz, *Phenomenology of the Higgs Effective Lagrangian via FeynRules*, [arXiv:1310.5150](https://arxiv.org/abs/1310.5150).

[120] V. Cirigliano, B. Grinstein, G. Isidori, and M. B. Wise, *Minimal flavor violation in the lepton sector*, Nucl. Phys. **B728** (2005) 121–134, [[hep-ph/0507001](https://arxiv.org/abs/hep-ph/0507001)].

[121] S. Davidson and F. Palorini, *Various Definitions of Minimal Flavour Violation for Leptons*, Phys. Lett. **B642** (2006) 72–80, [[hep-ph/0607329](https://arxiv.org/abs/hep-ph/0607329)].

[122] A. L. Kagan, G. Perez, T. Volansky, and J. Zupan, *General Minimal Flavor Violation*, Phys. Rev. **D80** (2009) 076002, [[arXiv:0903.1794](https://arxiv.org/abs/0903.1794)].

[123] M. Gavela, T. Hambye, D. Hernandez, and P. Hernandez, *Minimal Flavour Seesaw Models*, JHEP **0909** (2009) 038, [[arXiv:0906.1461](https://arxiv.org/abs/0906.1461)].

[124] T. Feldmann, M. Jung, and T. Mannel, *Sequential Flavour Symmetry Breaking*, Phys. Rev. **D80** (2009) 033003, [[arXiv:0906.1523](https://arxiv.org/abs/0906.1523)].

[125] R. Alonso, M. B. Gavela, L. Merlo, and S. Rigolin, *On the Scalar Potential of Minimal Flavour Violation*, JHEP **07** (2011) 012, [[arXiv:1103.2915](https://arxiv.org/abs/1103.2915)].

[126] R. Alonso, G. Isidori, L. Merlo, L. A. Munoz, and E. Nardi, *Minimal Flavour Violation Extensions of the Seesaw*, JHEP **06** (2011) 037, [[arXiv:1103.5461](https://arxiv.org/abs/1103.5461)].

[127] R. Alonso, M. Gavela, D. Hernandez, and L. Merlo, *On the Potential of Leptonic Minimal Flavour Violation*, Phys.Lett. **B715** (2012) 194–198, [[arXiv:1206.3167](https://arxiv.org/abs/1206.3167)].

[128] Z. Lalak, S. Pokorski, and G. G. Ross, *Beyond MFV in Family Symmetry Theories of Fermion Masses*, JHEP **1008** (2010) 129, [[arXiv:1006.2375](https://arxiv.org/abs/1006.2375)].

[129] A. L. Fitzpatrick, G. Perez, and L. Randall, *Flavor anarchy in a Randall-Sundrum model with 5D minimal flavor violation and a low Kaluza-Klein scale*, Phys.Rev.Lett. **100** (2008) 171604, [[arXiv:0710.1869](https://arxiv.org/abs/0710.1869)].

[130] B. Grinstein, M. Redi, and G. Villadoro, *Low Scale Flavor Gauge Symmetries*, JHEP **11** (2010) 067, [[arXiv:1009.2049](https://arxiv.org/abs/1009.2049)].

[131] A. J. Buras, M. V. Carlucci, L. Merlo, and E. Stamou, *Phenomenology of a Gauged $SU(3)^3$ Flavour Model*, JHEP **03** (2012) 088, [[arXiv:1112.4477](https://arxiv.org/abs/1112.4477)].

[132] K. Agashe, R. Contino, and A. Pomarol, *The Minimal Composite Higgs Model*, Nucl.Phys. **B719** (2005) 165–187, [[hep-ph/0412089](https://arxiv.org/abs/hep-ph/0412089)].

[133] I. Brivio, T. Corbett, O. Eboli, M. Gavela, J. Gonzalez-Fraile, *et. al.*, *Disentangling a dynamical Higgs*, JHEP **1403** (2014) 024, [[arXiv:1311.1823](https://arxiv.org/abs/1311.1823)].

[134] W. D. Goldberger, B. Grinstein, and W. Skiba, *Distinguishing the Higgs Boson from the Dilaton at the Large Hadron Collider*, Phys.Rev.Lett. **100** (2008) 111802, [[arXiv:0708.1463](https://arxiv.org/abs/0708.1463)].

[135] R. Contino, D. Marzocca, D. Pappadopulo, and R. Rattazzi, *On the Effect of Resonances in Composite Higgs Phenomenology*, JHEP **1110** (2011) 081, [[arXiv:1109.1570](https://arxiv.org/abs/1109.1570)].

[136] R. Contino, L. Da Rold, and A. Pomarol, *Light Custodians in Natural Composite Higgs Models*, Phys.Rev. **D75** (2007) 055014, [[hep-ph/0612048](https://arxiv.org/abs/hep-ph/0612048)].

[137] B. Gripaios, A. Pomarol, F. Riva, and J. Serra, *Beyond the Minimal Composite Higgs Model*, JHEP **0904** (2009) 070, [[arXiv:0902.1483](https://arxiv.org/abs/0902.1483)].

[138] E. Halyo, *Technidilaton Or Higgs?*, Mod.Phys.Lett. **A8** (1993) 275–284.

[139] L. Vecchi, *Phenomenology of a Light Scalar: the Dilaton*, Phys.Rev. **D82** (2010) 076009, [[arXiv:1002.1721](https://arxiv.org/abs/1002.1721)].

[140] B. A. Campbell, J. Ellis, and K. A. Olive, *Phenomenology and Cosmology of an Electroweak Pseudo-Dilaton and Electroweak Baryons*, JHEP **1203** (2012) 026, [[arXiv:1111.4495](https://arxiv.org/abs/1111.4495)].

[141] S. Matsuzaki and K. Yamawaki, *Is 125 GeV Techni-Dilaton Found at LHC?*, [arXiv:1207.5911](https://arxiv.org/abs/1207.5911).

[142] Z. Chacko, R. Franceschini, and R. K. Mishra, *Resonance at 125 Gev: Higgs Or Dilaton/Radion?*, [arXiv:1209.3259](https://arxiv.org/abs/1209.3259).

[143] B. Bellazzini, C. Csaki, J. Hubisz, J. Serra, and J. Terning, *A Higgslike Dilaton*, [arXiv:1209.3299](https://arxiv.org/abs/1209.3299).

[144] R. Contino, *The Higgs as a Composite Nambu-Goldstone Boson*, [arXiv:1005.4269](https://arxiv.org/abs/1005.4269).

[145] I. Brivio, O. Eboli, M. Gavela, M. Gonzalez-Garcia, L. Merlo, *et. al.*, *Higgs Ultraviolet Softening*, [arXiv:1405.5412](https://arxiv.org/abs/1405.5412).

[146] H. Georgi, D. B. Kaplan, and L. Randall, *Manifesting the Invisible Axion at Low-Energies*, Phys.Lett. **B169** (1986) 73.

[147] K. Hagiwara, R. Peccei, D. Zeppenfeld, and K. Hikasa, *Probing the Weak Boson Sector in $E^+ E^- \rightarrow W^+ W^-$* , Nucl.Phys. **B282** (1987) 253.

[148] W. J. Marciano and A. Queijeiro, *Bound on the W Boson Electric Dipole Moment*, Phys.Rev. **D33** (1986) 3449.

[149] **ACME** Collaboration, J. Baron *et. al.*, *Order of Magnitude Smaller Limit on the Electric Dipole Moment of the Electron*, Science **343** (2014), no. 6168 269–272, [[arXiv:1310.7534](https://arxiv.org/abs/1310.7534)].

[150] C. Baker, D. Doyle, P. Geltenbort, K. Green, M. van der Grinten, *et. al.*, *An Improved Experimental Limit on the Electric Dipole Moment of the Neutron*, Phys.Rev.Lett. **97** (2006) 131801, [[hep-ex/0602020](https://arxiv.org/abs/hep-ex/0602020)].

[151] S. Dawson, S. K. Gupta, and G. Valencia, *CP violating anomalous couplings in $W\gamma$ and $Z\gamma$ production at the LHC*, Phys.Rev. **D88** (2013), no. 3 035008, [[arXiv:1304.3514](https://arxiv.org/abs/1304.3514)].

[152] **OPAL** Collaboration, G. Abbiendi *et. al.*, *Measurement of W boson polarizations and CP violating triple gauge couplings from W^+W^- production at LEP*, Eur.Phys.J. **C19** (2001) 229–240, [[hep-ex/0009021](https://arxiv.org/abs/hep-ex/0009021)].

[153] **DELPHI** Collaboration, J. Abdallah *et. al.*, *Study of W boson polarisations and Triple Gauge boson Couplings in the reaction $e^+e^- \rightarrow W^+W^-$ at LEP 2*, Eur.Phys.J. **C54** (2008) 345–364, [[arXiv:0801.1235](https://arxiv.org/abs/0801.1235)].

[154] **ALEPH** Collaboration, S. Schael *et. al.*, *Improved measurement of the triple gauge-boson couplings gamma $W W$ and $Z W W$ in $e^+ e^-$ collisions*, Phys.Lett. **B614** (2005) 7–26.

[155] O. Eboli, J. Gonzalez-Fraile, and M. Gonzalez-Garcia, *Scrutinizing the $Z W + W^-$ vertex at the Large Hadron Collider at 7 TeV*, Phys.Lett. **B692** (2010) 20–25, [[arXiv:1006.3562](https://arxiv.org/abs/1006.3562)].

[156] **ATLAS** Collaboration, G. Aad *et. al.*, *Measurement of WZ production in proton-proton collisions at $\sqrt{s} = 7$ TeV with the ATLAS detector*, Eur.Phys.J. **C72** (2012) 2173, [[arXiv:1208.1390](https://arxiv.org/abs/1208.1390)].

[157] N. D. Christensen and C. Duhr, *FeynRules - Feynman rules made easy*, Comput.Phys.Commun. **180** (2009) 1614–1641, [[arXiv:0806.4194](https://arxiv.org/abs/0806.4194)].

[158] J. Alwall, M. Herquet, F. Maltoni, O. Mattelaer, and T. Stelzer, *MadGraph 5 : Going Beyond*, JHEP **1106** (2011) 128, [[arXiv:1106.0522](https://arxiv.org/abs/1106.0522)].

[159] T. Sjostrand, S. Mrenna, and P. Z. Skands, *PYTHIA 6.4 Physics and Manual*, JHEP **0605** (2006) 026, [[hep-ph/0603175](https://arxiv.org/abs/hep-ph/0603175)].

[160] J. Conway, *PGS4*, <http://www.physics.ucdavis.edu/~conway/research/software/pgs/pgs4-general.htm>.

[161] S. Dawson, X.-G. He, and G. Valencia, *CP violation in W gamma and Z gamma production*, Phys.Lett. **B390** (1997) 431–436, [[hep-ph/9609523](https://arxiv.org/abs/hep-ph/9609523)].

[162] J. Kumar, A. Rajaraman, and J. D. Wells, *Probing CP-violation at colliders through interference effects in diboson production and decay*, Phys.Rev. **D78** (2008) 035014, [[arXiv:0801.2891](https://arxiv.org/abs/0801.2891)].

[163] T. Han and Y. Li, *Genuine CP-odd Observables at the LHC*, Phys.Lett. **B683** (2010) 278–281, [[arXiv:0911.2933](https://arxiv.org/abs/0911.2933)].

[164] M. Spira, A. Djouadi, D. Graudenz, and P. Zerwas, *Higgs boson production at the LHC*, Nucl.Phys. **B453** (1995) 17–82, [[hep-ph/9504378](https://arxiv.org/abs/hep-ph/9504378)].

[165] D. McKeen, M. Pospelov, and A. Ritz, *Modified Higgs branching ratios versus CP and lepton flavor violation*, Phys.Rev. **D86** (2012) 113004, [[arXiv:1208.4597](https://arxiv.org/abs/1208.4597)].

[166] **CMS** Collaboration, S. Chatrchyan *et. al.*, *Study of the Mass and Spin-Parity of the Higgs Boson Candidate Via Its Decays to Z Boson Pairs*, Phys.Rev.Lett. **110** (2013) 081803, [[arXiv:1212.6639](https://arxiv.org/abs/1212.6639)].

[167] **CMS** Collaboration, S. Chatrchyan *et. al.*, *Measurement of the properties of a Higgs boson in the four-lepton final state*, Phys.Rev. **D89** (2014) 092007, [[arXiv:1312.5353](https://arxiv.org/abs/1312.5353)].

[168] **ATLAS** Collaboration, G. Aad *et. al.*, *Evidence for the spin-0 nature of the Higgs boson using ATLAS data*, Phys.Lett. **B726** (2013) 120–144, [[arXiv:1307.1432](https://arxiv.org/abs/1307.1432)].

[169] **ATLAS** Collaboration, *Measurements of the properties of the Higgs-like boson in the four lepton decay channel with the ATLAS detector using 25 fb⁻¹ of proton-proton collision data*, ATLAS-CONF-2013-013, ATLAS-COM-CONF-2013-018 (2013).

[170] **CMS** Collaboration, *Projected Performance of an Upgraded CMS Detector at the LHC and HL-LHC: Contribution to the Snowmass Process*, [arXiv:1307.7135](https://arxiv.org/abs/1307.7135).

[171] R. Alonso, M. Gavela, L. Merlo, S. Rigolin, and J. Yepes, *Minimal Flavour Violation with Strong Higgs Dynamics*, JHEP **1206** (2012) 076, [[arXiv:1201.1511](https://arxiv.org/abs/1201.1511)].

[172] T. Appelquist, M. J. Bowick, E. Cohler, and A. I. Hauser, *The Breaking of Isospin Symmetry in Theories with a Dynamical Higgs Mechanism*, Phys. Rev. **D31** (1985) 1676.

[173] G. Cvetič and R. Kogerler, *Fermionic Couplings in an Electroweak Theory with Nonlinear Spontaneous Symmetry Breaking*, Nucl. Phys. **B328** (1989) 342.

[174] D. Espriu and J. Manzano, *CP Violation and Family Mixing in the Effective Electroweak Lagrangian*, Phys.Rev. **D63** (2001) 073008, [[hep-ph/0011036](https://arxiv.org/abs/hep-ph/0011036)].

[175] L. Mercolli and C. Smith, *EDM Constraints on Flavored CP-Violating Phases*, Nucl. Phys. **B817** (2009) 1–24, [arXiv:0902.1949](https://arxiv.org/abs/0902.1949).

[176] J. Ellis, J. S. Lee, and A. Pilaftsis, *A Geometric Approach to CP Violation: Applications to the MCPMFV SUSY Model*, JHEP **10** (2010) 049, [arXiv:1006.3087](https://arxiv.org/abs/1006.3087).

[177] J. Brod and M. Gorbahn, *Next-to-Next-to-Leading-Order Charm-Quark Contribution to the CP Violation Parameter ϵ_K and ΔM_K* , Phys.Rev.Lett. **108** (2012) 121801, [[arXiv:1108.2036](https://arxiv.org/abs/1108.2036)].

[178] **LHCb** Collaboration, R. Aaij *et. al.*, *Measurement of the CP-Violating Phase Φ_s in the Decay $B_S^0 \rightarrow J/\Psi \Phi$* , Phys.Rev.Lett. **108** (2012) 101803, [[arXiv:1112.3183](https://arxiv.org/abs/1112.3183)].

[179] J. Laiho, E. Lunghi, and R. S. Van de Water, *Lattice QCD Inputs to the CKM Unitarity Triangle Analysis.*, Phys. Rev. **D81** (2010) 034503. Updates available on <http://latticeaverages.org/>, [[arXiv:0910.2928](https://arxiv.org/abs/0910.2928)].

[180] **UTfit** Collaboration, <http://www.utfit.org/UTfit/ResultsWinter2013PreMoriond>.

[181] **BaBar Collaboration** Collaboration, J. Lees *et. al.*, *Measurement of $B(B \rightarrow X_s \gamma)$, the $B \rightarrow X_s \gamma$ Photon Energy Spectrum, and the Direct CP Asymmetry in $B \rightarrow X_{s+d} \gamma$ Decays*, Phys.Rev. **D86** (2012) 112008, [[arXiv:1207.5772](https://arxiv.org/abs/1207.5772)].

[182] P. Gambino and M. Misiak, *Quark Mass Effects in $\bar{B} \rightarrow X_s \gamma$* , Nucl. Phys. **B611** (2001) 338–366, [[hep-ph/0104034](#)].

[183] M. Misiak *et. al.*, *The First Estimate of $BR(\bar{B} \rightarrow X_s \gamma)$ at $\mathcal{O}(\alpha_s^2)$* , Phys. Rev. Lett. **98** (2007) 022002, [[hep-ph/0609232](#)].

[184] M. Misiak and M. Steinhauser, *NNLO QCD Corrections to the $\bar{B} \rightarrow X_s \gamma$ Matrix Elements Using Interpolation in m_c* , Nucl. Phys. **B764** (2007) 62–82, [[hep-ph/0609241](#)].

[185] G. Buchalla, A. J. Buras, and M. E. Lautenbacher, *Weak Decays Beyond Leading Logarithms*, Rev. Mod. Phys. **68** (1996) 1125–1144, [[hep-ph/9512380](#)].

[186] T. Inami and C. S. Lim, *Effects of Superheavy Quarks and Leptons in Low-Energy Weak Processes $K_L \rightarrow \mu \bar{\mu}$, $K^+ \rightarrow \pi^+ \nu \bar{\nu}$ and $K^0 \leftrightarrow \bar{K}^0$* , Prog. Theor. Phys. **65** (1981) 297.

[187] A. J. Buras, L. Merlo, and E. Stamou, *The Impact of Flavour Changing Neutral Gauge Bosons on $\bar{B} \rightarrow X_s \gamma$* , JHEP **08** (2011) 124, [[arXiv:1105.5146](#)].

[188] T. Appelquist, M. J. Bowick, E. Cohler, and A. I. Hauser, *Isospin Symmetry Breaking in Electroweak Theories*, Phys. Rev. Lett. **53** (1984) 1523.

[189] A. De Rujula, M. B. Gavela, P. Hernandez, and E. Masso, *The Selfcouplings of Vector Bosons: Does Lep-1 Obviate Lep-2?*, Nucl. Phys. **B384** (1992) 3–58.

[190] F. Feruglio, A. Masiero, and L. Maiani, *Low-Energy Effects of Heavy Chiral Fermions*, Nucl. Phys. **B387** (1992) 523–561.

[191] T. Hurth, G. Isidori, J. F. Kamenik, and F. Mescia, *Constraints on New Physics in MFV Models: a Model-Independent Analysis of $\Delta F = 1$ Processes*, Nucl. Phys. **B808** (2009) 326–346, [arXiv:0807.5039](#).

[192] G. Isidori and P. Paradisi, *Hints of Large Tan(Beta) in Flavour Physics*, Phys. Lett. **B639** (2006) 499–507, [hep-ph/0605012](#).

[193] **D0** Collaboration, V. M. Abazov *et. al.*, *Measurement of the Anomalous Like-Sign Dimuon Charge Asymmetry with 9 Fb^{-1} of $p\bar{p}$ Collisions*, Phys. Rev. **D84** (2011) 052007, [arXiv:1106.6308](#).

[194] A. Lenz, *Theoretical Status of the CKM Matrix*, [arXiv:1108.1218](#).